UNIVERSITY OF TRENTO - Italy

International PhD Programme in Biomolecular Sciences

Department of Cellular, Computational and Integrative Biology – CIBIO

Cycle XXXII

"Investigating antigen delivery and presentation of OMV-based cancer vaccines"

Tutor

Prof. Guido Grandi

CIBIO – University of Trento

PhD Thesis of

Samine Jessica Isaac

Laboratory of Synthetic and Structural Vaccinology

CIBIO – University of Trento

Academic Year 2018-2019

Declaration

I, Samine J. Isaac, confirm that this is my own work or work I have done together with other members of our group and the use of all material from other sources has been properly and fully acknowledged.

Signed: 

Date: 24th September 2020

Thesis submitted for doctoral degree (PhD)

Defence: 27th October 2020

For Janita Isaac, your strength, courage and tenacity.

Abstract

Immunisation is the single most successful medical intervention to date. With the improved understanding of cancer immunity, cancer vaccines have quickly become weapons to be honed in the fight against cancer. The low immunogenicity of malignant cells hampers cancer immunotherapies. Cancer vaccines promise to overcome this problem.

Outer membrane vesicles (OMVs) are spherical structures shed from all gram-negative bacterial outer membranes. Currently, OMV-based vaccines focus on infectious disease. There are gaps in their use as cancer antigen delivery vehicles for cancer vaccines. Due to their adjuvanticity and simplicity for genetic engineering, OMVs have great potential as a cancer vaccine platform.

Here the aim is to show that it is possible to express an antibody derived single-chain variable fragment (scFv), specific for dendritic cell receptor DEC205, on the surface of OMVs using a bacterial protein as a carrier. Then demonstrate OMVs can be used to elicit good $CD8^+$ T cell responses. And finally show that their adjuvant and delivery vehicle properties lend them for use in *in situ* cancer vaccination.

I have shown we can engineer OMVs to express a functional scFv specific for the dendritic cell receptor DEC205 using a carrier. And that our proteome-minimised OMVs improved surface expression of the scFv fusion protein. The expression of the dendritic cell specific scFv increases internalisation of OMVs in dendritic cells. Importantly, this demonstrates an effective method for modifying OMV interaction with antigen presenting cells. Moreover, our OMVs, without additional dendritic cell targeting, are efficient vehicles for antigen delivery and can be used to elicit strong $CD8^+$ T cell responses. Finally, we show that our proteome-minimised OMVs alone induce anti-tumour immunity when injected intratumorally. Additionally, in the presence of tumour-specific neoepitopes we elicit an improved anti-tumour response.

The flexibility of OMVs both as adjuvants and vehicles for antigen delivery means they make a versatile vaccine platform, which can be fine-tuned using the techniques demonstrated.

Table of Contents

Declaration i

Abstract 1

Table of Contents 2

List of Tables 5

List of Figures 6

Abbreviations 8

Chapter 1: Introduction 10

1.1. Cancer background 10

1.2. Immunity 12

1.2.1. Dendritic cells 15

1.3. Cancer immunity and immunotherapy 20

1.3.1. A brief history 20

1.3.2. Mechanisms of cancer immunology 21

1.3.3. Cancer immunotherapy 26

1.3.4. Cancer vaccines 29

1.4. Outer membrane vesicles as a vaccine platform 36

1.5. Aim of the thesis 39

Chapter 2: Targeting OMVs to dendritic cells using single-chain variable fragments 41

2.1. Introduction 41

2.2. Results 46

2.2.1. The hunt for a novel carrier of scFv for surface expression in OMVs 46

2.2.2. Expression of FhuD2-scFv-αmDEC205 in BL21(DE3)Δ*60* derived OMVs 50

2.2.3. FhuD2 as a carrier for other scFv 53

2.2.4. Internalisation of mDEC205 targeting OMVs 55

2.2.5. Analysis of DC biomarker expression 58

2.3. Discussion 60

Chapter 3: Antigen processing and presentation 62

3.1. Introduction 62

3.2. Results 67

3.2.1. $OMV_{\Delta 60}$ adjuvanticity and reactogenicity 67

3.2.2. Immunogenicity of $OMVs_{\Delta 60}$ adsorbed with MHC I specific peptide antigens 70
3.2.3. Antigen peptide processing affects the elicitation of an antigen-specific T cell response 72
3.3. Discussion 75
Chapter 4: *In situ* vaccination of tumours with OMVs 77
4.1. Introduction 77
4.2. Results 80
4.2.1. $OMV_{\Delta 60}$ induced cancer cell lysis 80
4.2.2. *In situ* vaccination of OMVs inhibits growth of established tumours in the C57BL6-B16-OVA cancer model 81
4.2.3. *In situ* vaccination of OMVs with neoepitopes inhibits tumour growth in both injected and lateral tumours 82
4.3. Discussion 85
Chapter 5: Final discussion 87
Chapter 6: Material and methods 89
6.1. Bacterial strains and culture conditions 89
6.1.1. Chemically competent cell preparation 89
6.1.2. Chemically competent cell transformation 89
6.2. Fusion protein construct generation 90
6.2.1. Cloning of fusion protein constructs 91
6.3. OMV generation and purification 94
6.3.1. Small scale production for fusion protein expression 94
6.3.2. Medium scale fermentation for empty OMV production 94
6.4. SDS-PAGE and Western Blots 95
6.4.1. SDS-PAGE 95
6.4.2. Western blot 95
6.5. Phase partitioning with Triton X-114 95
6.6. Flow cytometry of Bacteria 96
6.7. Mammalian cell lines and culture 96
6.7.1. Cell lines and complete culture media 96
6.7.2. Cell thawing, passage and cryopreservation 98
6.8. *In vitro* cell assays 99
6.8.1. Internalisation of OMVs 99
6.8.2. Internalisation analysis 99

6.8.3. DC biomarker analysis 99
6.8.4. THP-1 cell hIL-6 release assay for adjuvanticity and reactogenicity 100
6.8.5. HEK Blue™ TLR activation assays 101
6.8.6. Lactate dehydrogenase (LDH) release cytotoxicity assay 101
6.9. *In vivo* experiments 102
6.9.1. Animal studies 102
6.9.2. Vaccination for T cell response analysis 102
6.9.3. Splenocyte re-stimulation assay 103
6.9.4. *In situ* vaccination of mice bearing two tumours 103
Bibliography 105
Publications 125
Acknowledgements 126

List of Tables

Table 1: Classes of tumour antigens 23
Table 2: Tumour escape mechanisms at each step of the cancer immunity cycle 25
Table 3: Statistical significance analysis of internalisation 58
Table 4: Peptides for $CD8^+$ T cell response experiments 73
Table 5: List of plasmids 91
Table 6: List of primers used for cloning 92
Table 7: Antibodies for the detection of DC biomarkers 100

List of Figures

Figure 1: A brief overview of immunity 13
Figure 2: Antigen presentation in dendritic cells. 14
Figure 3: Schematic representation of types of pattern recognition receptors (PRRs) in DCs. 17
Figure 4: Dendritic cell subsets. 19
Figure 5: Flow chart of cancer immunotherapy approaches 27
Figure 6: Correlation between tumour mutational burden and objective response rate with checkpoint inhibitors (anti–PD-1 or anti-PD–L1) in 27 tumour types.. 28
Figure 7: Overview of cancer vaccines 30
Figure 8: Classical antibody structure and scFv structure. 44
Figure 9: Schematic representation of plasmids contain fusion constructs and fusion protein structure. 47
Figure 10: SDS-PAGE of lysates and OMVs from BL21(DE3)ΔompA expressing with fusion proteins.. 48
Figure 11: The expression of FhuD2 in OMVs. 51
Figure 12: Western blot of triton X-114 – phase partitioned OMVs. 51
Figure 13: FhuD2-scFv is surface exposed in bacteria. 53
Figure 14: The expression and membrane localisation of three different FhuD2-scFv in OMVs 54
Figure 15: All three FhuD2-scFvs are surface exposed in bacteria. 55
Figure 16: Images of JAWSII cells with internal OMVs.. 56
Figure 17: Scatter plot of the number of internalised OMVs per cell.. 57
Figure 18: expression of DC biomarkers in JAWSII cells incubated with OMVs. 59
Figure 19: Antigen cross-presentation by dendritic cells. 62
Figure 20: T cell activation and tumour growth inhibition with $OMVs_{\Delta ompA}$. 64
Figure 21: schematic overviw of LPS and hexa-acylated or penta-acylated lipid A components. 65
Figure 22: Mouse TLR4 and human TLR2 dose-response curves by OMV stimulation.. 68
Figure 23: THP-1 cells stimulated with OMVs for IL-6 release dose-response curve..... 69

Figure 24: Vaccination with OMVs plus OVA peptide elicits a $CD8^+$ T cell response. 70
Figure 25: Percentage of epitope-specific $CD8^+$ $IFN\gamma^+$ T cells induced by vaccination with OMVs + peptide epitope..... 71
Figure 26: Percentage of epitope-specific $CD8^+$ $IFN\gamma^+$ T cells induced by vaccination with OMVs + the single SV40 peptide or double SV40 peptide. 73
Figure 27: Immunisation with OVA peptide or longOVA peptide adsorbed to OMVs affects the extent of $CD8^+$ T cell activation. 74
Figure 28: OMV vaccine with pentatope peptides adsorbd induces pentatope specific T cells and protects mice from CT26 tumours..... 79
Figure 29: Analysis of OMV cytotoxicity to CT26 cells..... 80
Figure 30: C57BL6 B16-OVA tumour growth with in situ vaccination tumour treatment. 82
Figure 31: BALB/c CT26 tumour growth with in situ vaccination tumour treatment. ... 83

Abbreviations

Acronym	Full name
Ab	Antibody
ADCC	Antibody-dependent cellular cytotoxicity
APC	Antigen presenting cell
BCG	Bacillus Calmette-Guérin (vaccine)
BCR	B cell receptor
CAR-T	Chimeric antigen receptor T cells
CCR7	C-C chemokine receptor type 7
CD	Cluster of differentiation
cDC	Conventional dendritic cell
CDC	Complement-dependent cytotoxicity
CDCC	Complement-dependent cell-mediated cytotoxicity
CDR	Complementarity-determining regions
CGA	Cancer germline antigen
CLR	C-type lectin receptor
CTLA-4	Cytotoxic T-lymphocyte-associated protein 4
DAMP	Damage-associated molecular pattern
DC	Dendritic cell
DEC205	DC receptor, type I endocytic CLR, with molecular weight 205 kDa
DNA	Deoxyribonucleic acid
EMA	European Medicines Agency
FDA	Food and Drug Administration
GM-CSF	Granulocyte-macrophage colony-stimulating factor
HBV	Hepatitis B virus
HER2	Human epidermal growth factor receptor 2
HPV	Human papillomavirus
HSV	Herpes simplex virus
IDO	Indoleamine 2,3-dioxygenase
IFNγ	Interferon gamma
IL	Interleukin
ILC	Innate lymphoid cell
LDH	Lactate dehydrogenase

LPS	Lipopolysaccharide
mAb	Monoclonal antibody
MAMP	Microbial-associated molecular pattern
MDSC	Myeloid-derived suppressor cell
MHC I	Major histocompatibility complex class I
MHC II	Major histocompatibility complex class II
mo-DC	Monocyte-derived dendritic cell
NK	Natural killer
NLR	NOD-like receptor
OMV	Outer membrane vesicle
$OMV_{\Delta 60}$	Outer membrane vesicle derived from strain BL21(DE3)Δ*60*
$OMV_{\Delta ompA}$	Outer membrane vesicle derived from strain BL21(DE3)Δ*ompA*
OVA	Ovalbumin (epitope SIINFEKL)
PD-1	Programmed cell death protein 1
pDC	Plasmacytoid dendritic cell
PD-L1	Programmed death-ligand 1
PMA	Phorbol 12-myristate 13-acetate
PRR	Pattern recognition receptor
scFv	Single-chain variable fragment
SV40	Simian Virus 40 large tumour antigen (IV epitope VVYDFLKL)
TAA	Tumour-associated antigen
TCR	T cell receptor
T_{FH}	T follicular helper
TGFβ	Transforming growth factor beta
T_H	T helper
TLR	Toll-like receptor
TLR	Toll-like receptor
TNFα	Tumour necrosis factor alpha
T_{REG}	Regulatory T
TSA	Tumour-specific antigens
VEGF	Vascular endothelial growth factor
VH	Variable heavy chain region
VL	Variable light chain region

Chapter 1: Introduction

1.1. Cancer background

Cancer is a large group of diseases defined by the uncontrollable proliferation and invasive growth of abnormal cells. This occurs when normal cells transform into tumour cells, in a multistep process involving the acquisition of mutations. It is generally the result of exposure to carcinogens together with genetic factors. Cancer can affect any part of the body, and overtime is able to spread from its original localisation to other organs, this mechanism is known as metastasis. Crucially, it is the metastatic disease that causes the majority of cancer deaths (Hanahan and Weinberg 2000; Dillekås *et al.* 2019).

The discovery and development of novel and highly effective cancer therapies are of the utmost importance considering the global burden of cancer. It is the second leading cause of death globally and in 2018 alone was responsible for an estimated 9.6 million deaths worldwide (Bray *et al.* 2018). The number of new cases per year is also on the rise, from an incidence of 18.1 million in 2018 to an estimated 29.5 million in 2040 (Bray *et al.* 2018). Ageing also greatly increases the risk of cancer due to the accumulation of somatic mutations, the decreased efficiency of DNA repair mechanisms and impaired immune responses. Therefore, cancer incidence rises with age and over 80% of all cancers occur in people over the age of 50 (Lin *et al.* 2019).

Fortunately, our understanding of cancer and its complexities has greatly developed in the last 20 or so years, and as it continues to do so, we create more tools and medicines with which to fight cancer. For example, in 2000 Hanahan and Weinberg proposed six hallmarks of cancer, present in all forms of the disease. They consist in the gain of following capabilities; ability to resist cell death, evasion of growth suppressors, sustained proliferative signalling, replicative immortality, induction of angiogenesis, and invasion and metastasis (Hanahan and Weinberg 2000). At the time, targeted cancer therapies, specific for these characteristics made significant breakthroughs in clinical research. These included the first monoclonal antibodies and tyrosine kinase inhibitors, such as trastuzumab and imatinib respectively (Chabner and Roberts 2005). Despite the success of targeted therapies, usually targeting growth factors and angiogenesis, it was quickly realised that targeting these characteristics alone did not fully encompass all the

aspects of cancer, and in fact left out some important features, in many cases accountable for patient relapses and non-response. Therefore these features: genetic instability, altered metabolism, tumour-promoting inflammation and evasion of immune-mediated destruction, were included and cancer hallmarks updated (Hanahan and Weinberg 2011). Cancer researchers are working to understand each hallmark in-depth and this understanding eventually leads to new treatment methods. The inclusion of immunological features has been instrumental in understanding disease progression. Moreover, studies elucidating how cancer evades immune-mediated destruction have led to various breakthroughs. Cancer immunotherapy has expanded and accelerated in the last decade, with much clinical success (Emens *et al.* 2017). This is due to the amalgamation of both new and old knowledge of cancer immunity.

1.2. Immunity

The role of the immunity in cancer development and progression has been one of the most challenging concepts in both immunology and oncology.

Immunity is the body's self-defence mechanism to resist pathogenic microorganisms to which we are continually exposed. The immune system can be divided into the innate and adaptive immune systems. The former is evolutionarily conserved and the latter a highly evolved complex system. It is able to recognise "foreign" particles as well as damage in order to remove internal threats to the body.

Innate immunity comprises a general response to infection, which is rapid, taking just hours. It consists of complement proteins and cytokines, as well as cellular components including dendritic cells (DCs), macrophages, granulocytes (neutrophils, eosinophils and basophils), mast cells, natural killer (NK) and innate lymphoid cells (ILCs). Whereas adaptive immunity has a slow (days or weeks), but antigen-specific response, and is able to induce memory. It consists of two major types of lymphocytes, B cells and T cells, responsible for humoral and cell-mediated immunity respectively. Some cytotoxic lymphocytes such as NK T cells and γδ T cells overlap into both innate and adaptive immunity (Murphy and Weaver 2016).

For an effective immune response, there is usually interaction between the two systems. The innate immune system in a non-specific first line of defence. Sensor cells such as DCs and macrophages, express pattern recognition receptors (PRRs) which are able to detect microbial-associated molecular patterns (MAMPs) present on invading microorganisms. Additionally, they are able to recognise damage-associated molecular patterns (DAMPs), and danger and stress signals. Subsequently, these cells respond directly with effector activity, and inflammatory cytokines, such as tumour necrosis factor α (TNFα), interleukin-12 (IL-12) and interferons, are released that act on other immune cells, such as the innate NK cells and ILCs. These are recruited into target tissues and kill infected cells or amplify the signals from innate recognition towards adaptive immunity. Generally, adaptive responses are initiated when the innate immune response fails to reduce or eliminate a new infection. DCs are professional antigen-presenting cells (APCs) and are the crucial link between the innate and adaptive immune system (Figure 1). They are phagocytes that take up the invading microbe. Once active, they mature and migrate to draining lymph nodes. Here they present microbe-derived

antigens, along with co-stimulatory molecules, to naïve T cells. Antigens are presented at the DC surface as peptides bound by major histocompatibility complex (MHC) molecules. This peptide-MHC complex binds the T cell receptor (TCR), which is in a complex with the cluster of differentiation 3 (CD3) molecule. Depending on the class of MHC molecule and co-stimulator expression, this interaction will cause polarisation and expansion of T cells into distinct subsets (Murphy and Weaver 2016).

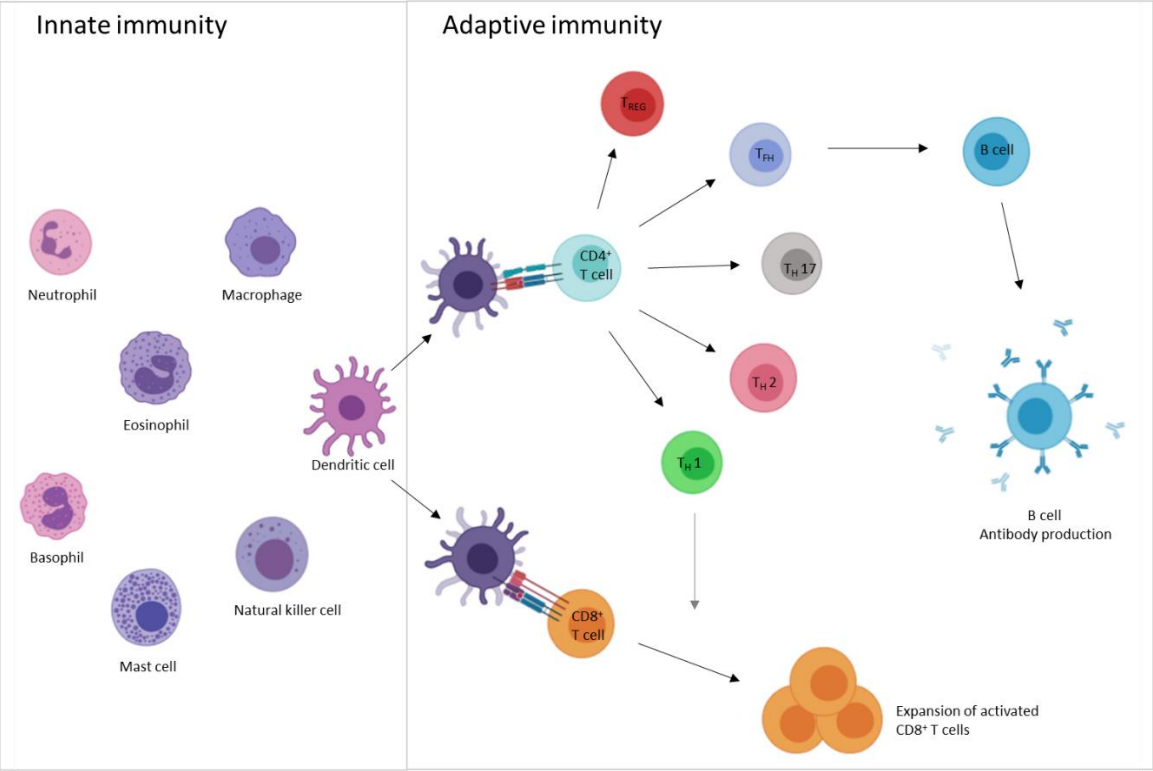

Figure 1: A brief overview of immunity *– Innate immune cells are the first to detect invading pathogens. Importantly, dendritic cells act as the interface between innate and adaptive immunity. Dendritic cells mature and prime T cells. They are the conductors of the type of adaptive immune response generated. Image created using BioRender.com*

MHC molecules can also be divided into class I and class II (MHC I and MHC II respectively). MHC I are expressed by every nucleated cell in the body. They bind peptides derived from intracellular antigens such as viral proteins, and other cytosolic proteins, to check for damage or infection. These peptides are 8-10 amino acids long. The peptide-MHC I complex is recognised by cytotoxic T cells ($CD8^+$ T cells). MHC II molecules are expressed by all APCs (DCs, macrophages and B cells), they bind peptides derived from extracellular antigens taken up by phagocytosis. These are longer peptides and generally more variable in length, often ranging 13-20 amino acids. This peptide-MHC II complex is recognised by helper T cells ($CD4^+$ T cells). Additionally, DCs can

present extracellular antigens as peptides on MHC I to $CD8^+$ T cells by cross-presentation (Figure 2). This requires internalisation of antigens and intracellular processing, whereby antigens are broken down into peptide by the proteasome. They are then loaded onto MHC I molecules for presentation (Joffre *et al.* 2012).

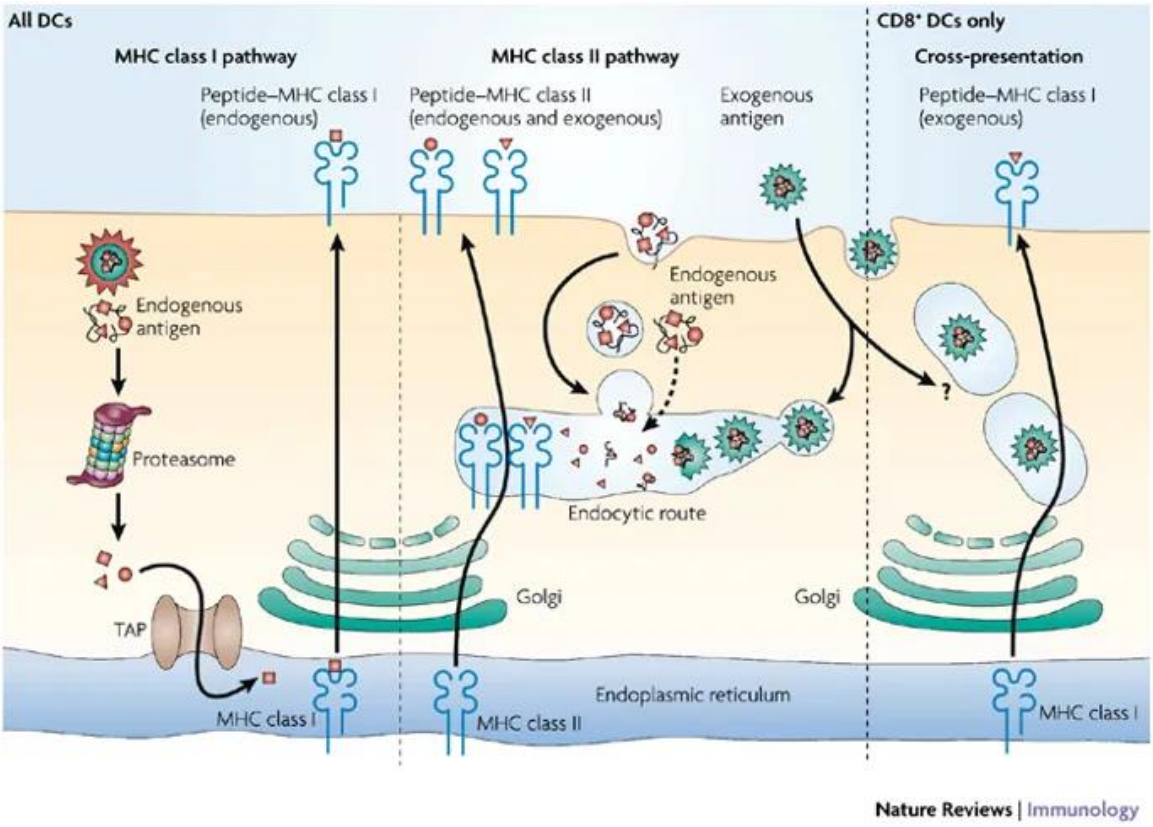

Figure 2: Antigen presentation in dendritic cells *(Villadangos and Schnorrer 2007) – All dendritic cells (DCs) have MHC I and MHC II presentation pathways. MHC I molecules present peptides that are mainly derived from endogenous proteins. MHC II molecules present peptides derived from exogenous antigens. They are endocytosed and peptides generated by proteolytic degradation in endosomal compartments. $CD8^+$ DCs have a unique ability to deliver exogenous antigens to the MHC I pathway, this phenomenon is called cross-presentation. The precise mechanism of cross-presentation is still not fully understood.*

$CD8^+$ T cells are known as cytotoxic T cells because their function is to kill target cells (usually infected cells) by recognition of specific antigens presented on MHC I. On the other hand, $CD4^+$ T cells are able to activate other immune cells, such as B and T cells. Thus earning the name T helper (T_H) cells. These can be broken down into five subsets, which have distinct roles. T_H1, T_H2, T_H17, and T_{FH} (follicular helper), activate their respective target cells; and regulatory T cells (T_{REG} cells), which are involved in damage limitation of immune responses by suppressing the activity of the other lymphocytes. T_H1 cells activate macrophages to kill intracellular pathogens and aid $CD8^+$ T cell activity. T_H2 cells active eosinophils, basophils and mast cells. T_H17 cells recruit

neutrophils to the infection site and promote antimicrobial peptide production by epithelial cells. Finally, T_{FH} cells are specialised B cell activators; they stimulate B cells for isotype switching and antibody production, the humoral response (Figure 1).

Anti-antigen B cell activity requires both interactions with T_H cells and binding of the antigen by the B cell receptor (BCR), a B cell membrane-bound antibody. B cells with high affinity for the antigen proliferate and differentiate, leading to affinity maturation of the antigen-specific antibody and antibody release. Antibodies defend the host in three ways. Neutralisation, whereby they bind pathogens or toxins, inactivating them. Opsonisation, in which pathogens are coated in antibodies, and this signals for phagocytosis and destruction by macrophages and neutrophils. Alternatively, complement activation, where bacteria bound antibodies activate the first protein of the complement cascade, leading to bacteria lysis and phagocytosis (Murphy and Weaver 2016).

Cells expressing MHC I are able to display both self and foreign antigens. The immune system is responsible for removing cells that present foreign antigens. Lymphocytes with an affinity for self-antigens are usually eliminated by negative selection, creating immune tolerance. Mutations in cancer create foreign antigens, but tumour suppression of the immune system mean that these antigens are not always recognised by immune cells. So, not only does the immune system have an effect on cancer but cancer has an effect on the immune system. Herein lies to the complexity of cancer immunity.

1.2.1. Dendritic cells

Dendritic cells are considered “professional” antigen-presenting cells because they are specialised at recognising invading microbes or antigens, are approximately 100-fold more potent adaptive immune response initiators than macrophages or monocytes (Steinman and Witmer 1978), and can cross-present exogenous antigens on MHC I. They are found in most tissues, especially barrier tissues such as the skin, lungs and gut. Though dendritic cells were discovered in 1973 by Ralph Steinman and Zanvil Cohn (Steinman and Cohn 1973), DC biology is just coming of age in terms of understanding and importance in immunology.

In the absence of infection or inflammation, they are in an immature state. Meaning they express low levels of MHC molecules and co-stimulatory molecules. When infection occurs, the presence of MAMPs or DAMPs stimulates DC maturation, leading to increased expression of MHC molecules, co-stimulatory molecules CD80, CD86 and CD40, as well as upregulation of chemokine receptors such as CCR7 and CD62L, which enable DC migration to secondary lymphoid tissues, where they interact with T and B cells for an adaptive immune response.

For optimal detection of molecular patterns DCs express a plethora of PRRs summarised in figure 3, via which they fine-tune immune responses. Expression of these PRRs depends on DC subset and maturity.

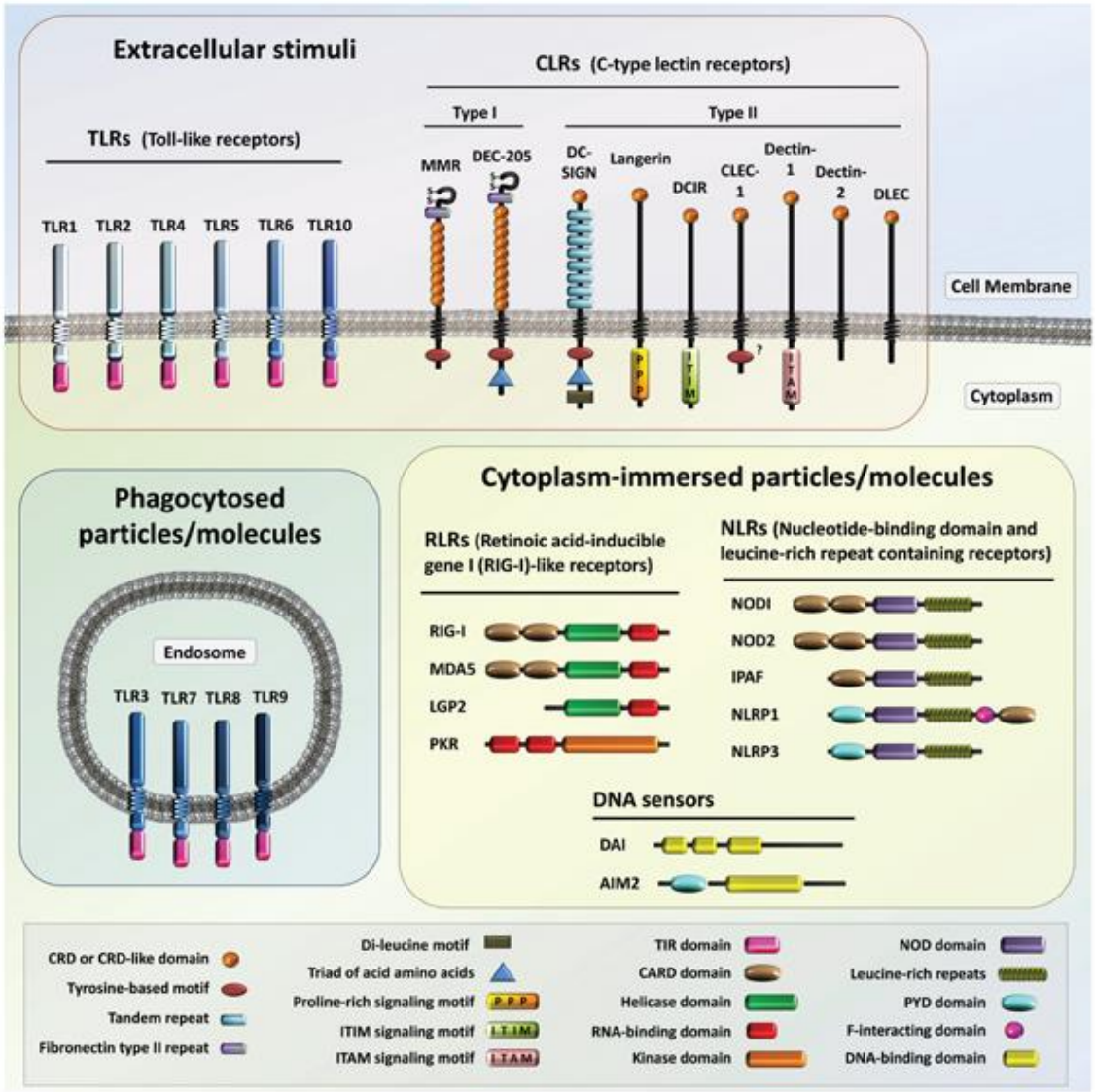

Figure 3: Schematic representation of types of pattern recognition receptors (PRRs) in DCs. *Toll-like receptors (TLRs) are found on the cell surface membrane and in the membrane of endosomes. C-type lectins (CLRs) are cell surface transmembrane receptors for glycans containing carbohydrate recognition domains (CRDs), which bind ligands in a Ca_2^+-dependent manner. Cytoplasmic PRRs include the nucleotide-binding oligomerisation domain (NOD) and leucine-rich repeat (LRR)-containing receptors (NLRs) involved in inflammasomes; The retinoic acid-inducible gene I (RIG-I)-like receptors (RLRs) and DNA sensor. Commonly occurring motifs and domains are shown. AIM2 = absent in melanoma 2; CLEC-1 = C-type lectin receptor 1; DAI = DNA-dependent activator of interferon-regulatory factors; DCIR = dendritic cell immunoreceptor; DC-SIGN = dendritic-cell specific ICAM-3 grabbing non-integrin; DEC-205 = dendritic cell receptor for endocytosis 205; DLEC = dendritic cell lectin; IPAF = ice protease-activating factor; ITAM = immunoreceptor tyrosine-based activation motif; ITIM = immunoreceptor tyrosine-based inhibitory motif; LGP2 = laboratory of genetics and physiology 2; MDA5 = melanoma differentiation-associated gene 5; MMR = macrophage mannose receptor; NLRP1/3 = nucleotide-binding oligomerisation domain, leucine-rich repeat and pyrin domain containing 1/3; PKR = double-stranded RNA activated protein kinase; PYD = Pyrin domains; TIR = Toll/interleukin-1 receptor homology domain. (Miyaji et al. 2011)*

As previously outlined, antigen presentation on MHC I or MHC II is crucial to the type of immune response elicited. Dendritic cells are the conductors of the type of immune response. They determine whether $CD4^+$ T cells are activated to become T_H cells, thus releasing various cytokines to direct the response, e.g. interleukin-12 (IL-12) promotes a T_H1 response responsible for cellular immunity, whereas IL-4 release

stimulates a T_H2 response leading to IL-10 and further IL-4 secretion, signalling a humoral (B cell) response (Chen *et al.* 2016). T_H1 cells primarily produce interferon-γ (IFNγ) and IL-2 that are responsible for T cell activation and inflammation. $CD8^+$ T cells are activated to release tumour necrosis factor α (TNFα), IFNγ and to enact cytotoxic effects on cells presenting the cognate antigen.

Dendritic cells can be broadly divided into two subsets; plasmacytoid DCs (pDCs) and conventional DCs (cDCs) (Figure 4). The pDCs are mainly recognised by being $B220^+$ in mice, and $CD123^+$ in humans. The cDC subset can be further divided into cDC1 ($CD8^+$ in mice and $CD141^+$ in humans) and cDC2 ($CD8^-/CD11b^+$ in mice and $CD1c^+$ in humans). $CD8^+$ DCs have a high expression of CLRs such as DEC205, which is involved in antigen capture and cross-presentation. As well as Clec9A, which has also been shown to facilitate antigen presentation (Macri *et al.* 2016). TLR3 is also highly expressed in this subset. However, $CD8^-$ DCs express Clec4A4, a CLR involved in antigen capture and presentation on MHC II (Den Haan *et al.* 2000; Uto *et al.* 2016). The pDCs are not as good antigen presenters as cDCs, though they can also be stimulated to activate $CD8^+$ T cells by cross-presentation, they often correlate with poor cancer prognosis. The role of cDC2 is less clear because it is context-dependent. They are involved in humoral and cellular immunity against extracellular pathogens, including $CD4^+$ T cell immunity in cancer, while cDC1s are involved in T_H1 and $CD8^+$ T cell immunity against cancer and intracellular pathogens. They specialise in cross-presentation and correlate with a beneficial cancer prognosis (Wculek *et al.* 2019). Dendritic cell lineage correlates with expression of transcription factors interferon regulatory factor 4 and 8 (IRF4 and IRF8 respectively). Monocyte-derived DCs (mo-DCs) are distinct entities derived from primitive myeloid progenitors. Monocyte are IRF4/8 low but can be induced to differentiate into mo-DCs.

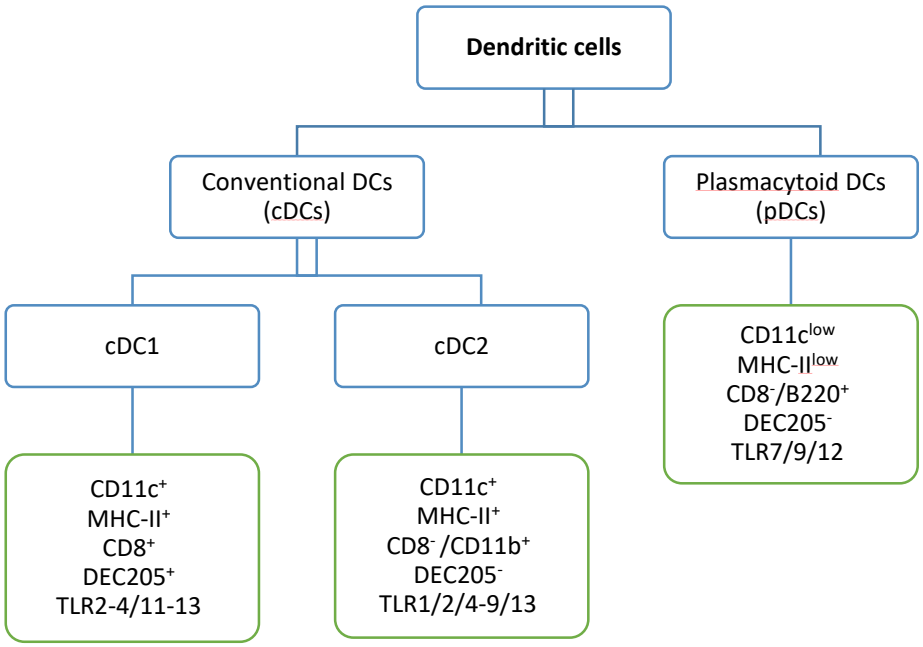

Figure 4: Dendritic cell subsets. *Different DC subsets in blue boxes, with corresponding differentially expressed surface markers in green boxes. Markers correspond to those expressed in mouse DCs for simplicity. DC subsets in humans closely resemble their mouse counterparts. Simplified from DC subset reviews (Collin and Bigley 2018; Wculek et al. 2019) in order to highlight markers relevant to this PhD thesis.*

1.3. Cancer immunity and immunotherapy

1.3.1. A brief history

Although the role of the immune system in cancer was studied by oncologist Dr William Coley over a century ago, it remained unappreciated and largely unacknowledged until relatively recently. This is partly due to the discovery of radiotherapy and chemotherapy, but also because of the lack of understanding of the immune system (McCarthy 2006). Now it is accepted that tumours suppress immune responses and evade anti-tumour immunity in a number of ways (Schreiber *et al.* 2011).

In 1891 Dr Coley began systematically studying the activation of an immune response to treat malignant tumours. He started by injecting a patient with inoperable bone sarcoma with streptococcal bacteria in order to cause an infection, thus stimulating the immune system. Finding that the tumour disappeared, he was encouraged to test this practise on other patients. To prevent patients dying from infection, he began to work with heat-killed *Streptococcus pyogenes* combined with *Serratia marcescens* (then known as *Bacillus prodigiosus*), this type of concoction was known as Coley's toxin (McCarthy 2006; Sell 2017). Throughout his career, he used Coley's toxin to treat hundreds of patients with inoperable bone and soft-tissue sarcomas. He demonstrated for the first time, that stimulation of the immune system could inhibit cancer growth. His work was widely discussed, and despite successes, heavily criticised by many in the scientific community. The combination of a lack of understanding of immunology, the breakthrough and support of radiotherapy, and inconsistencies and poor reproducibility of Coley's own work, meant that his method saw limited clinical investigation for the treatment of cancer (McCarthy 2006).

However, in 1909 Paul Ehrlich proposed the concept that tumour formation is usually suppressed by the immune system. Nascent transformed cells appear frequently but the immune system detects and eliminates these cells before they develop into cancer, a concept now known as immunosurveillance (Ehrlich 1909). This concept, much like Dr Coley's work, would pass through various phases of acceptance and scepticism. Until the 1950s, when Lewis Thomas and Frank Macfarlane Burnet published works supporting the theory of cancer immunosurveillance. They proposed that the host could

be protected from cancer growth by early immune recognition and subsequent elimination of neoplastic cells (Burnet 1957; Dunn *et al.* 2002).

Due to the early observations that infection can cause tumour regression, the efficacy of the Bacillus Calmette–Guérin (BCG) vaccine, a live attenuated *Mycobacterium bovis* tuberculosis vaccine, was demonstrated in the treatment of bladder cancer by Bast et al. in the 1970s (Bast *et al.* 1974). However, due to ongoing scepticism, it was not approved for superficial bladder cancer until 1990 (Lum and Torti 1991; Lamm 1992).

The 1990s yielded a big turnaround for cancer immunotherapy when immunocompetent knockout mouse models were used to demonstrate that IFNγ protects against tumour growth and formation, and has a role in tumour surveillance (Dighe *et al.* 1994; Kaplan *et al.* 1998). Meanwhile, in the clinic, interleukin 2 (IL-2), known as an activator of cytotoxic T cells, was being trialled for treatment of metastatic renal cell carcinoma and melanoma. Of the fraction of patients that had an objective response (approximately 15%), half of them were completely cured (Rosenberg and Lotze 1986; Fyfe *et al.* 1995; Atkins *et al.* 1999), leading to FDA approval of IL-2 in both settings. These discoveries and FDA approvals meant that finally there was widespread acceptance of cancer immunity. This was solidified by the work of Robert Schreiber's group on immunoediting in which they outlined a mechanism for cancer immunity (Dunn *et al.* 2002).

1.3.2. Mechanisms of cancer immunology

Now there are two concepts that explain the role of the immune system in cancer: cancer immunoediting and the cancer immunity cycle. Understanding these mechanisms has led to key breakthroughs in cancer immunotherapy. Cancer immunoediting describes the seemingly paradoxical roles of the immune system in suppressing tumour growth, yet also promoting tumour progression. It was elegantly delineated using "the three E's", elimination, equilibrium and escape (Dunn *et al.* 2002, 2004).

The elimination phase encompasses cancer immunosurveillance, in which both the innate and adaptive immune systems together are able to detect and destroy a developing tumour before it manifests clinically (Dunn *et al.* 2002). The immune system

becomes aware of the nascent tumour through danger signals, damage-associated molecular pattern molecules (DAMPs) and stress signals. PRRs on innate immune cells are activated, causing the release of cytokines and creating a microenvironment with anti-tumour adaptive immune responses (Guerra *et al.* 2008). Anti-tumour immune responses, like most other immune responses, require the activation of both innate and adaptive immune systems to confer efficient protection. Therefore, tumour elimination requires the expression of tumour antigens, which can be presented on MHC molecules for the activation and expansion of both $CD4^+$ and $CD8^+$ T cells (Schreiber *et al.* 2011).

Tumour antigen expression is the result of the build-up of various mutations, and dysregulation of normal cellular processes, that defines cancer. There are various types of tumour antigen, detailed in *Table 1: Classes of tumour antigens*, they are dependent on how the tumour originated (spontaneous versus carcinogen-induced mutations), anatomic location (e.g. prostate, breast etc), and rate of growth (Chen and Mellman 2013). Tumour antigens have the potential to be presented as peptides bound to MHC I on the surface of the tumour cell. These allow the tumour cell to be distinguished from normal, healthy cells. If complete tumour elimination occurs, cancer immunosurveillance has been successful and the process of immunoediting finishes here.

Table 1: Classes of tumour antigens Tumour antigens can be divided into three classes (adapted from Janeway's Immunobiology(Murphy and Weaver 2016) and (Hollingsworth and Jansen 2019))

Class	Subclass (derivation/origin)	Patient prevalence	Central tolerance	Example	Cancer type
Tumour-associated antigen (TAA)	Differentiation	high	High	Tyrosinase	Melanoma
	Over-expression	high	High	HER2	Breast / Ovary
	Post-translational modification	high	High	MUC-1	Breast/ pancreas
	Post-transcriptional modification	high	High	NA17	Melanoma
Cancer germline antigen (CGA)	Cancer testis antigens	high	Low	MAGE / NY-ESO	Melanoma / Breast / Glioma
Tumour-specific antigens (TSA)	Oncoviral	high	None	HPV type 16, E6 and E7 proteins	Cervical cancer
	Mutated driver oncogene	high	None	BCR-ABL	Leukaemia
	Mutated oncogene	low	None	β-catenin	Colorectal cancer
	Mutated suppressor gene	low	None	Cyclin-dependent kinase 4	Melanoma

The equilibrium phase occurs when a rare differentiated tumour cell acquires the ability to survive elimination. Here adaptive immune responses inhibit tumour cell proliferation and shape tumour immunogenicity. The tumour cells are maintained in a dormant state. In this phase, tumour cells may go undetected in patients for decades. Until eventually, growth is resumed as either metastases or a recurrent tumour. The role of adaptive immunity mechanistically distinguishes equilibrium from elimination. It was shown that only adaptive responses, $CD4^+$ and $CD8^+$ T cells, IFNγ and interleukin-12 (IL-12), were responsible for the maintenance of tumour cells in equilibrium, causing growth inhibition and tumour cell killing (Koebel *et al.* 2007). Selective pressures mean that tumour cells that acquire immuno-evasive mutations can progress on to the next phase.

Tumour cells in the escape phase have evaded immune recognition and destruction. This can happen for several reasons: when in response to the first two phases of immunoediting, differentiated tumour cells are selected for, with an increased ability to survive immune responses. Immune responses in the microenvironment

change due to cancer-induced immunosuppression or age-related immune deterioration. There are a number of mechanisms for tumour immune escape. Tumour proliferation and establishment can be caused by increased cellular resistance to immune cytotoxicity. Tumour cells may also lose antigen expression. This can occur in several ways: loss of MHC I molecules, loss of antigen processing functions (no peptide production or inability to load peptide on MHC I), or lack of expression of strong rejection antigens. These changes are driven by genetic instability and immunoselection (Dunn *et al.* 2002; Khong and Restifo 2002). They make the tumour undetectable to the immune system, allowing it to escape, sometimes referred to as a "cold" tumour. Additionally, tumour cells can also promote the formation of an immunosuppressive microenvironment. Thus aiding immune escape (Radoja *et al.* 2000). By releasing cytokines such as vascular endothelial growth factor (VEGF), transforming growth factor–b (TGF-b), galectin, or indolamine 2,3-dioxygenase (IDO) they active immunosuppression. Moreover, immunosuppression is propagated by the recruitment of T_{REG} cells and myeloid-derived suppressor cells (MDSCs) that inhibit protective immunes responses.

While cancer immunoediting describes how tumours eventually escape immune regulation. It is difficult to see exactly where cancer immunotherapies should be aiming. We know that cancer immunity is controlled by a series of highly regulated events. The cancer immunity cycle allows us to address these events as a whole, rather than singularly. In this way, we can understand how the immune system can control, and crucially, be manipulated to improve cancer immunity.

The effective killing of cancer cells by the immune system can be regarded as a seven-step process. Once initiated it should proceed and expand, continuing in a cycle. This is known as the Cancer-Immunity cycle (Chen and Mellman 2013). Step one, the tumour cell releases tumour antigens, which are captured and processed by DCs. An immunogenic, rather tolerogenic, response must be achieved by proinflammatory cytokine signalling and danger/stress signalling. Step two, DCs perform MHC I and II presentation of the antigens to T cells. Step three, T cells are thus primed and activated against tumour antigens. At this stage, it is critical that an immunogenic, rather than tolerogenic immune response is induced. Step four, the activated effector T cells traffic to the tumour. Step five, they infiltrate the tumour. Step six, via the TCR recognition of

antigen peptide-bound MHC I, T cells specifically bind tumour cells. Step seven, the cytotoxic T cells kill their target tumour cell, causing additional release of tumour antigens, thus restarting and expanding the cycle. Continued cycles increase the breadth and depth of the anti-tumour immune response (Chen and Mellman 2013). When this cycle is performing optimally, complete elimination can occur. Conversely, escape and the clinical manifestation of cancer occurs when any of the steps in the cancer-immunity cycle are dysregulated.

The aim of cancer immunotherapy must be to initiate (or reinitiate) and allow the continuation of the cancer immunity cycle. Therefore, therapies must overcome escape mechanisms at each step, as in *Table 2*.

Table 2: Tumour escape mechanisms at each step of the cancer immunity cycle

Step	Cells involved	Dysregulation	Mechanism
1) Release of tumour antigens	Tumour cells	Reduced expression of tumour antigens	Selection of tumour cells that lack tumour antigen expression Induction of Tolerogenic cell death
2) Tumour antigen presentation	DCs (APCs)	Deficient antigen presentation	Lack of MHC expression (+ co-stimulatory molecules) Lack of proinflammatory stimulation (cytokines and DAMPs etc) Anti-inflammatory signalling (IL-10, IL-4, IL-13) Tolerogenic presentation
3) Priming and activation of T cells	DCs→ T cells	Induction of tolerance	Expression of checkpoint inhibitors (CTLA4, PD-L1) T_{REG} activation
4) Trafficking of T cells to tumours	T cells	Decreased trafficking	Lack of chemokines (CX3CL1, CXCL9, CXCL10, CCL5)
5) Infiltration of T cell into tumours	T cells	Decreased tumour infiltration	VEGF, endothelin Lack of LFA1/ICAM1
6) Recognition of tumour cells by T cells	T cells → tumour cells	Faulty recognition	Recognised to tolerate Reduced peptide-MHC expression → not recognised
7) Killing of tumour cells	T cells → tumour cells	Resistant to apoptosis, suppression in the microenvironment	Lack of IFNy Checkpoint inhibition (PD-1, PD-L1, LAG-3 etc)

1.3.3. Cancer immunotherapy

Cancer immunotherapies cover a wide range of therapies (Figure 5). They can be classified as active or passive depending on whether they are designed to act directly on the immune system (active) or the tumour (passive). Passive immunotherapies such as tumour targeting monoclonal antibodies (mAbs) have had widespread success in the clinic since the late 1990s (Dougan and Dranoff 2009). Spurred by the landmark approvals of Rituximab for B cell lymphoma in 1997 and Trastuzumab for HER2-positive breast cancer in 1998.

Antibodies are useful therapeutic agents because of their multi-functionality. Using their variable domains, they are able to target specific epitopes, their binding can be used to block or even activate the target. In addition, through their constant domains they can engage Fc receptors, allowing antibody-dependent cellular cytotoxicity (ADCC), as well as engaging complement immune mechanisms such as complement-dependent cytotoxicity (CDC) or complement-dependent cell-mediated cytotoxicity (CDCC) (Peters and Brown 2015).

In the last decade the biopharmaceutical industry has made substantial advances in developing antibody therapeutics, almost tripling the number of licensed antibody therapeutics in the clinic (Kaplon *et al.* 2020). Technical developments involving protein engineering of antibody formats have also increased their flexibility. Allowing the development of fragment antibodies and bispecific or multi-valent antibodies (Labrijn *et al.* 2019). This versatility has had a significant impact on the development of cancer immunotherapies.

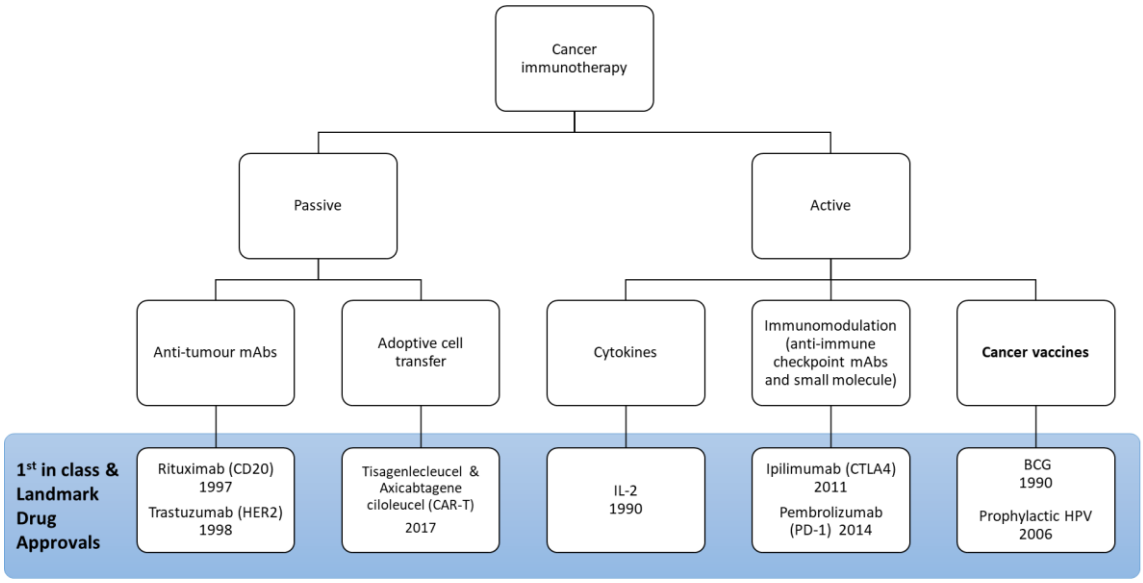

Figure 5: Flow chart of cancer immunotherapy approaches *– Cancer immunotherapy can be either passive or active. Passive immunotherapy involves giving antibodies or adoptive cell transfer in patients with a weak immune system. Once inside the bodies these molecules can compensate for deficient immune functions. Active immunotherapy involves stimulating the cancer patients own immune system to fight the cancer. Flowchart adapted from the IASLC Atlas of PD-L1 immunohistochemistry testing in lung cancer (Tsao et al. 2017)*

In the last 10 years, active immunotherapies, specifically mAbs that block regulatory immune checkpoint inhibitors have had a huge impact on cancer treatment. First in class was Ipilimumab, a cytotoxic T lymphocyte antigen 4 (CTLA-4) blocking mAb. Shortly followed by mAbs targeting programmed cell death protein 1 (PD-1), or its ligand, PD-L1 (Topalian *et al.* 2015; Postow *et al.* 2015; Baumeister *et al.* 2016). These are immune checkpoint inhibitors, when the respective ligand-receptor pairs bind (e.g. PD-1:PDL1 or CTLA-4:CD80/CD86) they signal a down-regulation of T cell activity. Blocking these targets is designed to "release the breaks" on immunosuppression, allowing effector T cell stimulation. Releasing the breaks implies that at some point there was an effective anti-tumour immune response. Anti-tumour $CD8^+$ T cell cytotoxicity is dependent on tumour cell expression of antigenic peptides on MHC I, the effectiveness of these treatments has demonstrated that patient tumours are recognised by the immune system, and can elicit tumour-specific $CD4^+$ and $CD8^+$ T cell responses. Meaning that tumour-specific antigens are being recognised. In fact, tumour mutational burden and neoantigen frequency, correlate with treatment success

(Schumacher and Schreiber 2015; Tran *et al.* 2017; Yarchoan *et al.* 2017). In turn, resistance often occurs due to tumour antigen loss or low mutations burden (Figure 6).

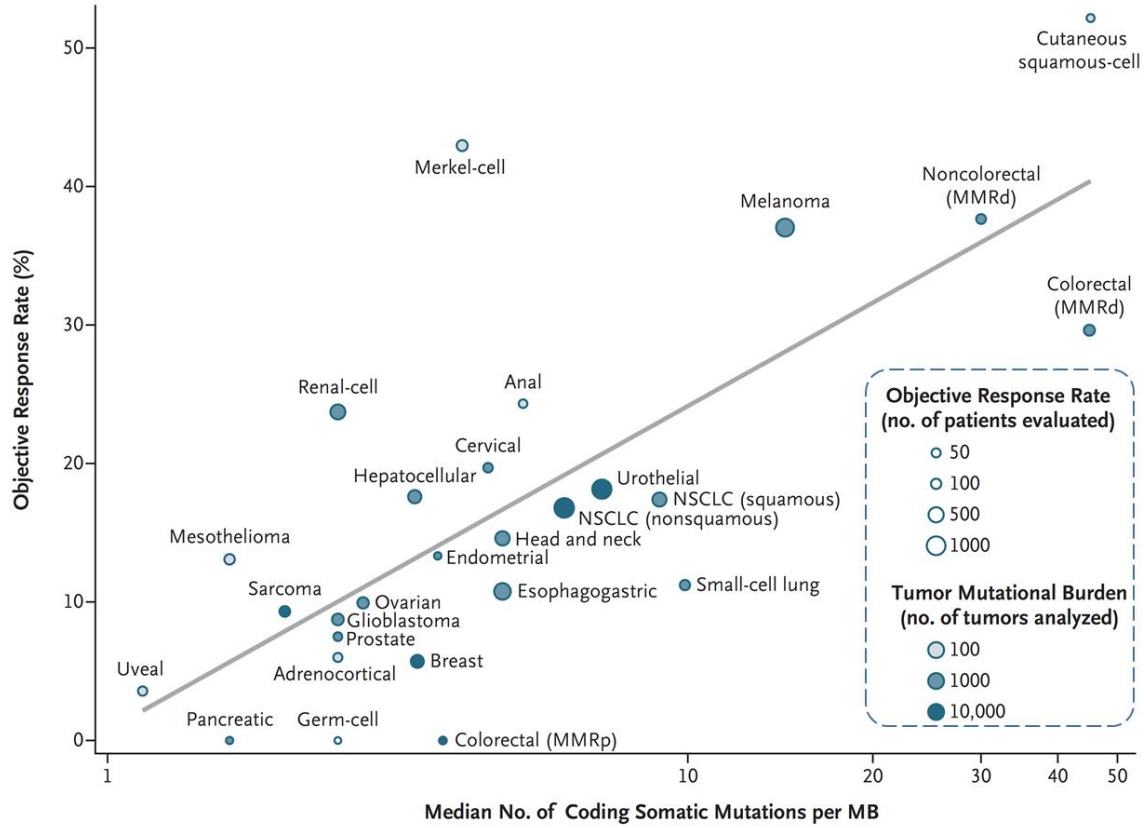

Figure 6: Correlation between tumour mutational burden and objective response rate with checkpoint inhibitors (anti–PD-1 or anti-PD–L1) in 27 tumour types. *The x-axis (logarithmic scale) shows the median number of coding somatic mutations per megabase (MB) of DNA in 27 tumour types or subtypes among patients who received PD-1 or PD-L1 inhibitors. The y-axis shows the objective response rate of these patients to the treatment. The number of patients who were evaluated for the objective response rate is shown for each tumour type (size of the circle), along with the number of tumour samples that were analysed to calculate the tumour mutational burden (degree of shading of the circle). MMRd denotes mismatch repair-deficient, MMRp mismatch repair-proficient, and NSCLC non–small-cell lung cancer (Yarchoan et al. 2017).*

Cellular immunotherapy has also greatly progressed in the last decade. In 2010, Sipuleucel-T was the first FDA approved cellular immunotherapy. It is a therapeutic vaccine against hormone-refractory prostate cancer expressing prostatic acid phosphatase (PAP). It is comprised of autologous DCs, stimulated and matured *ex vivo* with PAP-GM-CSF. In the USA it is used to treat castration-resistant prostate cancer patients (Gardner *et al.* 2012). Though initially approved by the EMA, its market authorisation was withdrawn by the holder due to financial issues. Partly because European governments were reluctant to fund this personalised cell therapy due to issues with cost-benefit rules. But also because of the technical challenges of

leukapheresis (obtaining patient leukocytes) (Gardner *et al.* 2012). However, adoptive cell transfer, particularly of chimeric antigen receptor T cells (CAR-T cells) have been a technological success. In 2017, both Tisagenlecleucel (Kymriah™) and Axicabtagene ciloleucel (Yescarta™) were approved by the FDA, and the EMA the following year. Both are CD19 specific CAR-T cells used in the treatment of B-cell cancers and have complete remission rates of over 50% (Hopfinger *et al.* 2019). Tisagenlecleucel, for the treatment of B-cell precursor acute lymphoblastic leukaemia (ALL) in patients aged 0-25 years (Prasad 2018). Axicabtagene ciloleucel for the treatment of large B-cell lymphomas in adult patients.

As outlined in figure 5, there are many types of cancer immunotherapy. Here I will focus on cancer vaccines in detail because they are most relevant to my PhD thesis.

1.3.4. Cancer vaccines

In general, immunisation is the single most significant and successful medical intervention to date. Traditionally, vaccines are given as a prophylactic therapy, in that healthy people are vaccinated so the immune system is primed and ready to respond to prevent specific diseases. As has already been discussed, the idea of using this very effective intervention against cancer is not new. However, it is only now that cancer immunity is well understood, that cancer vaccines have become significant weapons in the fight against cancer.

One of the main problems hindering cancer immunotherapies is the low immunogenicity of malignant cells. Tumour cells can present self-antigens, downregulate the antigen presentation process or secrete regulatory cytokines to create an immunosuppressive microenvironment resulting in immune evasion as previously described. Cancer vaccine therapies are best equipped to overcome this problem.

Cancer vaccines can be broadly divided into prophylactic or therapeutic vaccines, though there is beginning to be some overlap. Cancer vaccine mechanisms are diverse and usually depend on vaccine administration methods (see Figure 7).

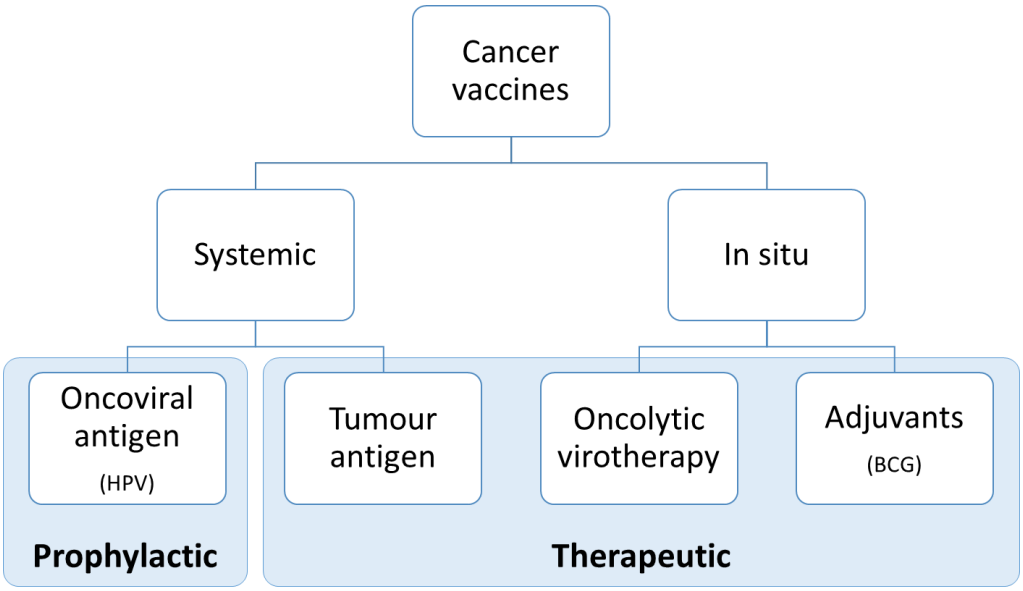

Figure 7: Overview of cancer vaccines *– Cancer vaccines can be broken down by treatment administration method and vaccine approach. The type of vaccine approach is generally meant for either prophylactic or therapeutic treatments, though with new developments the lines are beginning to blur. Administration is traditionally systemic but in situ (or intratumoral) cancer vaccination is being more frequently explored.*

Prophylactic cancer vaccines targeting oncogenic viral antigens have already been successful in the clinic. Such as vaccines against human papillomavirus (HPV) (Kenter *et al.* 2009; Karaki *et al.* 2016; Yang *et al.* 2016) and hepatitis B virus (HBV) (Lee *et al.* 1998; Chang 2009; Pol 2015), which are causes of cervical and liver cancer respectively. In fact, the universal HBV vaccination campaign launched in Taiwan over 30 years ago provided the first evidence that vaccination could prevent cancer in humans (Chang 2009). It has been estimated that the protective efficacy of HBV vaccination for primary liver cancer is 84% (Qu *et al.* 2014). Yet oncogenic virus vaccines are limited because oncogenic viruses and their antigens are expressed and causative in just a fraction of cancers. However, there is now a focus on researching these oncogenic virus vaccines for therapeutic cancer treatment. As such, the HPV vaccine is being repurposed for therapeutic treatment of HPV-associated head and neck cancers due to oncoviral antigens being ideal tumour antigens for vaccines (Wang *et al.* 2018).

Creating therapeutic cancer vaccines, which can be administered as a treatment once the disease clinically manifests, is the current challenge of the field. This is because the appearance of tumour antigens comes hand in hand with the appearance of the diseased cells. The goal is to achieve an immune response to the tumour that is durable

and self-propagating. To achieve this, T cells must be optimally primed, and the activation state of dendritic cells and antigen source are key to this function. Therefore, an effective cancer vaccine ought to include three critical components. One, protective tumour antigens against which the immune response must be elicited; two, an immunostimulatory adjuvant; and three, a delivery mechanism for effective engagement of an anti-tumour immune response (Grandi *et al.* 2016).

In terms of administration, there currently two approaches to cancer vaccination: systemic and *in situ* vaccination (Dougan *et al.* 2019).

1.3.4.1. In situ vaccination

In situ vaccination is an effective strategy, yet is perhaps the simplest in terms of vaccine design. It dates back to Coley's toxin and the BCG bladder cancer vaccination. The main principle is to inject adjuvants directly into the tumour and tumour microenvironment, thus stimulating an immune response at the tumour site. Antigens are not required in the formulation because the rationale is that the induction of tumour cell death causes the release of tumour-specific antigens, which are phagocytosed by the dendritic cells. With the help of adjuvants, the DCs become active and prime T cells, leading to the development of a potent anti-tumour T and B cell response (Sagiv-Barfi *et al.* 2018). Therefore, effective *in situ* cancer vaccines require an adjuvant and a tumour cell death mechanism because that is how the tumour-specific antigens are supplied to the system. The right adjuvant alone may incite tumour cell death directly via the cytotoxic immune response. It is this simplicity that allows *in situ* vaccination to be considered both off-the-shelf and personalised, i.e. it is patient-specific on delivery, without the need to identify and formulate tumour-specific antigens. In addition, efficacious *in situ* vaccinations induce an abscopal effect, meaning the anti-tumour immune response is observed at distant, metastatic tumour sites, not only where the vaccine was injected (Pierce *et al.* 2015; Hammerich *et al.* 2015, 2019; Sagiv-Barfi *et al.* 2018; Khalil *et al.* 2019).

In situ vaccination with the BCG vaccine for superficial bladder cancer was the first FDA approved *in situ* cancer vaccination. The only other approved *in situ* vaccine is T-VEC (talimogene laherparepvec), the first FDA approved oncolytic virotherapy, discussed below. There are currently several adjuvants in clinical trials for intratumoral

administration, TLR agonists dominate this area. The TLR7/8 agonist imiquimod, for topical treatment of skin carcinomas, is being used in combination with various intratumoral approaches (Green *et al.* 2007; Kidner *et al.* 2012). Poly I:C based formulations are also of interest, such as Poly-ICLC, which mimics viral dsRNA and stimulates TLR3 (Ammi *et al.* 2015; Kyi *et al.* 2016). BO-112 is another synthetic dsRNA, based on poly I:C in clinical trials (Aznar *et al.* 2019). Bacterial LPS and CpG-enriched DNA, targeting TLR4 and TLR9 respectively, have also shown efficient microenvironment activation when administered *in situ* (Maito *et al.* 2012; Hammerich *et al.* 2016; Frank *et al.* 2018). The stimulator of interferon gene (STING) agonists are also gaining significant attention due to their ability to activate APCs and generate cytotoxic and T_H1 T cell responses (Sallets *et al.* 2018). Thus, adjuvanticity is recognised as key to *in situ* vaccination in terms of turning the immunosuppressive microenvironment into an immunologically active one. However, their use as a potentiator in combination with other therapies, maybe be the key to the most effective *in situ* treatments (Aznar *et al.* 2017; Sato-Kaneko *et al.* 2017). The other important aspect of *in situ* vaccination is tumour cell death. It may be achieved through the creation of a pro-inflammatory environment alone, or in combination with classical radio- and chemotherapies. Though these classical cancer therapies are known for their cell-killing ability, they are indiscriminately cytotoxic, meaning they also kill healthy cells, including immune cells. However, designed to be precision tumour cell killers, oncolytic virotherapies are particularly adept as *in situ* therapeutic modalities. I have included them with *in situ* cancer vaccines because they are currently only injected into accessible tumours (Dougan *et al.* 2019) and have an immunogenic component. Although they are often considered a stand-alone therapy.

1.3.4.2. Oncolytic virotherapies

As mentioned, the recently approved *in situ* vaccination oncolytic virotherapy T-VEC, in now in use against melanoma. It is based on an attenuated Herpes simplex virus type 1 (HSV-1), engineered to replicate within tumour cells and synthesise GM-CSF (Rehman *et al.* 2016). HSV-1 neurovirulence and antigen presentation blocking genes have been deleted, preventing blister development and allowing antigen recognition. T-VEC targets and propagates in tumour cells by binding surface nectins to enter the cell.

It preferentially replicates in cancer cells by exploiting dysregulated oncogenic and antiviral signalling pathways. Notably, the protein kinase R (PKR) and type I IFN pathways. The generation of an immune response is also enhanced by the expression of GM-CSF, for the recruitment and activation of DCs (Kohlhapp and Kaufman 2016).

There are several oncolytic viruses in development based on various RNA and DNA viruses, though most are herpesvirus or adenovirus-based (Kaufman *et al.* 2015). In general, oncolytic virotherapies specifically recognise and kill tumour cells, resulting in a mixture of apoptosis, necrosis and phagocytosis, aimed at eradicating the tumour mass. The virus-mediated killing effect is enhanced because the specific tumour cell death also causes the release of tumour-specific antigens derived from those cells. The virus itself introduces MAMPs meaning that the therapy activates both the innate and adaptive immune responses at the site of injection, triggering a cytotoxic effect against tumour cells (Bartlett *et al.* 2013). They can also induce the abscopal effect by subsequent migration of T cells to other tumour sites (Raja *et al.* 2018). There are currently a large number of oncolytic viruses in clinical trials (Harrington *et al.* 2019).

1.3.4.3. Systemic cancer vaccines

The systemic vaccine approach was anticipated to mirror the achievement of conventional vaccinations for infectious disease. However, the development of efficacious cancer vaccines has been extremely challenging. Expectations were that by choosing the right adjuvant and right antigen, cancer vaccines could eradicate cancer in the way that vaccines have done for so many infectious diseases. Initially, cancer vaccines failed to live up to their hype. Many strategies involved single or few antigens in the form of long peptides, or irradiated or lysed tumour cells (Wong *et al.* 2016). In 2011 a paper was published analysing the results of cancer vaccine trials in multiple solid cancers since 2004, they observed an overall objective response rate of 3.7% in 856 patients (Klebanoff *et al.* 2011). These initial setbacks were largely down to difficulties in identifying tumour-specific antigens and effective adjuvants.

Mutations in cancer cell genes can generate neoepitopes, which are mutation-derived peptides that can be bound by MHC molecules. Neoepitopes are tumour-specific antigens, not present in normal cells, that can be presented on MHC molecules, inducing tumour-specific T cells which exert an anti-tumour response (Mumberg *et al.* 1996; Dudley

and Roopenian 1996; Lennerz *et al.* 2005). Along with the progress in next-generation sequencing, vaccines based on cancer neoepitopes formulated with novel adjuvants are showing high efficacy in the preclinical setting. Additionally, clinical trials are showing promising results, particularly in combination with other immunotherapies (Ott *et al.* 2017; Sahin *et al.* 2017). Due to their nature, neoepitopes based cancer vaccines are usually personalised.

Two groups have made key breakthroughs in the personalised neoepitope cancer vaccine field. Sahin and colleagues showed that RNA-based vaccines formulated with neoepitopes identified using *in silico* prediction tools are highly effective in preventing tumour growth in various mouse models (Kreiter *et al.* 2015). This work also highlighted the importance of MHC II epitopes in driving immune responses to cancer. They have now also validated this approach in the first personalised neoepitope vaccine in humans (Sahin *et al.* 2017). In thirteen patients with stage III and IV melanoma, they identified non-synonymous tumour-specific mutations. Then, by predicting high MHC II and I binding affinity and high epitope expression, they selected ten mutations in order to create a personalised RNA neoepitope vaccine for each patient. Vaccination significantly reduced metastatic events in all thirteen patients, resulting in sustained progression-free survival. One patient experienced rapid disease progression following vaccination, but after combination with PD-1 blockade experienced a complete response (Sahin *et al.* 2017).

In the same year, another small clinical trial was published, including six melanoma patients also achieved successful results with neoepitope vaccination. The patients were vaccinated with 13-20 long peptide neoepitopes (15-30 amino acids in length) mixed with poly ICLC adjuvant Hiltonol (TLR3 and melanoma differentiation-associated protein 5 (MDA-5) agonist). This time, neoepitopes were predicted based on their MHC I binding affinities. Despite this prediction method, vaccination-induced neoepitope specific T cells that were $CD8^+$ but mostly $CD4^+$ T cells. After resection and vaccination, stage III melanoma patients remained without disease recurrence for over two years. The two patients with stage IV melanoma experienced lung metastases and recurrent disease after vaccination. However, as in the previous study, they both achieved complete tumour regression after PD-1 immune checkpoint inhibitor therapy (Ott *et al.* 2017).

These two clinical studies demonstrate the safety, feasibility and efficacy of personalised multi-neoepitope cancer vaccination. They also provide strong evidence for the benefit of the combination therapy using neoepitope vaccination and immune checkpoint inhibitors therapies, such as pembrolizumab. These data offer renewed promise for the future of personalised neoepitope cancer vaccination in the clinic.

1.4. Outer membrane vesicles as a vaccine platform

Gram-negative bacteria naturally produce outer membrane vesicles (OMVs). They are derived from budding out of the outer membrane to form a spherical, bilayered, membranous structure of ~20-300 nm in diameter (Grandi et al. 2016). These particles are primarily made up of lipopolysaccharide (LPS), phospholipids and outer membrane and periplasmic proteins. The production of OMVs by gram-negative bacteria is an evolutionarily conserved process, which serves the purpose of performing a multitude of biological functions including; intra- and inter-species communication, biofilm formation, genetic transformation, resistance to environmental stresses and delivery of toxins to host (Kulp and Kuehn 2010; Schwechheimer and Kuehn 2015).

The presence of MAMPs, such as LPS and lipoproteins, confer OMVs with inherent adjuvanticity, giving them great potential as a vaccine platform (Ellis and Kuehn 2010; van der Pol *et al.* 2015). By binding and activating immune cell pattern recognition receptors (PRRs), such as toll-like receptor 4 (TLR4) they can stimulate innate and adaptive immunity (Ellis *et al.* 2010; Moshiri *et al.* 2012; Gerritzen *et al.* 2017). They are readily phagocytosed, able to activate DCs, inducing maturation and the production of pro-inflammatory cytokines (Kaparakis-Liaskos and Ferrero 2015). Studies have shown that OMVs elicit a T_H1 dominant immune response (Kim *et al.* 2013; Fantappiè *et al.* 2014; Rosenthal *et al.* 2014). This is required for the elimination of both pathogens and tumour cells (Rosenthal and Zimmerman 2006). Importantly, we and other groups, have demonstrated that OMVs induce both B and T cell responses specific for the delivered antigens (Alaniz *et al.* 2007; Kim *et al.* 2013; Fantappiè *et al.* 2014; Laughlin *et al.* 2015; Gerritzen *et al.* 2017; Grandi *et al.* 2017, 2018; Irene *et al.* 2019)

OMVs can be used to display and deliver heterologous antigens by adsorption or genetic engineering of the OMV producing strain. Engineered protein antigens can co-localise in the lumen or on the surface of the OMV (Kesty and Kuehn 2004; Chen *et al.* 2010; Fantappiè *et al.* 2014). We have shown that heterologous lipoproteins can be incorporated into the OMV membrane and that is possible to deliver heterologous antigens as fusion proteins to the OMV surface (Fantappiè *et al.* 2017; Grandi *et al.* 2017, 2018; Irene *et al.* 2019).

The concept of using OMV-based vaccines against infectious pathogens has been around for a long time. OMV-based vaccines against *Neisseria meningitidis* serogroup B

have been successfully used in the clinic for over 20 years (Sierra *et al.* 1991; Rosenqvist *et al.* 1995; Arnold *et al.* 2011). The OMV-based vaccine Bexsero has been approved by the EMA and FDA, among others, to prevent *N. meningitidis* serogroup B infections (Giuliani *et al.* 2006; Serruto *et al.* 2012). This demonstrates both the safety and efficacy of OMV vaccines.

Recently, OMV-based vaccines have gained in popularity for use against infectious diseases. Initiatives such as the Vacc-iNTS project help launch phase I clinical trials of an OMV-based vaccine against invasive non-typhoidal salmonellosis disease (https://vacc-ints.eu/). In addition, an OMV-based vaccine against *Shigella sonnei*, for the prevention of the diarrheal disease shigellosis, demonstrated good safety and immunogenicity profiles in early phase clinical trials (NCT03527173) (Obiero *et al.* 2017; Launay *et al.* 2019). However, the use of OMV-based vaccines in cancer therapy is still in its infancy (Zhang *et al.* 2019). This is because a successful cancer vaccine requires three essential components that must be carefully balanced: the right adjuvant, the right tumour antigens and effective delivery. The wrong type or amount of any of these components could lead to an ineffective immune response or even cause immune evasion.

In our laboratories, we have been fine-tuning the characteristics of our OMVs. The hypervesiculating *Escherichia coli* (*E.coli*) strain BL21(DE3)Δ*ompA* is used as a progenitor strain, our starting point. This mutant strain derives from the *E. coli* BL21(DE3) strain carrying a deletion in the *ompA* gene, causing subsequent loss of the transmembrane outer membrane protein A (OmpA). OmpA plays a key role in anchoring the outer membrane to the bacterial peptidoglycan and loss of this interaction causes the hypervesiculating phenotype (Bernadac *et al.* 1998; Deatherage *et al.* 2009; Park *et al.* 2012). We call these $OMVs_{\Delta ompA}$.

In order to refine our OMV platform, our group has been working to reduce the number of endogenous protein in $OMVs_{\Delta ompA}$ and reduce the reactogenicity. Reduction in endogenous protein load was achieved by the identification and subsequent deletion of “dispensable” genes potentially coding for immunogenic OMV proteins. This was done using an in house validated CRISPR/Cas9 knockout protocol (Zerbini *et al.* 2017). The procedure led to the successful knockout of 58 genes and importantly, their encoded proteins and the strain was named *E. coli* BL21(DE3)Δ*58* (Zanella 2019). OMVs

from this strain (called $OMVs_{\Delta 58}$) allow us to reduce the burden of immunity not specific for our antigen of interest. As previously stated, OMVs have intrinsic adjuvanticity due to the presence of several MAMPs. LPS represents a large portion of OMVs (Park *et al.* 2010) and is a ligand for TLR4. Stimulation of TLR4 leads to the cytokine production responsible for OMV adjuvanticity. However, it is also responsible for OMV reactogenicity, which may cause adverse reactions to vaccines. Therefore, the reactogenicity must be moderated for clinical use. In *E. coli*, the lipid A portion of LPS is naturally present in the hexa-acylated form. However, it has been shown that penta-acylated LPS has reduced agonistic activity on TLR4 and thus reduces reactogenicity (Steeghs *et al.* 2008). Deletions of *msbB* and *pagP*, acyl-transferase genes of the LPS biosynthesis pathway, have been shown to produce LPS containing penta-acylated lipid A (Somerville *et al.* 1996; Bishop *et al.* 2000; Irene *et al.* 2019). By including the inactivation of these two genes to our strain, we developed the *E. coli* BL21(DE3)Δ*60* strain, to give us proteome-minimised, reactogenicity-minimised OMVs, called $OMVs_{\Delta 60}$ hereafter (Zanella *et al.* 2020).

Hypervesiculating strains such as *E. coli* BL21(DE3)Δ*ompA*, and *E. coli* BL21(DE3)Δ*60* even more so, allow for simple purification of high yields of OMVs from bacterial cultures (Deatherage *et al.* 2009; Fantappiè *et al.* 2014, 2017; Gerritzen *et al.* 2017; Zanella *et al.* 2020). The supernatant is easily separated from the biomass by centrifugation, then vesicles can be purified using tangential flow filtration, potentially achieving yields of 100 mg of OMVs per litre of culture (Berlanda Scorza *et al.* 2012). These features make our OMVs good potential vaccine tool.

1.5. Aim of the thesis

In the laboratory of synthetic and structural vaccinology, we study the use of OMVs as a vaccine platform, focusing on infectious disease and cancer vaccines. Here I investigate the use of OMVs for antigen delivery and presentation. I aim to discover the most efficacious approaches to cancer vaccination using the OMV platform.

As discussed previously, DCs play a key role in determining the effectiveness of an anti-cancer immune response. To optimally exert their function, they should (1) avidly bind the antigen, (2) efficiently process the antigen and present antigen derived peptides in the context of MHC molecules, and (3) rapidly reach the site where their action is needed.

The aim of my thesis is to understand how we can best use our OMV platform by trying to optimise each of the three steps described above. Therefore, I aim to:

1. Understand whether it is possible to engineer OMV to express an antibody derived single-chain fragment variable (scFv) on the surface enabling OMV targeting to the DEC205 receptor on dendritic cells (optimisation of antigen binding)
    a. Develop constructs with carrier proteins fused to the scFv to enable scFv expression in OMV.
    b. Characterise the expression of protein carrier-scFv fusion proteins in OMVs.
    c. Understand whether the FhuD2-αmDEC205 fusion protein is functional when expressed on OMVs and whether it can improve the efficacy of OMVs over those not targeting mDEC205.
2. Study the ability of OMVs to induce $CD8^+$ T cell responses *in vivo* (optimisation of presentation of antigen-derived peptides)
    a. Using model $CD8^+$ T cell epitopes, immunise mice with OMV-associated epitopes and measure the $CD8^+$ T cell response.
    b. By studying long and short peptides encompassing $CD8^+$ T cell epitopes, understand how the peptide processing and presentation may affect the immune response.

3. Investigation the use of OMVs *in situ* cancer vaccination using mouse models (optimisation of DC recruitment)
    a. Demonstrate *in situ* adjuvanticity and cancer cell cytotoxicity of OMVs.
    b. Study tumour growth after *in situ* vaccination with OMVs.

Chapter 2: Targeting OMVs to dendritic cells using single-chain variable fragments

2.1. Introduction

Advances in DC biology have led to improvements in strategies for vaccine development, such as specific DC targeting (Apostolopoulos *et al.* 2013; Macri *et al.* 2016). In particular, methods using antigens bound to antibodies have been used to target the antigen to a DC receptor for internalisation, processing and presentation. Antigens have been delivered to MHC molecules via targeting various DC receptors, mostly C-type lectins (CLRs) such as DEC205 and Clec9A, and Fc receptors. Many vaccines rely on humoral immunity, thus their effectiveness measured by antibody titres. However, effective cancer vaccines also require an effective T cell response, achieving which can be challenging. Given that CLRs are expressed diversely on DC subsets, targeting antigens to DC receptors is a way to guide the immune response toward a particular type of T cell response. Choosing the right target is challenging because there is still conflicting evidence as to which receptor allows the enhanced antigen presentation on MHC I or MHC II. For my PhD project, I have chosen to focus on DEC205 because it is a well characterised CLR, there is evidence for DEC205 targeting to MHC I for cross-presentation and there is an anti-mouse DEC205 antibody sequence available.

DEC205 is a type I endocytic CLR, with a molecular weight of 205 kDa, characterised by a cysteine-rich domain, fibronectin type-II domain and ten carbohydrate recognition domains (CRDs) (Jiang *et al.* 1995). Due to its expression in DCs, particularly $CD8^+$ DCs, DEC205-specific antibodies have been studied in order to target antigens for processing and improved presentation, and to elicit a better antigen-specific T cell response. A number of antigens have been tested in this way, e.g. ovalbumin, and HIV gag p24, among others. It has been demonstrated that vaccination by using antigen targeting via DEC205 increases the efficiency of T cell immunity (Bonifaz *et al.* 2004).

The function of DEC205 seems to involve binding necrotic cells for cross-presentation of debris-associate antigens (Shrimpton *et al.* 2009). It can also bind and uptake CpG oligonucleotides, which are ligands for TLR9 (Lahoud *et al.* 2012).

The induction of a robust MHC-I cross-presentation and OVA-specific $CD8^+$ T cell has been demonstrated by using ovalbumin (OVA) conjugated DEC205 antibodies to target mouse $CD8^+$ DCs (Bonifaz *et al.* 2002, 2004). In mice, injection of OVA-conjugated DEC205 antibodies alongside an adjuvant, induced proliferation and accumulation of OVA-specific naive $CD8^+$ and $CD4^+$ T cells, causing differentiation into effector T cells (Bonifaz *et al.* 2002, 2004). They found OVA-conjugated DEC205 antibodies produced much stronger immunity than soluble OVA at 1000-times higher doses. Prolonged antigen presentation by MHC-I, but not by MHC-II molecules was also observed (Bonifaz *et al.* 2004). Adjuvant administration in tandem with antigen-conjugated anti-DEC205 antibodies is necessary to induce a robust T cell immune response. In the absence of an adjuvant, DEC205 on immature DCs are targeted leading to T-cell tolerance (Petzold *et al.* 2012). A few hours after subcutaneous injection, antigens are detected at the surface of $CD8^+$ DCs in both lymph nodes and spleens, causing systemic antigen presentation by MHC-I and MHC-II molecules (Bonifaz et al. 2004).

There is also evidence that targeting DEC205 in humans, elicits a robust activation of T cells. *Ex vivo* human monocyte-derived DCs (moDCs) stimulated with anti-DEC205 antibodies conjugated to the human immunodeficiency virus (HIV) gag protein p24 potently induce $CD8^+$ T-cell proliferation and interferon-γ secretion (Bozzacco *et al.* 2007). Additionally, when incubated with moDCs, anti-DEC205 single-chain fragment fused to melanoma-associated antigen 3 (MAGEA3) caused increased secretion of IL-2 by antigen-specific $CD4^+$ T cells compared with antigen-electroporated or peptide-pulsed moDCs (Birkholz *et al.* 2010). In contrast to NY-ESO-1 antigen alone, NY-ESO-1 conjugated anti-DEC205 antibodies promote $CD8^+$ T cell activation (Tsuji *et al.* 2011). Moreover, the first phase I clinical trial of a protein vaccine targeting DCs, showed treatment of cancer patients with cutaneously administered NY-ESO-1 fused to anti-DEC205 with resiquimod and/or poly-ICLC induced antigen-specific antibodies and T cells, leading to a partial clinical response without toxicity (Dhodapkar *et al.* 2014).

A number of antigens have also been targeted to DEC205 using single-chain variable fragments (scFv) derived from antibodies. Demangel et al. demonstrated the

enhanced generation of effector T_H1 cells specific for Ag85B (a *Mycobacterium tuberculosis* antigen) by pDNA vaccination of the antigen fused to the DEC205-scFv (Demangel *et al.* 2005). Another DNA vaccine, encoding the heavy-chain domain of Botulinum neurotoxin serotype A fused to an anti-DEC205 scFv generated stronger humoral and T cell proliferative responses (Chen *et al.* 2017b). Another fusion, targeting the *Toxoplasma gondii* surface antigen SAG1 to DEC205 improved local and systemic humoral and cellular immune responses (Lakhrif *et al.* 2018). Recently, Ngu et al found that DC targeting of ovalbumin (OVA) antigen using recombinant DEC205 specific scFv-OVA induced a much higher antigen uptake and presentation to both $CD8^+$ and $CD4^+$ T cells compared to soluble OVA. They also found that vaccinating with DEC205 specific scFv-gag with poly ICLC, they induced strong and long-lasting specific $CD4^+$ T cells against HIV-gag p24 (Ngu *et al.* 2019).

Single-chain variable fragments (scFv) are derived from the variable region of IgG antibodies. Antibodies are used for tumour targeting and immune checkpoint targeting cancer therapies. However, they are not limited to this indication alone. Numerous mAbs are approved for multiple disease indications, such as autoimmune and cardiovascular diseases to name a couple. Not only are they used therapeutically, but they are also valuable research tools due to their specificity and diversity. The structure of an antibody is modular in nature, as shown in figure 8. The variable region is made up of fragments of the variable light chain and the variable heavy chain regions. A flexible glycine- and serine-rich linker can be used to link these two domains to create a scFv. The variable region is important because the antigen-binding specificity of an antibody is located here. There are three complimentary-determining regions (CDRs) in each VL and VH domain. The sequence variability in these regions allows diverse binding specificities (Holliger and Hudson 2005).

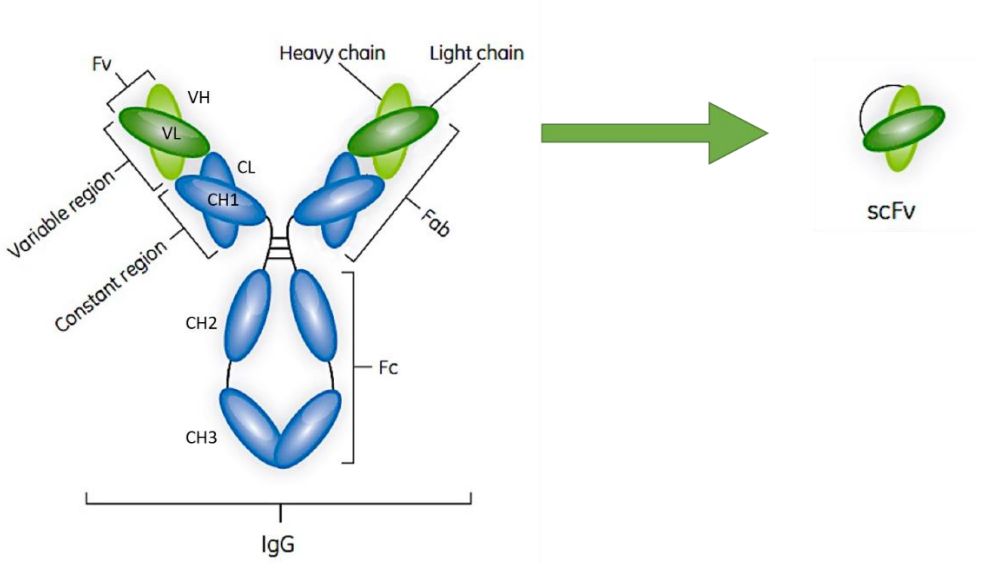

Figure 8: Classical antibody structure and scFv structure*. Antibody tools and therapeutic entities are generally based on immunoglobulin G (IgG). A classical antibody consists of two heavy and two light chains, held together by disulphide bonds, in a "Y" structure. The variable regions are responsible for the creation of the binding regions. The single-chain variable fragment (scFv) is made up of the variable heavy chain domain linked to the variable light chain domain. Image adapted from Rodrigo et al. 2015 (Rodrigo et al. 2015)*

Bird et al. first described the scFv in 1988 (Bird *et al.* 1988). These fragments have since gained popularity as a tool and well as a therapeutic entity for many reasons. Firstly, their small size of approximately 25 kDa makes them a better candidate for production in microbial systems in contrast to full-size antibodies (Holliger and Hudson 2005). Secondly, placing the VH and VL regions on a single chain allows the scFv to be expressed from a single transcript, conversely to the required expression of both the heavy and light chains of antibodies, usually in mammalian expression systems. Thirdly, they generally have better tissue penetration that full antibodies. Finally, not only are they used in many chimeric formats, but they are the binding module of CAR-T cells. For example, the CD19 binding specificity of Kymriah and Yescarta is due to the chimeric antigen receptor containing an anti-CD19 scFv (Makita *et al.* 2017).

Importantly, *E. coli* has been used for the production of soluble scFv (Miller *et al.* 2005; Gaciarz *et al.* 2016). As well as *E.coli* surface display of scFv for screening antibody libraries (Francisco *et al.* 1993; Daugherty *et al.* 1999). There is also evidence that some scFvs can be enriched in OMVs when fused to pore-forming toxin ClyA or lipoprotein SlyB (Kim *et al.* 2008b; Chen *et al.* 2017a). Specifically, fusion of a digoxin specific scFv to ClyA allowed functional display of the scFv on the OMV surface (Kim *et al.* 2008b). Considering these pieces of evidence, I believed there is potential for the expression of

scFv on the surface of our OMVs. In fact, in our laboratory we successfully engineered OMVs with carrier proteins to allow the expression of polypeptide antigens (Grandi *et al.* 2017, 2018)

With the aim of developing a novel carrier enabling OMV surface expression of scFvs, I studied a number of strategies for scFv expression in OMVs. I investigated the expression of anti-DEC205 scFv to enable targeting of OMVs to the DEC205 receptor with the final aim of improving OMV delivery of antigens to DC and antigen cross-presentation, thus improving vaccine efficiency.

2.2. Results

2.2.1. The hunt for a novel carrier of scFv for surface expression in OMVs

The aim of this part of my PhD project was engineer OMVs with DEC205 scFv. This required the fusion of the scFv to a carrier protein in order to allow expression of the scFv on the surface of our bacterial OMVs. This challenge requires the fusion protein to cross the inner membrane, attach to the outer membrane, and be surface exposed, rather than facing into the periplasm. Subsequently, the scFv must also be present on the shed OMV surface. For the development of the scFv fusion proteins, extensive cloning, using techniques such as the polymerase incomplete primer extension (PIPE) method were employed. The characterisation was analysed by assessing protein expression in bacteria lysates and OMVs using SDS-PAGE.

The anti-mouse DEC205 scFv sequence was taken from antibody NLDC-145 (Inaba *et al.* 1995; Demangel *et al.* 2005). The scFv was cloned using a DNA string that was codon optimised for expression in *E. coli*. The amino acid sequence of the VH and VL were linked together with a 15-residue standard linker $(G_4S)_3$ (Huston *et al.* 1988). The expression of the scFv fusion protein was verified by SDS-PAGE analysis of whole bacteria cells and OMVs.

In addition to the challenge of crossing the inner membrane and periplasm of gram-negative bacteria to be enriched in OMVs. The expression of scFv in OMVs is complex because scFv are themselves a truncated fusion protein of a mammalian antibody. Therefore, scFvs do not occur in nature and are not naturally expressed in bacteria. It is well known that scFv can be expressed in *E.coli* in soluble form (Miller *et al.* 2005; Kim *et al.* 2008a; Wang *et al.* 2013; Vaks and Benhar 2014; Gaciarz *et al.* 2016). There are also examples of scFv expression and anchoring on the *E. coli* surface (Francisco *et al.* 1993; Velga *et al.* 1999; Daugherty *et al.* 1999). Yet, there is only one example of scFv surface expression in OMVs, using the *E. coli* cytotoxin ClyA (Kim *et al.* 2008b).

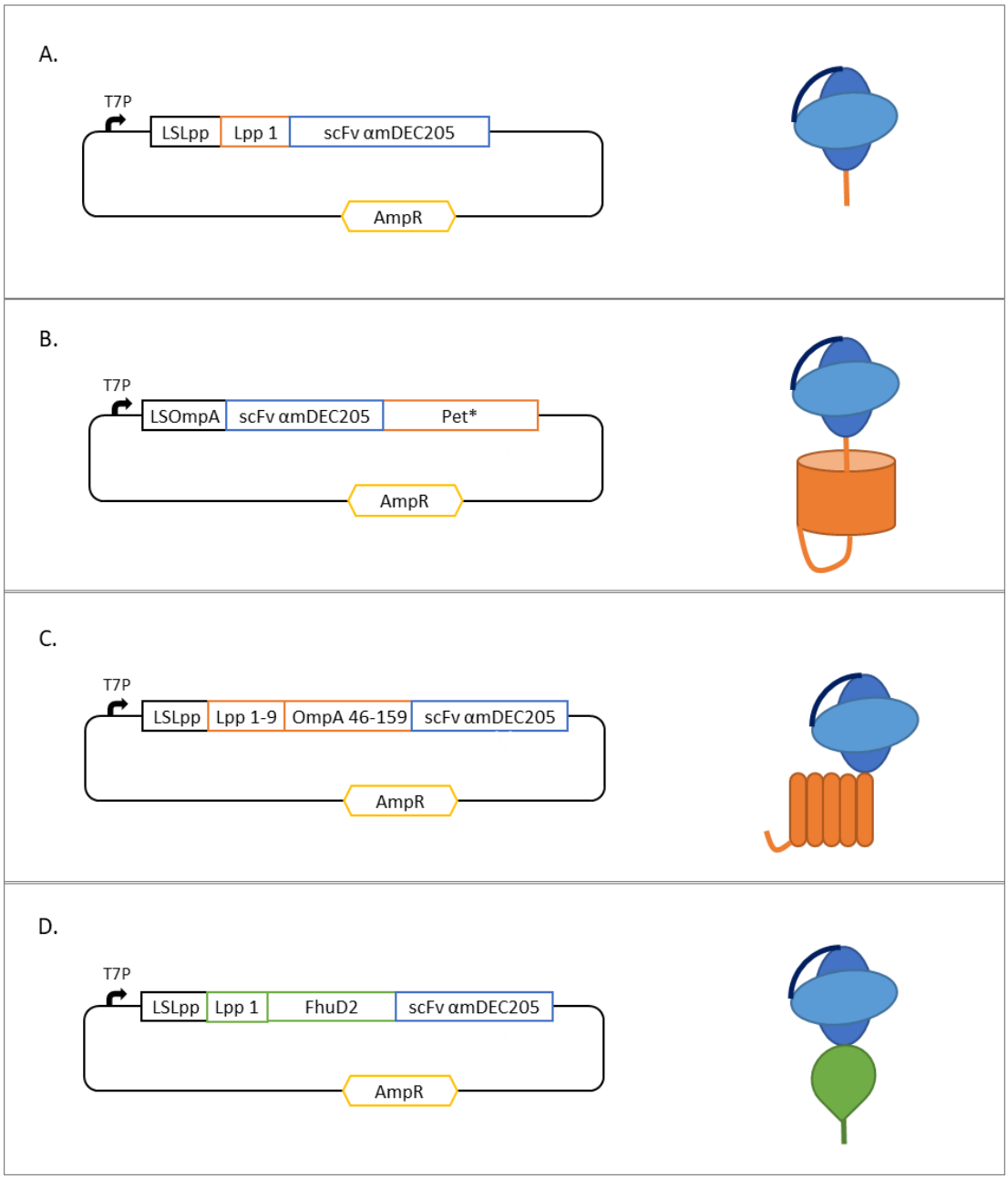

Figure 9: Schematic representation of plasmids contain fusion constructs and fusion protein structure. *A, shows the Lpp leader sequence (LSLpp) and the first amino acid of lpp (Lpp1) fused to the scFv for anti-mouse DEC205. B, shows the ompA leader sequence (LSompA) fused to the scFv sequence in the position of the passenger domain, fused to the autochaperone region and β-barrel, pet* protein. C, Depicts the LSLpp, fused to the first 9 amino acids of Lpp, then truncated ompA (TompA), containing transmembrane regions 3-7, fused to the scFv. D, Shows the Lpp leader sequence and first amino acid (allowing lipidation), fused to FhuD2, then the scFv.*

Initially, four distinct methods for cloning and expression of the scFv in OMVs were attempted, as described below. The fusion protein expression was analysed as follows: the BL21(DE3)Δ*ompA* strains containing each single fusion construct were grown at 30°C to an OD_{600} of 0.4-0.6. The expression of the fusion proteins was induced by addition of 0.1 mM of isopropyl-ß-D-1-thiogalactopyranoside (IPTG). At harvest, 1 ml

of cells were collected for lysate analysis, the rest were pelleted and OMVs purified as specified in materials and methods section. Finally, to assess the presence of the fusion proteins, lysates were separated by SDS-PAGE. When the fusion protein was present in the lysates, the OMVs were also analysed by SDS-PAGE.

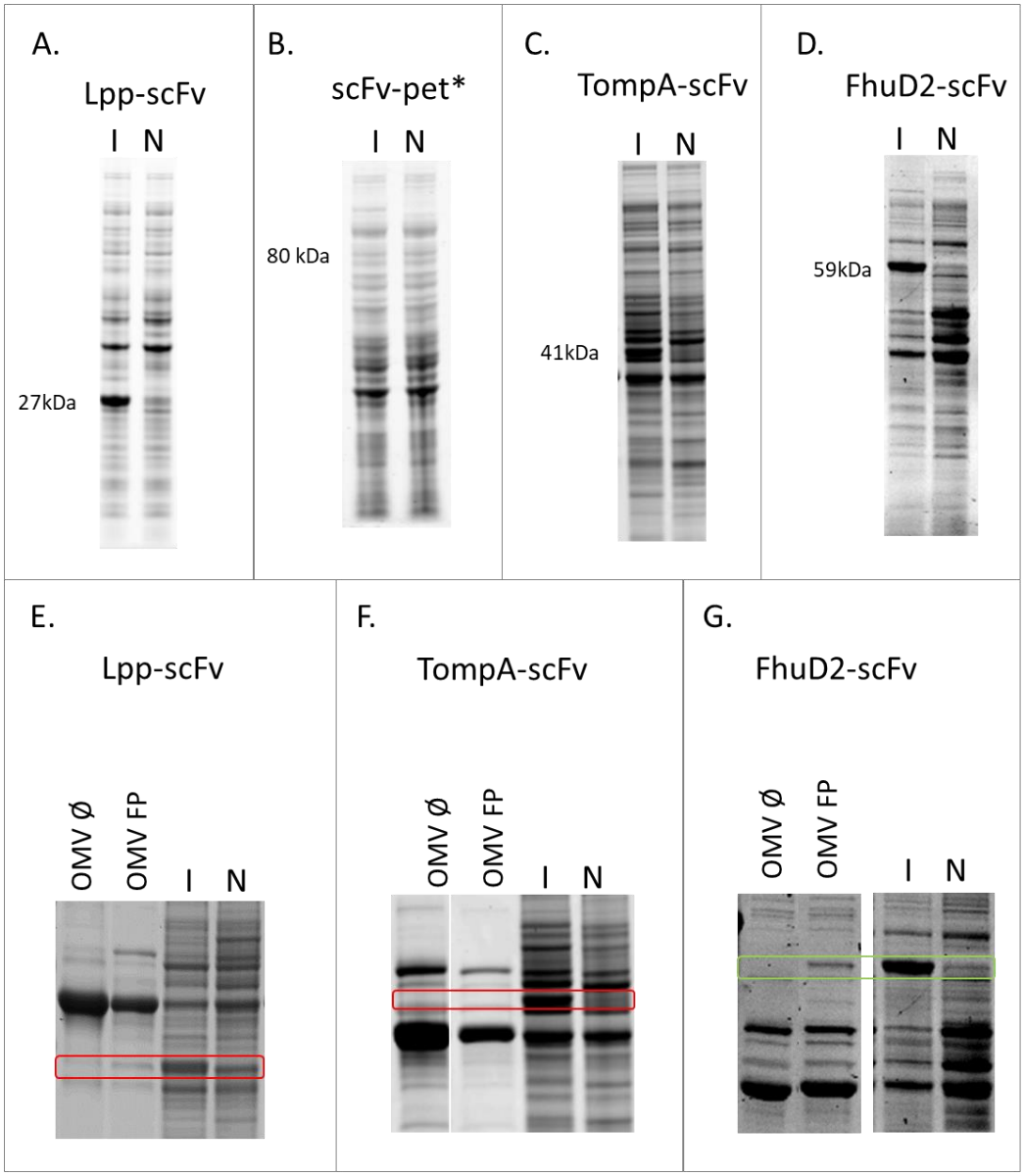

Figure 10: SDS-PAGE of lysates and OMVs from BL21(DE3)ΔompA expressing with fusion proteins. *A, Shows SDS-PAGE of lysates from BL21(DE3)ΔompA-lpp-scFv. The first lane show the separation of lysates from bacteria with expression induced (I). The second lane is the control, containing lysates from the same strain with the lpp-scFv construct not induced (N). The induced sample lane shows a band at 27kDa, corresponding to the size of the lpp-scFv fusion protein, it is not present in the not induced sample. B, Lysates from BL21(DE3)ΔompA-scFv-pet*, with expression induced (I) and not induced (N), no band observed at the expected molecular weight of 80 kDa. C, Lysates from BL21(DE3)ΔompA-lpp-TompA-scFv, with expression induced (I) and not induced (N), induced lane shows band at 41 kDa, corresponding to the size of the lpp-TompA-scFv fusion protein. D, Lysates from BL21(DE3)ΔompA-FhuD2-scFv, with expression induced (I) and not induced (N) induced lane shows a band at 59 kDa, corresponding to the size of the FhuD2-scFv fusion protein. E, SDS-PAGE of lysates and OMVs from BL21(DE3)ΔompA-lpp-scFv, OMV Ø denote empty OMVs (with a pET plasmid, without an engineered fusion protein construct), OMV FP is the lane with OMVs induced to express the fusion protein (FP). Again a band is observed in the induced bacteria lysates, but it is not enriched in OMVs. F, Lysate and OMVs from lpp-TompA-scFv, again induced lysate confirms expression of lpp-TompA-scFv in whole bacteria, but there is no corresponding band in the OMVs. G, Induced bacteria show a band in the lysates, there is a band in the corresponding OMVs with the same molecular weight, showing FhuD2 is expressed in OMVs.*

The first approach involved lipidation of the scFv by fusion to the lpp leader sequence and the cysteine residue of the lipobox (Cowles *et al.* 2011), plasmid map and schematic structure are shown in figure 9A. We have already shown that this is an effective method for delivery of heterologous bacterial proteins to the outer membrane and that some of these lipidated proteins have good OMV surface expression (Fantappiè *et al.* 2017; Irene *et al.* 2019). Using this method for this scFv fusion I was able to express the lipidated scFv in BL21(DE3)Δ*ompA* bacteria. Figure 10A shows the expression of lpp-scFv in the bacteria lysates, with a thick band at 27 kDa, corresponding to the molecular weight of the lpp-scFv fusion protein, not present in the control lane (N). However, I did not observe enrichment of lpp-scFv in OMVs from the same strain, as shown in figure 10E. Though there seems to be a faint band in OMVs, it is also present in all control empty OMVs.

The second method involved the fusion of the scFv to the β-barrel autotransporter protein, demonstrated for use in the extracellular expression of recombinant proteins (Sevastsyanovich *et al.* 2012). I used pet carrying a mutation at position 1081 (pet*) preventing cleavage of the passenger protein. The pet* β-barrel autotransporter contains an autochaperone region required to transport the fused protein though the pore created by the β-barrel and to the cell surface. This method involved N-terminal, rather than C-terminal, fusion of the scFv to the autochaperone region. This fusion protein has an estimated molecular weight of 80 kDa. It involved the scFv being transported through the pore to allow surface exposition (see figure 9B). Though I was able to express the pet* alone in bacteria (data not shown), I did not observe expression of the scFv-pet* fusion protein in our BL21(DE3)Δ*ompA* strain, as shown in figure 10B.

The third method involved the use of a truncated ompA fusion protein, commonly used for *E. coli* surface display and affinity maturation of scFv antibody libraries. The fusion protein was designed according to lpp'ompA$_{46\text{-}159}$ described by Stathopoulos et al (Stathopoulos *et al.* 1996), where the lipobox and first 9 amino acids of lpp were fused to a truncated ompA$_{46\text{-}159}$ then fused to the scFv, with expected molecular weight 41 kDa (Figure 9C). The truncated ompA$_{46\text{-}159}$ codes for the expression of transmembrane domains 3, 4, 5, 6 and 7, leaving out 1, 2 and 8. This fusion protein has been shown to display scFv on the *E. coli* cell surface (Francisco *et al.* 1993). While I

detected expression in the BL21(DE3)Δ*ompA* lysates, it was not enriched in OMVs, see figure 10C & 10F.

Finally, FhuD2, a ferrichrome-binding protein native to *Staphylococcus aureus*, was used for scFv fusion (Figure 9D). In our laboratory, we have already demonstrated that lipidated FhuD2 compartmentalises in OMV with high efficiency and is also surface exposed (Irene *et al.* 2019). We have also successfully engineered OMVs using lipidated FhuD2 as a carrier for a polypeptide B cell epitope. Demonstrating that FhuD2 is a good OMV surface carrier for polypeptides (Grandi *et al.* 2018). When the lipidated FhuD2 was used as a carrier and fused with the scFv, a good expression level was achieved both in BL21(DE3)Δ*ompA* whole bacteria and also enriched in OMVs from this strain, as demonstrated by bands corresponding to FhuD2-scFv at 59 kDa in figures 10D & 10G. The expression of the FhuD2-scFv fusion in BL21(DE3)Δ*ompA* derived OMVs was confirmed by western blot analysis using anti-FhuD2 antibodies as shown in figure 11A.

2.2.2. Expression of FhuD2-scFv-αmDEC205 in BL21(DE3)Δ*60* derived OMVs

Our laboratory recently produced a novel bacterial strain, named BL21(DE3)Δ*60*, for the production of OMVs for use as a vaccine platform. This novel strain has an improved OMV production capacity over BL21(DE3)Δ*ompA* and importantly, improved cell surface expression of heterologous antigens. Therefore, I decided to investigate whether I could improve the expression of the FhuD2-scFv fusion protein in OMVs by using this strain.

I transformed the FhuD2-αmDEC205 fusion plasmid to the new strain and produced OMVs (see materials and methods). I then analysed the FhuD2-αmDEC205 fusion protein expression in OMVs. First by SDS-PAGE as in figure 11B, then by western blot using the anti-FhuD2 antibody (Figure 11C).

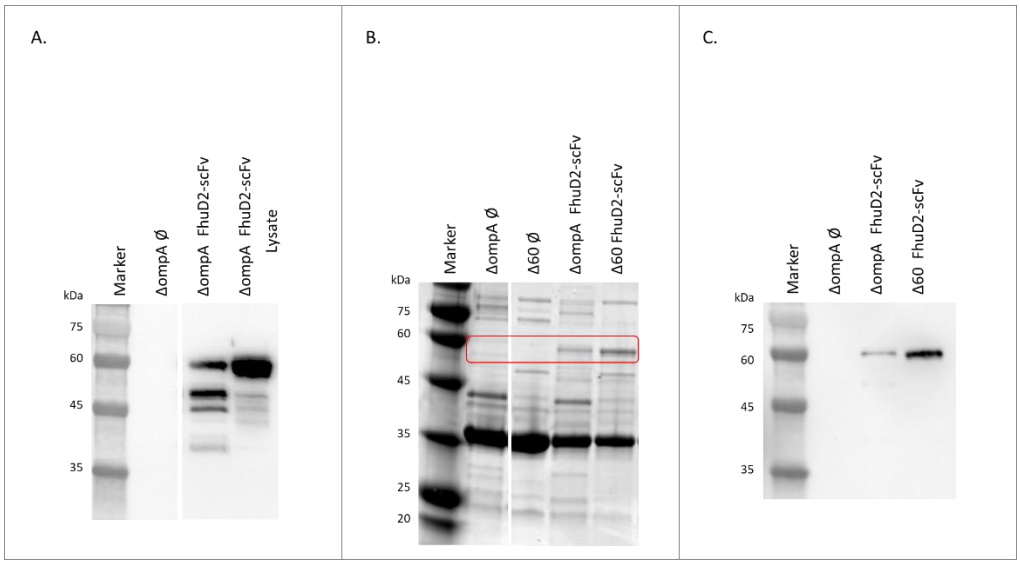

Figure 11: The expression of FhuD2 in OMVs. *A, Western blot confirming expression of the FhuD2-αmDEC205 in OMVs derived from the BL21 (DE3)ΔompA strain. B, SDS-PAGE comparing the expression of the FhuD2-scFv fusion protein in BL21 (DE3)ΔompA and BL21 (DE3)Δ60 derived OMVs. C, Western blot confirming the expression of FhuD2-αmDEC205 fusion in both $OMVs_{\Delta ompA}$ and $OMVs_{\Delta 60}$. These data show that the FhuD2-αmDEC205 fusion protein is better expressed in the $OMVs_{\Delta 60}$ compared with the $OMVs_{ompA}$.*

2.1.2.1. OMV membrane localisation of FhuD2-scFv-αmDEC205 in $OMVs_{\Delta 60}$

To analyse the fusion protein localisation in OMV I performed a phase partitioning experiment. OMVs were solubilised in a 1% solution of Triton X-114, a non-ionic detergent, in order to separate the membranous “hydrophobic” phase from the aqueous “hydrophilic” phase. Once the detergent phase and the aqueous phase were divided, they were analysed by SDS-PAGE and subsequent western blotting using anti-FhuD2 for FhuD2-αmDEC205 detection (Figure 12).

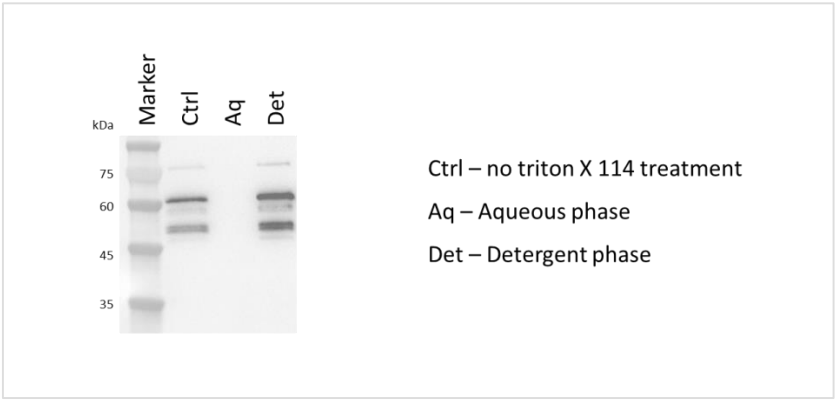

Figure 12: Western blot of triton X-114 – phase partitioned OMVs. *After solubilisation in Triton X-114, the OMV contents and membrane divide into either the detergent phase (membranous/lipid phase) or the aqueous phase. Each phase is run on SDS-PAGE alongside the total (non-partitioned) OMV control. Western blot using the anti-FhuD2 antibody detection shows that the FhuD2-αmDEC205 fusion protein is detected in the detergent phase showing it is membrane-bound.*

The fusion proteins co-localised in the detergent phase demonstrating that it is present in the membrane of OMVs. Whereas co-localisation to the aqueous phase would demonstrate presence in the OMV lumen. The use of OMVs derived from BL21(DE3)Δ*60* means that luminal proteins such as MBP have been deleted. We usually use MBP as a control for the presence of proteins in the aqueous phase. Since I could not use our MBP control for the aqueous phase, I simply checked the protein gel using UV-trans luminescence prior to western blotting, I observed the presence of some proteins in the aqueous phase, but no band corresponding to the fusion protein. This confirmed that the fusion protein is not expressed in the lumen.

2.1.2.2. Cell surface expression of FhuD2-scFv-αmDEC205 is greatly improved in the BL21(DE3)Δ*60 strain*

Flow cytometry of bacteria expressing FhuD2-αmDEC205 was used to analyse the cell surface expression of the FhuD2-αmDEC205 fusion protein in both BL21(DE3)Δ*ompA* and BL21(DE3)Δ*60* strains. The surface expression on BL21(DE3)Δ*60* bacteria is greatly improved over BL21(DE3)Δ*ompA* FhuD2-αmDEC205 expression, as seen across separate experiments. Bacteria were grown at 37°C, 200 rpm and induced (or not induced) with 0.1 mM IPTG when OD_{600} reached 0.4-0.6. They were harvested 2 hours after induction for staining. Cell stained with anti-FhuD2 as specified in material and methods, and analysed by flow cytometry. Cells positive for the FhuD2-αmDEC205 fusion were detected in the FITC channel.

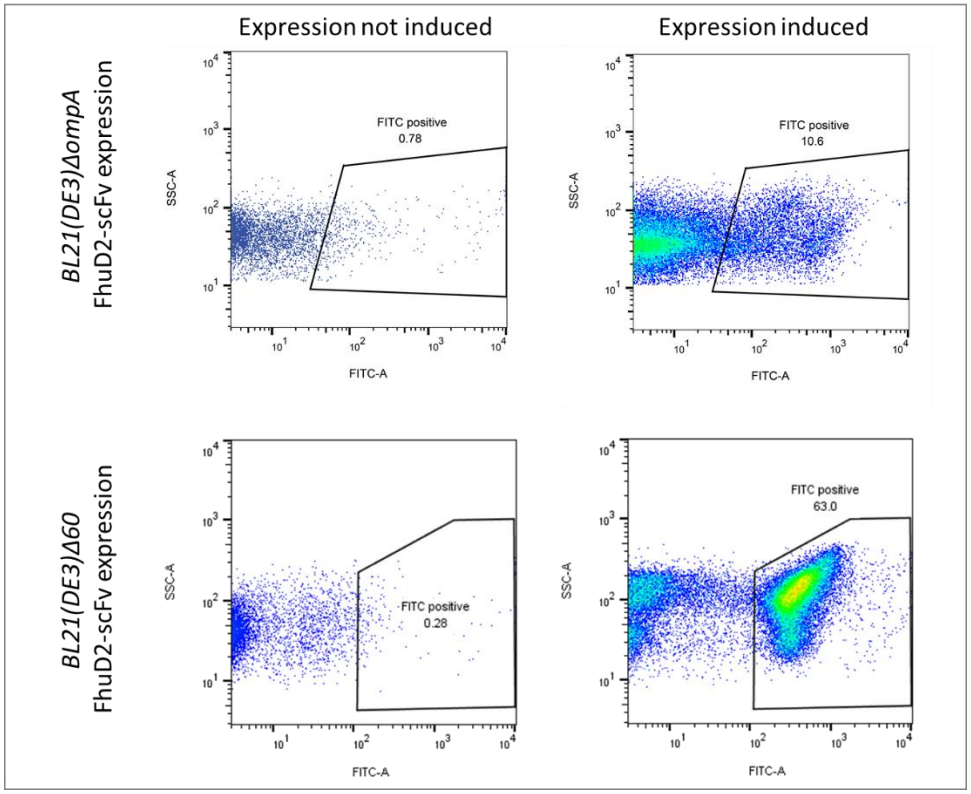

Figure 13: FhuD2-scFv is surface exposed in bacteria. *Flow cytometry analysis of BL21(DE3)ΔompA and BL21(DE3)Δ60 with and without induced expression of the FhuD2-αmDEC205 fusion protein. All cells were stained with anti-FhuD2 and secondary antibody anti-rabbit Alexa Fluor-488. The non-induced stained shows non-specific binding of the antibodies. The binding on induced cells shows the specific binding to FhuD2-αmDEC205.*

In figure 13 we observe that on BL21(DE3)Δ*ompA* FhuD2-αmDEC205 induced cells, I detected an increase of 10% in the population of cells positive for the fusion protein. When expression was induced in BL21(DE3)Δ*60*, there was 63% positive population staining for surface expression of the fusion protein. Given the surface expression on whole bacterial cells, I hypothesised that the fusion protein would also be surface exposed at the membrane of OMVs.

2.2.3. FhuD2 as a carrier for other scFv

To investigate whether FhuD2 could support the expression and surface localisation of other scFvs, two more scFv were cloned into the FhuD2 containing plasmid for expression of FhuD2-scFv fusions. The scFv named αHELD1.3 is a sequence derived from the antibody HELD1.3 (Ward *et al.* 1989; Souchon *et al.* 1990; Boulot *et al.* 1990), it is specific for hen egg lysozyme and thus can be used as a negative control. The other scFv is derived from the antibody FGK45 and is specific for mCD40 (Rolink *et al.* 1996; Szekeres *et al.* 2011).

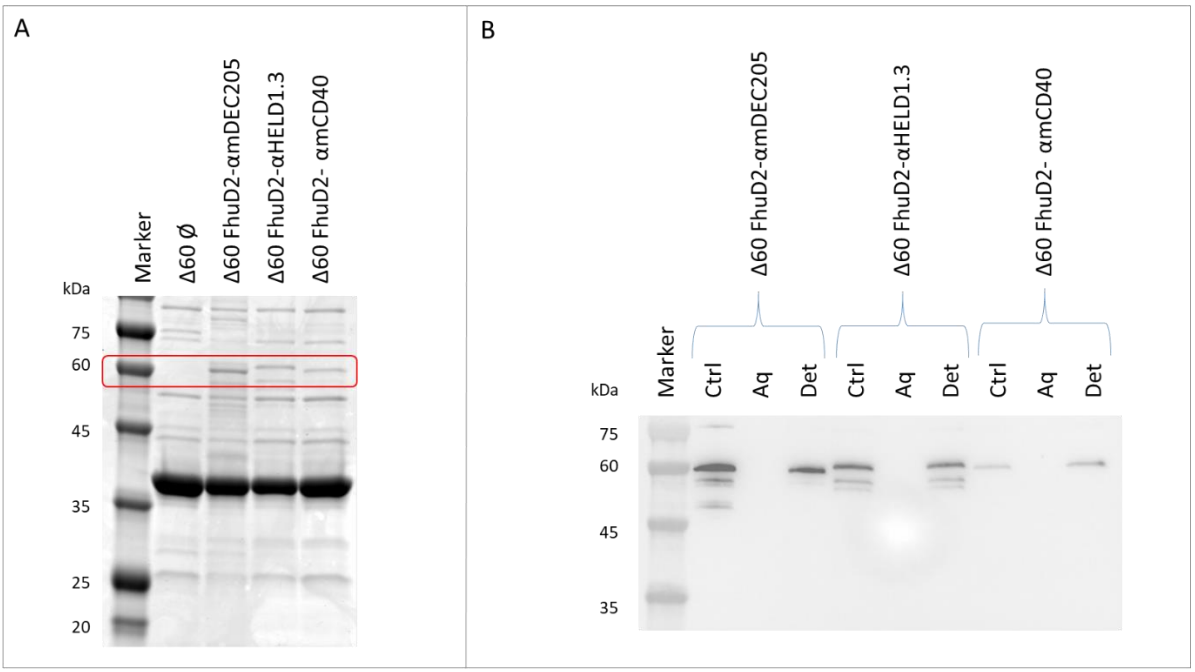

Figure 14: The expression and membrane localisation of three different FhuD2-scFv in OMVs. *A, SDS-PAGE confirming expression of all three FhuD2-scFvs in OMVs derived from the BL21(DE3)Δ60 strain. B, Western blot of phase partitioned OMVs confirming the expression of each FhuD2-scFv fusion protein in the OMV membrane. Ctrl, OMVs not partitioned. Aq, protein from the aqueous phase. Det, proteins from the detergent (membranous) phase.*

I analysed the expression of the FhuD2-scFv fusion proteins in OMVs by SDS-PAGE (see Figure 14A). Bands at approximately 60 kDa correlate to expression of the FhuD2-scFv fusion protein expression. All three sets of OMVs expressing each FhuD2-scFv fusion protein were subsequently phase partitioned in order to assess the membrane localisation of the fusion protein. By western blot I demonstrated the colocalisation of the fusion proteins in the OMV membrane, represented by the detergent phase (Figure 14B).

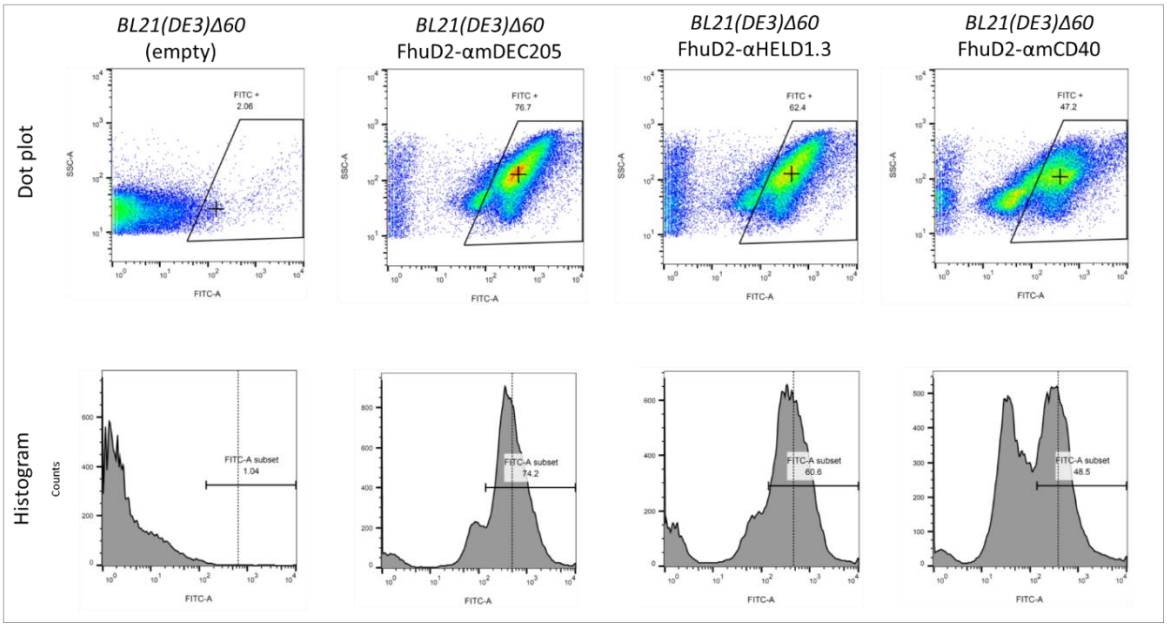

Figure 15: All three FhuD2-scFvs are surface exposed in bacteria. *Flow cytometry analysis of BL21(DE3)Δ60 empty, BL21(DE3)Δ60-FhuD2-amDEC205, BL21(DE3)Δ60-FhuD2-aHELD1.3 and BL21(DE3)Δ60-FhuD2-amCD40 with induced expression of the fusion proteins. All cells were stained with anti-FhuD2 and secondary antibody anti-rabbit Alexa Fluor-488. The dot plots show specific binding to FhuD2-scFvs and no binding in the empty control. The histogram beneath each dot plot represent the same data, but show more clearly a double population.*

Flow cytometry analysis of whole bacteria confirmed the surface expression of the FhuD2-scFv proteins in the BL21(DE3)Δ*60* strain. Using the same method as in figure 13, I observed that there was a positive population staining of 74.2%, 60.6 % and 48.5 % for FhuD2-αmDEC205, FhuD2-αHELD1.3 and FhuD2-αmCD40 fusion protein respectfully (Figure 15). This confirmed the cell surface exposure of the new scFv is similar to that of FhuD2-αmDEC205.

2.2.4. Internalisation of mDEC205 targeting OMVs

In order to understand whether the OMVs expressing αmDEC205 scFv are able to bind mDEC205, and thus internalise differently to non-targeting OMVs, I studied their internalisation on mouse dendritic cell line JAWSII. The JAWSII cell line is well characterised and known for its expression of mDEC205 (Jorgensen *et al.* 2002; Jiang *et al.* 2008; Zapala *et al.* 2011). The cells were seeded at 3 x 10^4 cells in 100 µl, in a 96-well optical plate for microscopy. The next day I incubated 10 µg/ml of OMVs from BL21(DE3)Δ*60-FhuD2-amDEC205* and BL21(DE3)Δ*60-FhuD2-aHELD1.3* with these cells for 2, 30, 90 and 180 minutes. Subsequently, I fixed and permeabilised the cells, stained for OMVs using an anti-LPS antibody and detected with an AlexFlour-488 conjugated secondary antibody. The cells were finally stained with a cell mask (deep red) and hoechst. Using spinning disk confocal microscopy I analysed images of the cells.

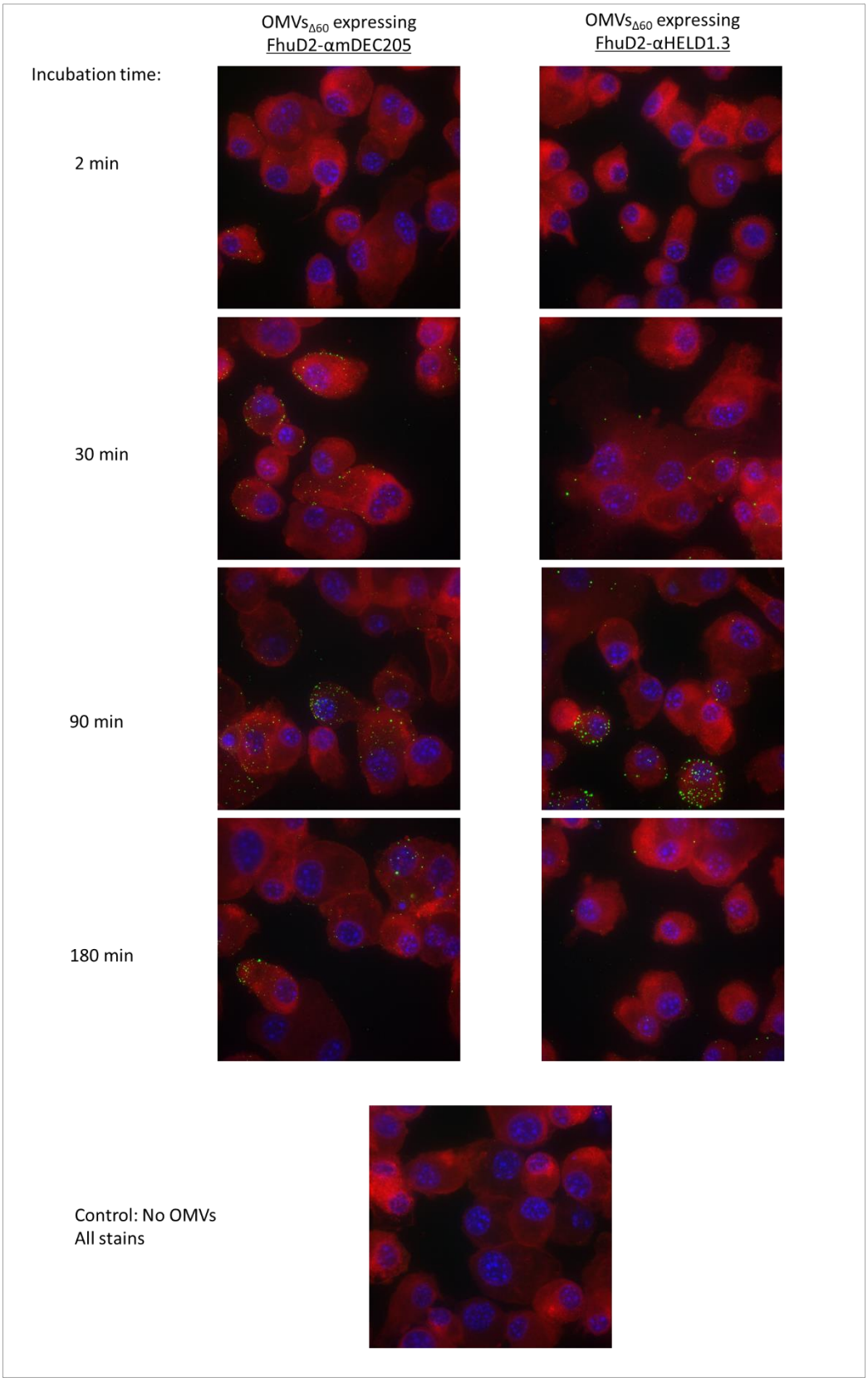

Figure 16: Images of JAWSII cells with internal OMVs. *Cells are stained red, nuclei blue and OMVs green. There is punctate staining of the vesicles throughout each time-point. Here I show a representation of just one field of view for each OMV and time-point. However, there is an average of three fields of view per group.*

Figure 16, shows an example of one field of view at each time point. I confirmed the presence of both OMVs inside the cells across different time-points. I analysed the images collected using ImageJ, in order to obtain a count of the number of OMVs per cell in each time-point for both the mDEC205 targeting OMVs and the control OMVs (see materials and methods). The graph in figure 17 shows the number of vesicles per cell, for each cell analysed in each group. Here we see that the results are similar for both type of OMV with one exception. At T=30 minutes there is a mean of 153 mDEC205-targeting OMVs per cell. Whereas at other time-points in cells with both mDEC205 targeting and non-targeting OMVs there is a mean of approximately 90-100 OMVs per cell. This is the only statistically significant difference in OMV internalisation in the cells. The groups were compared using the Kruskal-Wallis test, which demonstrates the reliability of the data and differences are not due to random sampling. The post-test Dunn's multiple comparison test, was used to analyse specific pairs as summarised in Table 3. These analyses seem to confirm that after a 30-minute incubation with OMVs targeting mDEC205, more of these OMVs are internalised by the cells than non-targeting OMVs at the same time-point. However, the difference is marginal, and disappears when longer incubations are used.

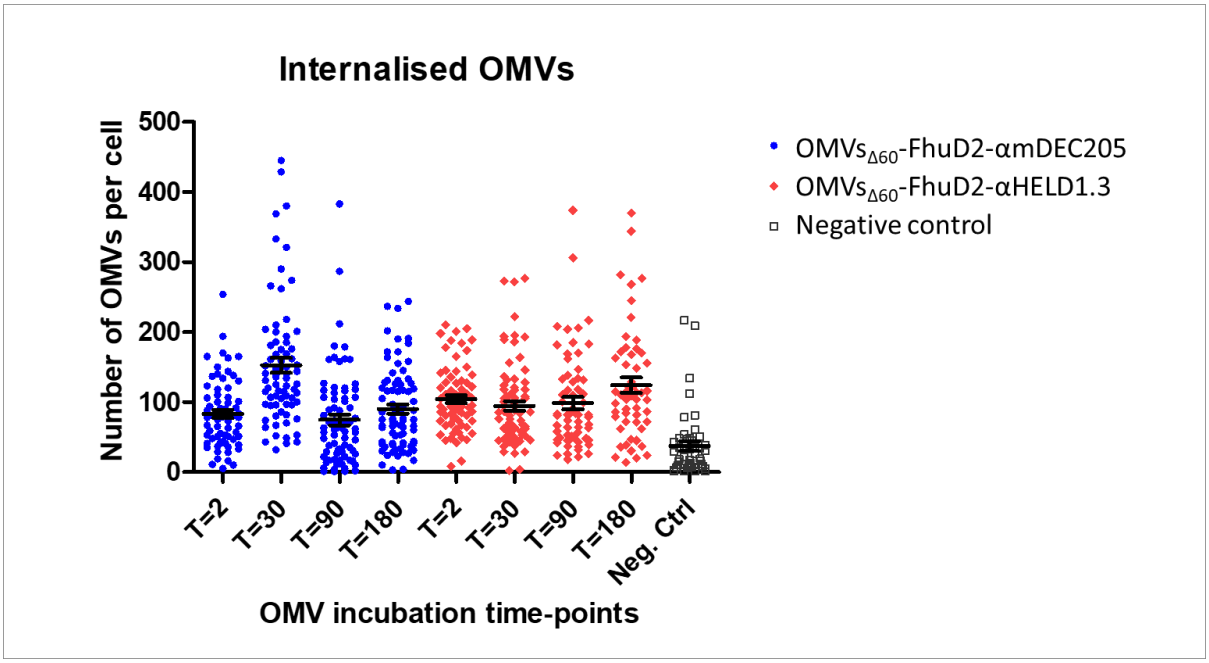

Figure 17: Scatter plot of the number of internalised OMVs per cell. *The x-axis show the number of OMVs per cell, each dot represent a cell. The y-axis shows the incubation time with the OMVs. Blue dots represent cells incubated with OMVs derived from BL21(DE3)Δ60-FhuD2-amDEC205 and red dots represent cells incubated with OMVs derived from BL21(DE3)Δ60-FhuD2-aHELD1.3 (negative control OMVs).*

Table 3: Statistical significance analysis of internalisation

Kruskal-Wallis test			
P value	< 0.0001		
Exact or approximate P value?	Gaussian Approximation		
P value summary	***		
Do the medians vary significantly (P < 0.05)?	Yes		
Number of groups	9		
Kruskal-Wallis statistic (H value)	118.3		
Dunn's Multiple Comparison Test	Difference in rank sum	Significant? (P < 0.05)	Summary
Comparison of OMV internalisation at matched time-points			
T=2 vs T=2	-72.81	No	ns
T=30 vs T=30	**124.7**	**Yes**	*******
T=90 vs T=90	-71.11	No	ns
T=180 vs T=180	-73.51	No	ns
Comparison over time for $OMVs_{\Delta 60}$-FhuD2-αmDEC205			
T=2 vs T=30	-150.2	Yes	***
T=30 vs T=90	194.2	Yes	***
T=90 vs T=180	-57.81	No	ns
T=2 vs T=180	-13.76	No	ns
Comparison over time for $OMVs_{\Delta 60}$-FhuD2-αHELD1.3			
T=2 vs T=30	47.4	No	ns
T=30 vs T=90	-1.659	No	ns
T=90 vs T=180	-60.2	No	ns
T=2 vs T=180	-14.46	No	ns

2.2.5. Analysis of DC biomarker expression

In order to assess whether the short-term increase in OMV internalisation by DCs could lead to an enhanced activation of the cells, I analysed the DC biomarker expression of the cells after incubation with the OMVs. The JAWSII cells were incubated with 25 µg/ml of mDEC205-targeting OMVs, non-targeting OMVs or PBS, for 72 hours. The OVA peptide SIINFELK or PBS control was added for the last 2 hours at 100 nM. Then cells harvested and Fcγ receptor blocked using Fc Block, prior to subsequent staining for the following biomarkers; CD80, CD86, MHC-II and MHC-I-OVA (MHC-I with the OVA (SIINFEKL) peptide in the binding groove).

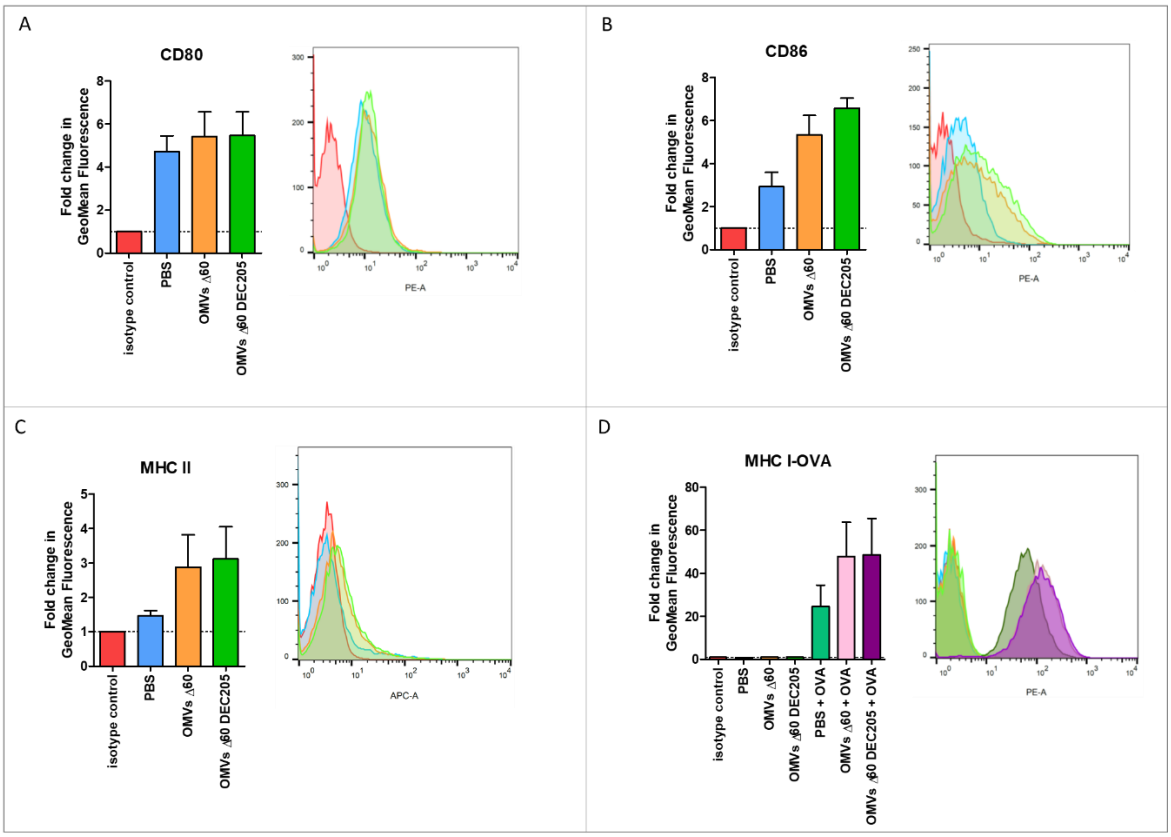

Figure 18: expression of DC biomarkers in JAWSII cells incubated with OMVs*. Each panel contains a bar graph representing the flog change in GeoMean fluorescence corresponding to marker expression, with the colour matched histogram representation of the fluorescence. In all representations Red is the isotype control, Blue, PBS control, Orange, OMVs derived from BL21(DE3)Δ60, green OMVs from BL21(DE3)Δ60-FhuD2-αmDEC205. Panel A, shows CD80 expression. B, CD86 expression. C, MHC-II expression. D, OVA bound MHC-I expression, only measurable when the OVA peptide SIINFEKL is added to the culture.*

I observed increased expression of CD86, MHC-II and MHC-I-OVA when the cell were incubated with OMVs compared to PBS. I did not observe an upregulation of CD80 over that of the PBS group, but I note that mouse GM-CSF was present in the media in all conditions at 5 ng/ml. However, there was not difference between expressions of these biomarkers when the cells were incubated with mDEC205-targeting OMV compared to non-targeting OMVs.

2.3. Discussion

The goal of this investigation was to identify a novel carrier which enables the expression of scFvs on OMVs. Then subsequent targeting of those OMV to the DEC205 DC receptor. The data presented support the use of FhuD2 as a carrier for expression of scFv in OMVs. They also demonstrate targeting of the OMVs to mDEC205 by fusion of a scFv specific for mDEC205. However, the functionality of the OMVs to DEC205 needs to be further explored.

I demonstrated that lipidated FhuD2 can be used as a carrier for large proteins, not just polypeptides. I showed FhuD2 enables the expression of a scFv on OMVs. In gram-negative bacteria surface exposition of heterologous proteins has generally been achieved using various carrier proteins fused to the protein of interest. Carrier proteins are often autotransporters or truncated forms of integral outer membrane proteins such as ompA. The efficiency with which the carrier protein can deliver the protein of interest to the bacterial surface varies greatly depending on the protein of interest. I had additional challenges being that the protein of interest a scFv, which has a globular protein structure not found in bacteria. Additionally, I needed it to be enriched in OMVs rather than whole bacteria. FhuD2 allows the use of lipoprotein transport machinery for delivery of fusion proteins to the surface of bacteria. In general, lipoproteins have a precursor consisting of an N-terminal leader sequence (LS) carrying a cysteine-containing lipobox. After transport through the inner membrane, the cysteine is diacylated. The protein is then cleaved upstream of the diacylated cysteine. In Gram-negative bacteria, the free NH_2 group of the cysteine receives another acyl group and the triacylated lipoprotein transported to the outer membrane by the Lol transport machinery (Narita and Tokuda 2017). However, the mechanism for the transport of lipidated FhuD2 in *E. coli* has not been elucidated, but it is like that the lipidation and natural location of FhuD2 on the surface of Staphylococcus aureus (Mishra *et al.* 2012) play a key role in translocation to the outer membrane.

Firstly, I showed that expression of scFv in OMVs is possible with the FhuD2 carrier protein (Figures 10, 11 and 14). Meaning that with the right carrier scFv can be translocated across the inner membrane of the bacteria, for subsequent enrichment in OMVs. I show that the FhuD2-scFv fusions can co-localise to the outer membrane, and is present at the OMV membrane (Figures 12 and 14B). On bacteria, the FhuD2-scFv

fusion protein is surface exposed, as demonstrated by detection of the fusion protein by flow cytometry (Figures 13 15). The surface exposition of the fusion protein was improved by expression in our novel BL21(DE3)Δ*60* strain derived OMVs (Figure 13). Since we know that the FhuD2 is on the membrane of OMVs, and that is it surface exposed in *E. coli*, I hypothesised that the scFv is also surface exposed on the outer membrane in OMVs. However, this should be confirmed. Unfortunately, I did not have a scFv-specific antibody to follow its localisation. Such antibodies could be conveniently used for flow cytometry as well as in immune-electron microscopy on both whole cells and purified OMVs.

While we know that NLDC-145 is an antibody specific for mDEC205 and that scFvs derived from this antibody have been shown to bind mDEC205 (Demangel *et al.* 2005), I am lacking specific binding data for our FhuD2-αmDEC205 fusion. The fact that I observed a marginal increment in OMV internalisation by the mouse dendritic cell line JAWSII seems to suggest that the scFv does bind mDEC205. However, further investigation is needed.

The possible differential internalisation of OMVs due to mDEC205 did not lead to increased DC biomarker expression on JAWSII cells compared to the biomarker expression on cells incubated with non-targeting OMV. CD86 and MHC class II molecules were upregulated in cell incubated with OMVs. However, OMVs that express the FhuD2-αmDEC205 fusion protein did not elicit and increased expression of MHC I-OVA over "naked" OMVs. This may be due to the fact that OMVs efficiently bind host cells *in vitro* (O'Donoghue and Krachler 2016) and their stimulatory molecules already saturate their activation. Such situation might be different *in vivo* where the presence of DCs is limiting. In this case, a better avidity of OMVs to DC receptors might play an important role in DC activation. However, further investigation is needed along this line.

Chapter 3: Antigen processing and presentation

3.1. Introduction

For an effective immune response dendritic cells must process and present exogenous antigens on MHC I molecules, a process known as cross-presentation. The efficiency of $CD8^+$ T cell priming by cross-presenting DCs is dependent on both the level of DC maturation and the amount of antigen peptide bound MHC I complexes on the DC surface. Cross-presentation is important for inducing T cell responses specific for tumour antigens. However, the mechanism of cross-presentation is still not fully understood. Broadly, two main pathways for antigen cross-presentation in DCs are considered: the cytosolic pathway and the vacuolar pathway (Figure 19).

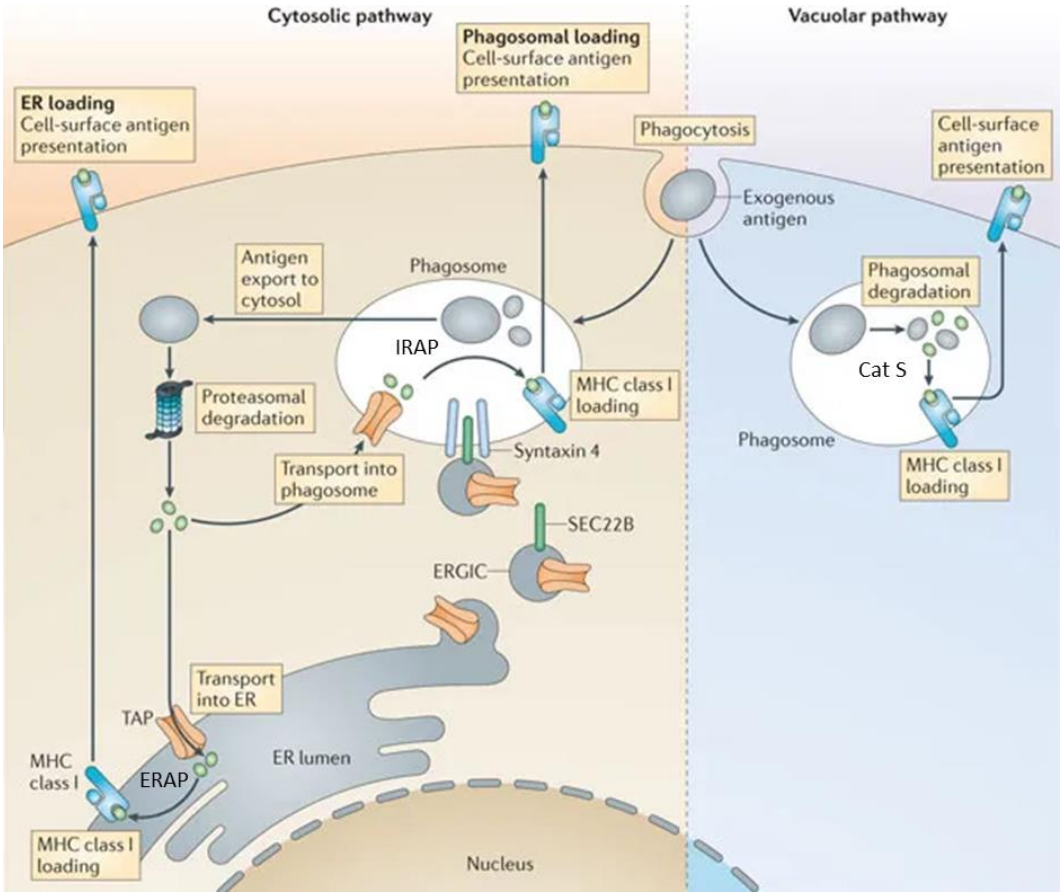

Figure 19: Antigen cross-presentation by dendritic cells*. After phagocytosis, exogenous antigens may enter the cytosolic or vacuolar pathway. In the cytosolic pathway, antigens are processed by proteasomal degradation. The processed antigen-derived peptides are transported back into the phagosome (soluble and particular antigens) or into the ER (particular antigens) via TAP. There, they are further trimmed by IRAP or ERAP and loaded onto MHC I. The SEC22B, which localises in the ER–Golgi intermediate compartment (ERGIC) and interacts with syntaxin 4 on phagosomes, mediates the recruitment of cross-presentation machinery towards phagosomes. Alternatively, in the vacuolar pathway, exogenous antigens are degraded in endosomes by Cathepsin S (Cat S) and loaded onto MHC I molecules. Image adapted from Joffre et al. 2012 (Joffre et al. 2012)*

In order to explore whether $OMV_{\Delta 60}$ adjuvanticity can confer a specific $CD8^+$ T cell response to peptide epitopes with which they are decorated we investigated two $CD8^+$ T cell-specific model antigen epitopes: SV40 $IV_{404-411}$ C411L, with peptide sequence VVYDFLKL, and $OVA_{257-264}$, with sequence SIINFEKL.

SV40 IV is an MHC I H2-K^b restricted epitope derived from the Simian Virus 40 (SV40) large tumour antigen (Tanaka and Tevethia 1988; Mylin *et al.* 1995). It is an immunodominant epitope able to induce a $CD8^+$ T cell-specific response. The C411L mutation is used to avoid the problematic cysteine oxidation of peptides, this mutated epitope is also more efficiently recognised than the wild-type epitope (Mylin *et al.* 2000). It is a commonly used tool to study T cell responses using the C57BL6 mouse model. From here on the SV40 IV epitope will be referred to as simply SV40.

$OVA_{257-264}$ is a $CD8^+$ specific peptide from the chicken ovalbumin protein, known to be highly immunogenic in C57BL6 mice (Moore *et al.* 1988; Rötzschke *et al.* 1991). It is also specific for the MHC I H2-K^b allotype expressed by these mice and has been used extensively both *in vitro* and *in vivo* for T cell analysis (Lipford *et al.* 1993). Therefore, it is a well-defined tool for studying T cell responses. In addition, there is a well-known murine syngeneic tumour model, using the C57BL6 mice with the B16F10-OVA melanoma cell line, stably transfected to express chicken ovalbumin. Meaning that we can use this model in our OMV tumour protection experiments if and when required. From here on $OVA_{257-264}$ will be referred to simply as OVA. Using these model antigen epitopes as tools we systematically analysed the $CD8^+$T cell response induced by our OMVs.

As previously stated, OVA is a well-studied model epitope therefore studies regarding peptide length are already published. One study clearly demonstrates that the short synthetic peptide SIINFEKL is rapidly presented to $CD8^+$ T cells causing a strong activation. Whereas the use of a 24 amino acid long peptide DEVSGLEQLESIINFEKLAAAAAK resulted in a lower potency of $CD8^+$ T cell stimulation. The addition of proteasome inhibitor epoxomicin caused a loss of MHC-I presentation, showing that intracellular processing of the long peptide is proteasome dependent. When TAP was knocked-out of DCs, they also became deficient at activated $CD8^+$ T cells (Rosalia *et al.* 2013). However, targeting the long peptide to DCs by conjugation to TLR-

ligands helped overcome the peptide processing barrier and enhanced antigen uptake (Khan *et al.* 2007). Currently, many systems for peptide delivery have been studied in order to overcome lack of synthetic peptide potency (He *et al.* 2018). Here we demonstrate how OMVs are a great delivery vehicle for peptides using model antigen epitopes OVA and SV40, because of their adjuvanticity and investigate the formulation of peptide antigens with OMVs.

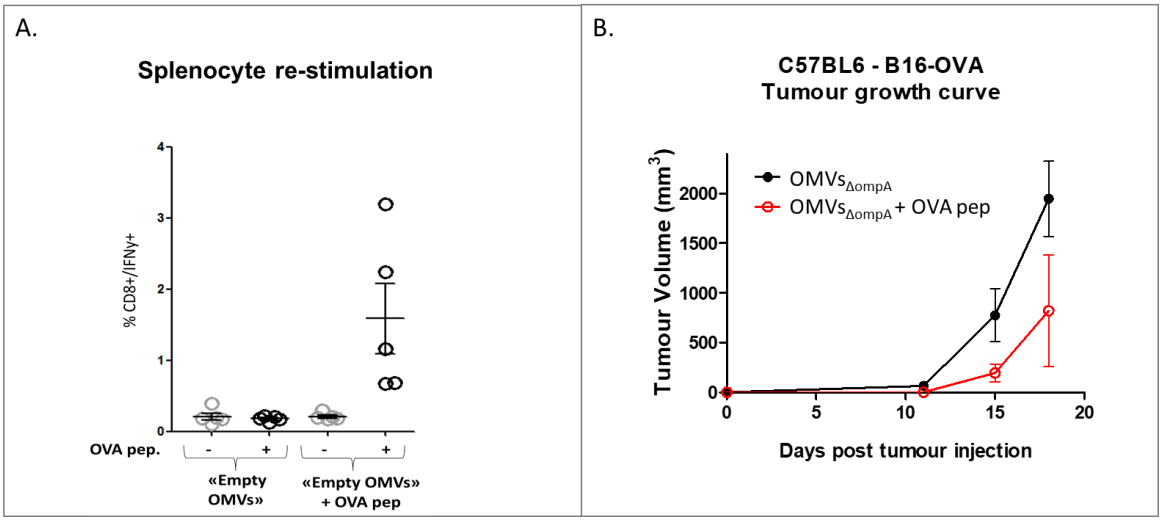

***Figure 20: T* cell activation and tumour growth inhibition with $OMVs_{\Delta ompA}$.** *A. C57BL6 mice were injected subcutaneously on day 0 and day 7, with 10 µg $OMVs_{\Delta ompA}$ or 10 µg $OMVs_{\Delta ompA}$ with 50 µg OVA peptide. On day 12 splenocytes prepared and stimulated with either 5µg/ml of OVA peptide or 5 µg/ml of negative control peptide. The percentage of $CD8^+$ T cells also positive for IFNγ was analysed by flow cytometry. B. C57BL6 mice were implanted with B16-OVA melanoma cells on day 0. Mice were vaccinated on day 1, 4, 8, 11 and 15 with 10 µg $OMVs_{\Delta ompA}$ or 10 µg $OMVs_{\Delta ompA}$ with 100 µg OVA peptide. Tumour growth was monitored from day 8.*

In our laboratory, we have already proven that $OMVs_{\Delta ompA}$ decorated with OVA can be used to immunise mice and elicit a $CD8^+$ T cell response (Figure 20A). Vaccination with this treatment can also confer anti-tumour protection in the B16-OVA melanoma in a syngeneic C57BL6 mouse model. On day 0, the mice were injected with B16-OVA tumour cells subcutaneously in one site, on the flank. On days 1, 4, 8, 11 and 15 mice were vaccinated by subcutaneous injection of OMVs alone, or OMVs with the OVA peptide adsorbed. Vaccination with OMVs + OVA peptide markedly reduced tumour growth (Figure 20B).

OMVs have unique adjuvant properties because they carry a number of MAMPs. The most notable of which is lipopolysaccharide (LPS), also referred to as endotoxin. LPS is the ligand for the PRR toll-like receptor4 (TLR4) and is abundant on OMVs. It is this TLR4 signalling, which greatly contributes to the adjuvanticity of OMVs. However, it is

also responsible for the reactogenicity of OMVs, which must be limited for clinical use to reduce adverse reactions such as inflammation, high fever and pain.

LPS consists of lipid A, core oligosaccharides and O-antigen chain. It is the Lipid A that constitutes the binding moiety for TLR4 and is therefore responsible for LPS activity on TLR4. Fortunately, there are a number of mutations in the LPS biosynthetic pathway, which allow the removal of acyl chains from lipid A. While native lipid A is hexa-acylated in different species including *E. coli*, the inactivation of acyltransferase genes *msbB* and *pagP* results in the production of a penta-acylated lipid A moiety (Somerville *et al.* 1996; Bishop *et al.* 2000). OMVs derived from BL21(DE3)Δ*60*, are not only OMV-proteome minimised compared to BL21(DE3)Δ*ompA* derived OMVS, but they also contain the *msbB*/*pagP* gene deletions, resulting in the presence of penta-acylated lipid A in their LPS (Figure 21). *N. meningitidis* serogroup B OMVs with penta-acylated LPS have reduced reactogenicity similar to that of detergent treated OMVs such as Bexsero (Zariri *et al.* 2016). Bexsero is an OMV-based meningitis B vaccine with both EMA and FDA approval. Thus, it is used as a guideline for safety and toxicity of OMVs in the clinic. OMVs derived from *Shigella sonnei* are also less reactogenic when LPS is penta-acyated (Gerke *et al.* 2015). In addition, phase I clinical trials showed they are well tolerated and have an acceptable safety profile in adults (Launay *et al.* 2019).

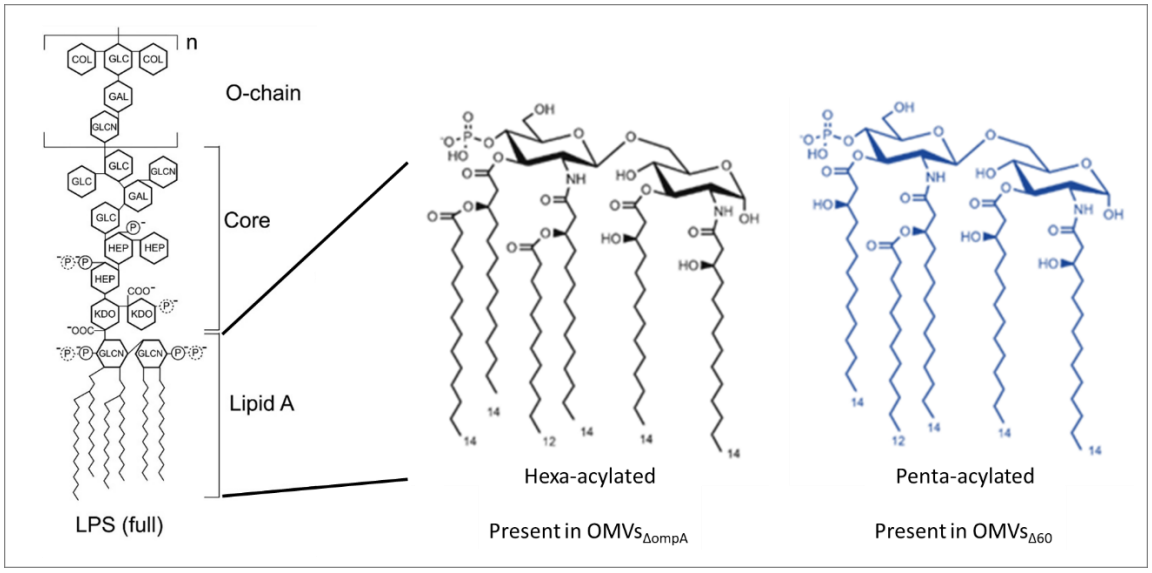

Figure 21: schematic overviw of LPS and hexa-acylated or penta-acylated lipid A components*. LPS is a large molecule consisting of an O-antigen chain, polysacharide core and lipid A. Hexa-acylated Lipid A is the native form of the lipid. Penta-acylated Lipid A occurs when msbB and PagP genes are deleted, creating a less reactogenic LPS.*

Several assays can be used to follow the adjuvanticity and reactogenicity of OMVs. One of these involves studying the TLR4 agonistic activity using the HEK-Blue™ TLR4 cells. When these cells are stimulated with TLR4 agonists, TLR4 signalling occurs, causing the activation of NFkB and subsequent nuclear signalling. In the case, these cells contain and reporter gene encoding inducible secreted embryonic alkaline phosphatase (SEAP). Stimulation of TLR4 activates NFkB, which induces the production of SEAP. The agonistic activity of our OMVs has been tested using the HEK-Blue humanTLR4 (hTLR4). We have previously shown that $OMVs_{\Delta 60}$ were almost one order of magnitude less agonistic than $OMVs_{\Delta ompA}$ at hTLR4 stimulation (Zanella *et al.* 2020).

OMVs confer good humoral immunity against various exogenous proteins (Fantappiè *et al.* 2014; Irene *et al.* 2019), as well as T cell responses (Grandi *et al.* 2017, 2018). Such responses are associated with the ability of OMVs to confer efficient delivery of the target antigen to dendritic cells (DCs) and, in the case of T cell responses, to cross-present the antigens to $CD8^+$ T cells. However, the optimal conditions for OMVs to induce T cells remain to be fully elucidated and this has become the second objective of my experimental work.

3.2. Results

3.2.1. $OMV_{\Delta 60}$ adjuvanticity and reactogenicity

Before investigating the OMV-induced T cell responses we first analysed the suitability of our $OMVs_{\Delta 60}$ for vaccination. Hence, we analysed their adjuvanticity and reactogenicity using cell-based assays. Having shown that we have good OMV activity profile in the hTLR4 assay (Zanella *et al.* 2020), we investigated whether we also have a good adjuvanticity and reactogenicity profile when we consider other PRRs. Though TLR4 is the main receptor for inducing OMVs reactogenicity and adjuvanticity, it is not the only one. TLR2 detects lipoproteins, which are also present in OMVs and is therefore important the hTLR2 receptor response to our OMVs. Human reactogenicity and adjuvanticity assays are important for clinical vaccine development. However, given that we use syngeneic mouse models for the *in vivo* studies, I also investigated mouseTLR4 stimulation by OMVs. This helped us confirm that the results we observe in mice are translatable to humans. The mTLR4 assay is also a HEK Blue™ TLR4 cell line experiment. The mouse TLR4 cell line was made by co-transfection of mTLR4, MD-2 and CD14 co-receptor genes, along with an inducible reporter gene secreted embryonic alkaline phosphatase (SEAP). The reporter gene is under the control of an IFN-β minimal promoter that is fused to five NFκB and AP-1 binding sites. Stimulation with a TLR4 ligand activates NFκB and AP-1, inducing the production of SEAP. The supernatant containing the SEAP was mixed with QUANTI-blue™ detection regent, which turns from pink to blue in the presence of alkaline phosphatase. The absorbance at 655nm is proportional to the mTLR4 activity. Whereas the hTLR2 assay is a HEK Blue™ TLR2 cell line experiment uses the same HEK Blu e™ cells with co-transfection of the hTLR2 receptor gene and the secreted embryonic alkaline phosphasate (SEAP) gene into HEK293 cells. The readout and detection is the same as in the mTLR4 assay, absorbance at 655nm is proportional to the hTLR2 activity.

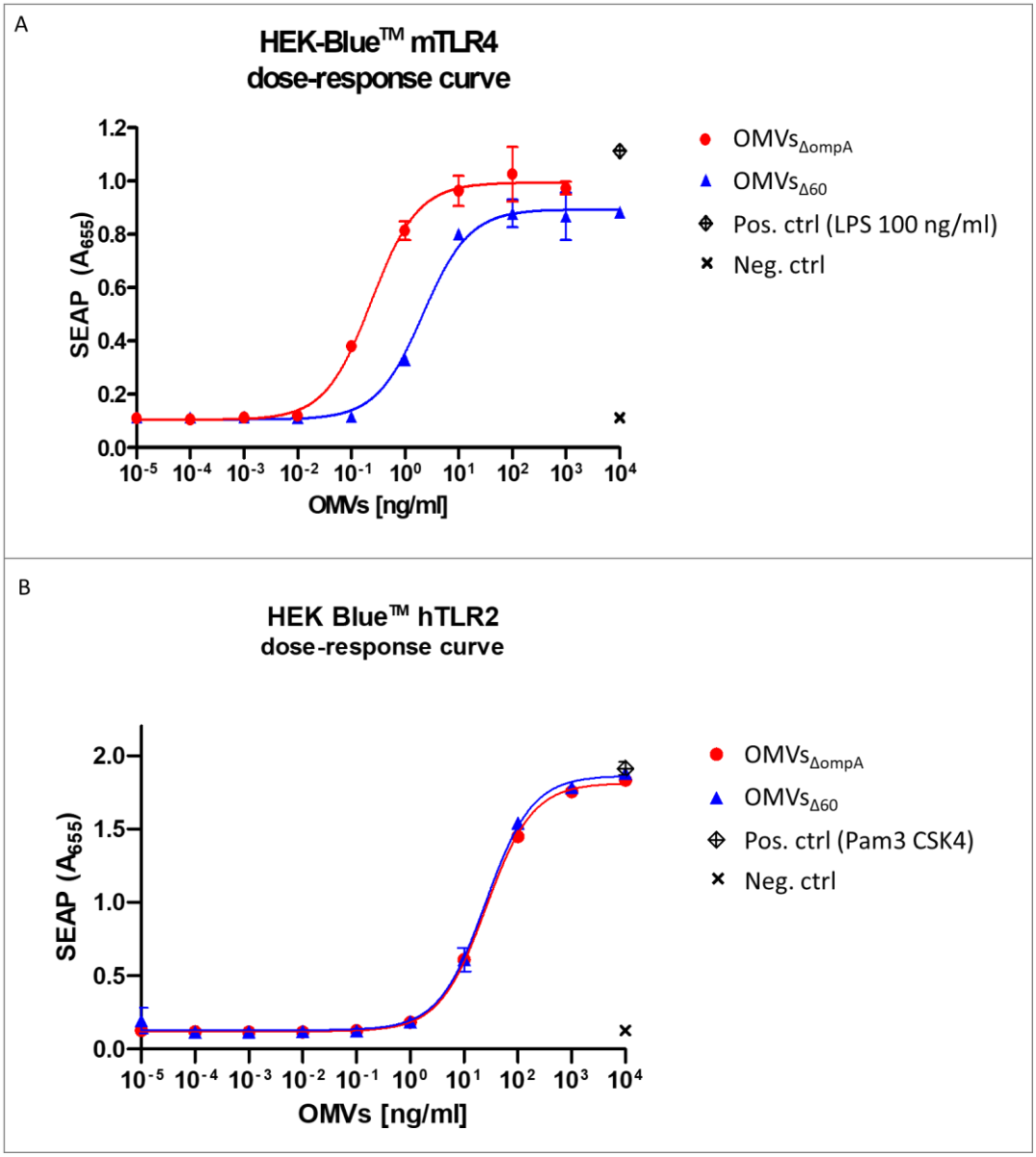

Figure 22: Mouse TLR4 and human TLR2 dose-response curves by OMV stimulation. *OMVs, ΔompA OMVs (red) and Δ60 OMVs (blue), derived from BL21(DE3)ΔompA and BL21(DE3)Δ60 strains respectively, were incubated with HEK-Blue™ mTLR4/hTLR2 cells for 17 hours at 37°C. Along with negative control (endotoxin-free H_2O) and positive controls LPS or Pam3CSK4 both at 100 ng/ml. TLR stimulation was measured by incubation of the supernatant with QUANTI-Blue™ and subsequent spectrophotometric analysis at A_{655}. The graphs are representative examples of repeat experiments*

In line with both data from the hTLR4 experiment, the mTLR4 experiments showed that both $OMVs_{\Delta 60}$ and $OMVs_{\Delta ompA}$ stimulate mTLR4. However, the $OMVs_{\Delta 60}$ are one log less potent than the $OMVs_{\Delta ompA}$ (Figure 22A). These data demonstrated that the reactogenicity of the OMVs is reduced in the BL21(DE3)Δ*60* derived OMVs compared to the BL21(DE3)Δ*ompA* derived ones. Yet the $OMVs_{\Delta 60}$ are still able to stimulate mTLR4, showing they still have adjuvanticity. We also demonstrated that both $OMVs_{\Delta ompA}$ and $OMVs_{\Delta 60}$ stimulate hTLR2 with the same potency and efficacy (Figure 22B).

Given the broad spectrum of PRRs present on antigen-presenting cells, other receptors may also be involved in OMV adjuvanticity and reactogenicity. Therefore, we used the THP-1 human monocyte cell line to assess these properties in an assay not reliant on just one receptor target. In fact, THP-1 cells express TLR1, TLR2, TLR4, TLR5, TLR6, TLR7, TLR8 and TLR9 (Ciabattini *et al.* 2006). They produce hIL-6, among other cytokines, in response to stimuli.

First, the THP-1 cells were differentiated into macrophages by incubation with phorbol 12-myristate 13-acetate (PMA). Once differentiated they were incubated with increasing concentration of OMVs derived from either BL21(DE3)Δ*ompA* or BL21(DE3)Δ*60*. After a 24 hour incubation with OMVs, the supernatants were collected and ELISA used to analyse the amount of hIL-6 released by the cells. With 10 ng/ml of $OMVs_{\Delta 60}$, there was no detectable hIL-6 released, whereas 10 ng/ml of $OMVs_{\Delta ompA}$ stimulated the production of 45 ng/ml of hIL-6. However, $OMVs_{\Delta 60}$ did stimulate hIL-6 release, though 3-log higher concentrations of $OMVs_{\Delta 60}$ than $OMVs_{\Delta ompA}$ were required (Figure 23).

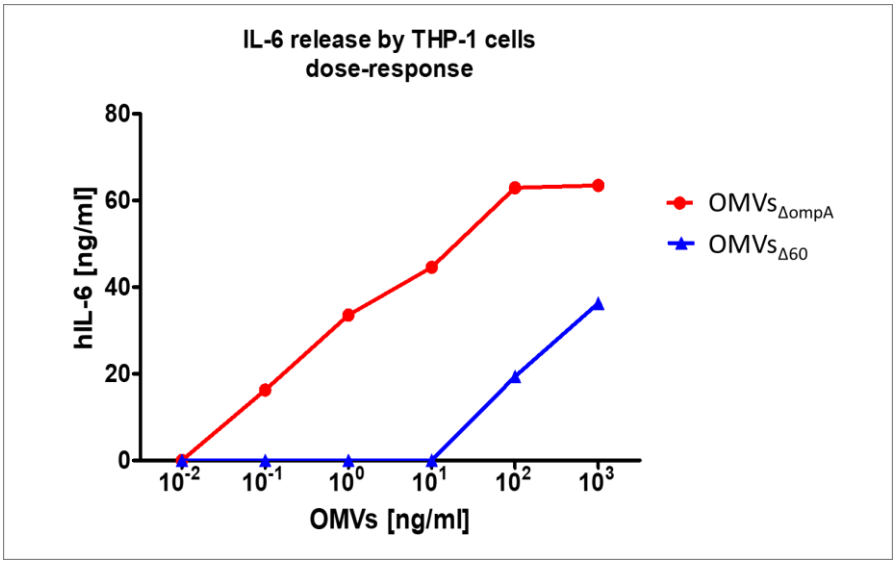

Figure 23: THP-1 cells stimulated with OMVs for IL-6 release dose-response curve. *Differentiated THP-1 cells were incubated with increasing concentrations of OMVs derived from BL21(DE3)ΔompA (red) and BL21(DE3)Δ60 (blue) strains and the level of hIL-6 in the culture medium was measured by ELISA.*

These data demonstrated that TLR4 response is probably the most important PRR response to OMVs in THP-1 cells and that $OMVs_{\Delta 60}$ are less potent than $OMVs_{\Delta ompA}$, therefore less reactogenic. However, they are equally efficacious and therefore should maintain adjuvanticity.

3.2.2. Immunogenicity of OMVs$_{\Delta 60}$ adsorbed with MHC I specific peptide antigens

We know that OMVs$_{\Delta ompA}$ are able to elicit CD8$^+$ T cell responses to OVA when decorated with the peptide (Tomasi 2018), but we want to know if OMVs$_{\Delta 60}$ can elicit the same CD8$^+$ T cell response. We performed a preliminary test to demonstrate that like OMVs$_{\Delta ompA}$, the OMVs$_{\Delta 60}$ also elicit a good T cell response when decorated with OVA (Figure 24A).

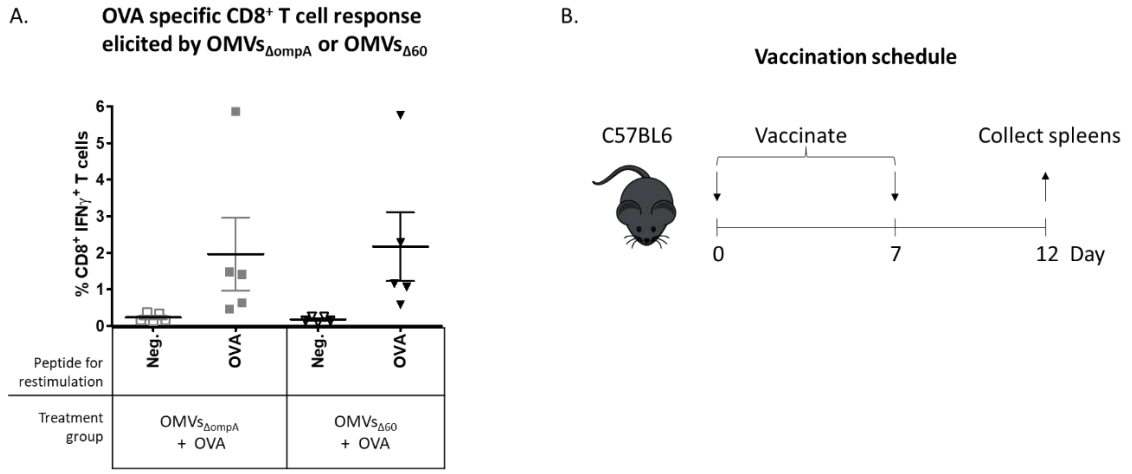

***Figure 24: Vaccination with OMVs plus OVA peptide elicits a CD8$^+$ T cell response**. A, Preliminary test of immunogenicity of OMVs$_{\Delta ompA}$ with 5µg OVA versus OMVs$_{\Delta 60}$ with 5 µg OVA adsorbed. Splenocyte re-stimulation with the OVA peptide or negative control peptide show that both OMVs$_{\Delta ompA}$ and OMVs$_{\Delta 60}$ induce an OVA-specific CD8$^+$ T cell response. B, Vaccination schedule.*

To analyse the CD8$^+$ T cell response to OMVs with peptide antigen adsorbed we immunised mice following this vaccination schedule (Figure 24B). C57BL6 mice were vaccinated subcutaneously with 10 µg of OMVs plus peptide on day 0 and day 7. On day 12, spleens were harvested for the splenocytes re-stimulation experiment. Spleens were processed to obtain a single-cell suspension of splenocytes, which are mostly T cell, B cells and some antigen-presenting cells. Splenocytes from each mouse were stimulated with 5 µg/ml of OVA peptide or negative control peptide. If vaccination induced an OVA-specific CD8$^+$ T cell immune response then the peptide would induce an antigen recognition response, leading to activation of CD8$^+$ T cells, demonstrated by IFNγ release. The negative control peptide is not present in the vaccine formulation or native to the mice, thus should result in no or minimal non-specific IFN-γ release by T cells.

We demonstrated that when the OVA peptide is adsorbed to $OMVs_{\Delta 60}$ and used to immunise mice, the mice develop an epitope-specific $CD8^+$ T cell response. To establish the general applicability of OMVs for eliciting $CD8^+$ T cell responses, we repeated the experiments using SV40 peptide. Moreover, we investigated the dose-dependent stimulation of T cells. C57BL6 mice were vaccinated subcutaneously with 10 µg $OMVs_{\Delta 60}$ plus 50, 5 or 0.5 µg of the peptide, on day 0 and day 7. On Day 12, Spleens were harvested for the splenocyte restimulation experiment and active $CD8^+$ T cells analysed (Figure 25).

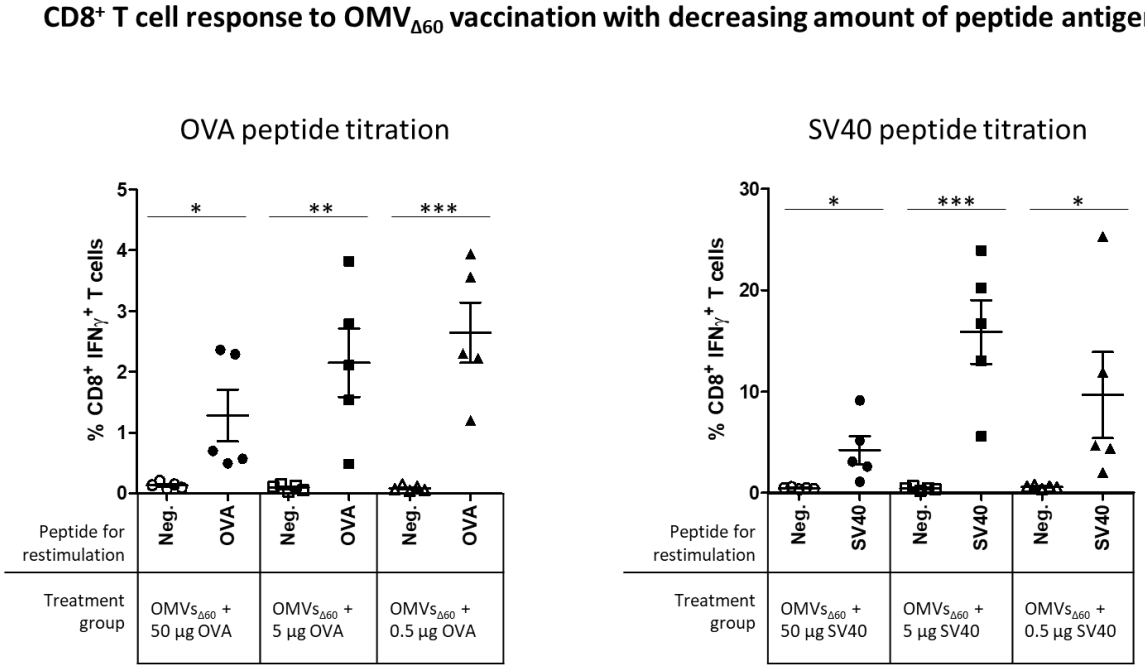

Figure 25: Percentage of epitope-specific CD8+ IFNγ+ T cells induced by vaccination with OMVs + peptide epitope. *Mice were injected subcutaneously on day 0 and day 7. For the OVA titration treatment groups were 10 µg OMV + 50 µg OVA, 10 µg OMVs + 5 µg OVA or 10 µg OMV + 0.5 µg OVA. The SV40 titration groups followed the same pattern, 10 µg OMV plus 50, 5 or 0.5 µg SV40. B, Splenocytes harvested on day 12 were stimulated with either 5 µg/ml of the vaccination peptide or 5 µg/ml of negative control peptide.*

When splenocytes were re-stimulated with the peptide epitope used for vaccination, the percentage of $CD8^+$ T cells expressing activation marker IFNγ was significantly increased over control peptide stimulation. The frequency of epitope-specific $CD8^+$ T cells was remarkably elevated, particularly in the case of SV40. Indeed, in our hands the observed frequencies were consistently higher than those we observed using other adjuvant, such as Hiltonol (data not shown). Interestingly, 50 µg of the peptide was the least effective dose for both epitopes, and based on these data we used the 5 µg dose for the following experiments.

3.2.3. Antigen peptide processing affects the elicitation of an antigen-specific T cell response

Normally, antigen presentation on MHC I occurs when (1) antigens present in the cytoplasm (either after internalisation from the outside the cell, or those synthesised inside the cell) are processed into peptides by the immuno-proteasome, (2) the peptides, transported into the ER through the TAP system, are trimmed down to the exact length (8-10 amino acids), and (3) the peptides are loaded into the groove of the MHC molecules. An alternative way for peptides to be presented on MHC I is that they bind directly extracellularly, replacing peptides with less affinity/stability sitting in the groove of surface-exposed MHC molecules. In the experiments described above, the OVA and SV40 $CD8^+$ T cell epitopes, being the exact length to bind MHC I, could be directly transferred from the OMV to MHC I, thus bypassing the digestion and TAP-mediated transport steps. This could explain the remarkably high frequency of epitope-specific T cells induced by OMV immunisation. Is the same frequency obtained if longer peptides, containing the SV40 and OVA epitopes, are adsorbed to OMVs? To induce epitope-specific T cells such peptides must be internalised and properly processed and presented to MHC I.

To address this question I designed the SV40 2X peptide which contained two copies of the SV40 epitope, as well as a GG linker and short native flanking regions (see Table 4). Flanking the epitope with two amino acids from the natural protein sequence and using two glycine linkers has been shown to improve presentation (Rueda *et al.* 2004). We vaccinated C57BL6 mice according to the schedule given previously (Figure 24B) with peptides carrying one or two copies of SV40 epitope adsorbed to $OMVs_{\Delta 60}$ (see Table 4). To keep the same molar concentration of the epitope, mice were given either 5 µg of SV40 1X or 7.41 µg SV40 2X in a 200 µl solution containing 10 µg of $OMVs_{\Delta 60}$. As shown in Figure 26, both peptide configurations induced high frequencies of epitope-specific T cell responses and using an unpaired T-test no statistical difference between the two vaccinations were observed. This strongly suggests that, under the condition used, the long SV40 peptide adsorbed to OMVs could efficiently be

internalised by APCs and processed to give the 8-amino acid SV40 epitope ready to be presented on MHC I molecules.

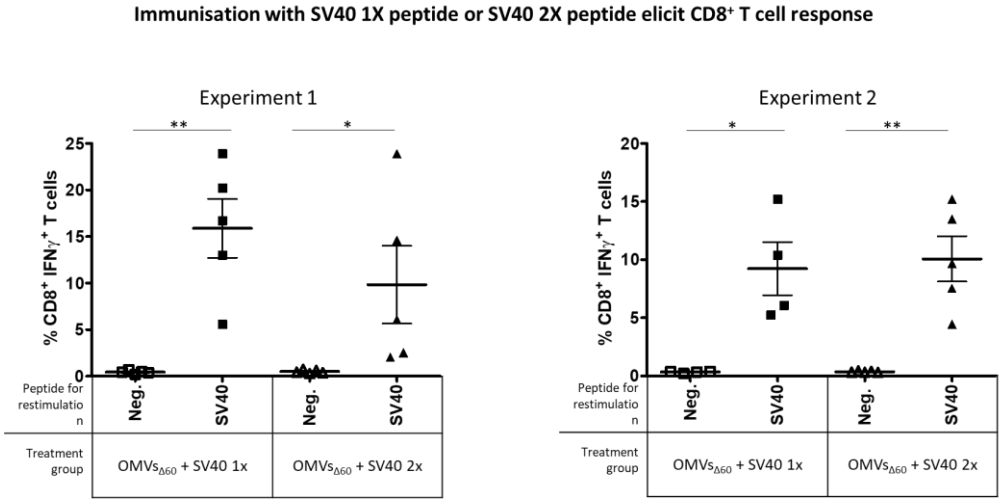

Figure 26: Percentage of epitope-specific CD8⁺ IFNγ⁺ T cells induced by vaccination with OMVs + the single SV40 peptide or double SV40 peptide. *Mice were vaccinated subcutaneously on day 0 and day 7, as in previous experiments. There were immunised with $OMVs_{\Delta 60}$ + SV40 1x or $OMVs_{\Delta 60}$ + SV40 2x. Splenocytes harvested on day 12 were stimulated with either 5 µg/ml of the SV40 1x peptide or 5 µg/ml of negative control peptide. Paired T-test.*

Table 4: Peptides for CD8⁺ T cell response experiments

Antigen	Epitope	MHC I binding epitope sequence	Peptide name	Peptide Sequence
SV40 large T antigen	SV40 IV 404-411 (C411L)	VVYDFLKL	SV40 1X	**VVYDFLKL**
			SV40 2X	DS**VVYDFLKL**MVGGDS**VVYDFLKL**MV
Chicken ovalbumin	OVA 257-264	SIINFEKL	OVA 1X	**SIINFEKL**
			OVA 2X	QLE**SIINFEKL**TEGGQLE**SIINFEKL**TE
			longOVA	GSQLE**SIINFEKL**TEWTSSNVMEERK
Murine leukaemia virus envelope gp70	gp70 423–431 (AH1)	SPSYVYHQF	Negative control	SPSYVYHQF

Peptide sequence amino acids in **bold** are the exact MHC I binding epitopes, in black is the natural protein sequence including the epitope and flanking regions, in grey are amino acid linkers.

We attempted the same experiment with the OVA peptide. However, the peptide carrying two copies of OVA could not be synthesised due to its high hydrophobicity (see Table 4). Therefore, I designed and had synthesised a "long OVA" peptide of 26 amino acids carrying the OVA epitope internally (see Table 4) and we compared the capacity of the "short OVA" peptide and the long OVA peptide to elicit OVA-specific T cells. Figure 27 shows that both the short OVA, consisting of the 8 amino acid MHC I epitope, and the long OVA, were able to induce a CD8⁺ T cell response. However, in this case, the short epitope was significantly more effective at eliciting a

good epitope-specific CD8$^+$ T cell response (P=0.0035, unpaired, one-tailed t-test). These results suggest that the design of the peptide for processing and presentation on DC plays a key role in allowing proper cross-presentation.

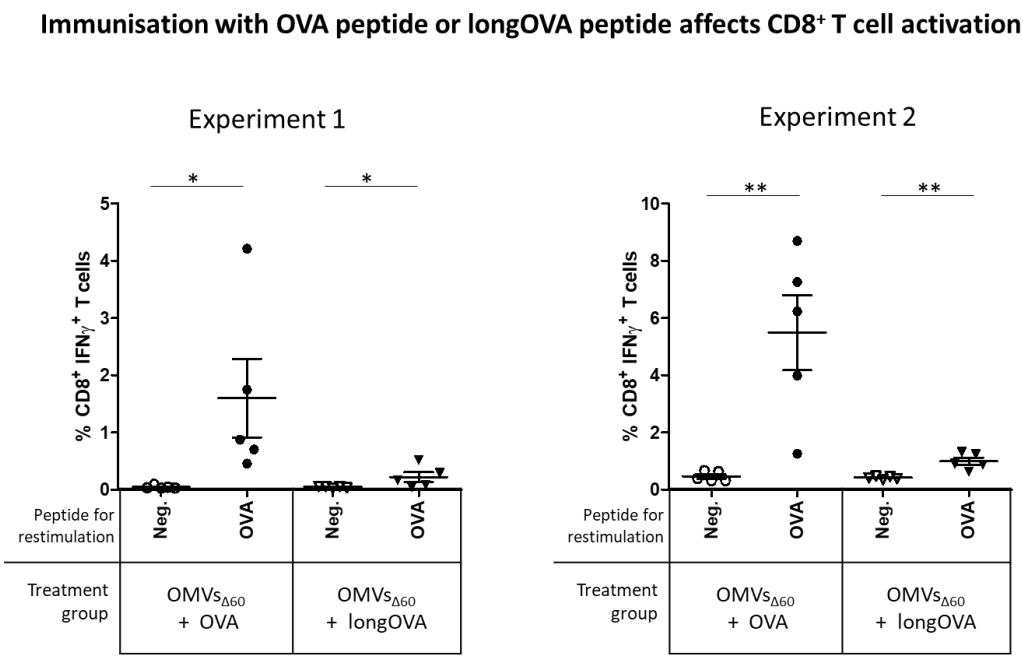

Figure 27: Immunisation with OVA peptide or longOVA peptide adsorbed to OMVs affects the extent of CD8$^+$ T cell activation. *Mice were vaccinated using the above schedule. One group was given 10 µg OMVs$_{\Delta 60}$ with 5 µg of OVA peptide. The other group was given 10 µg OMVs$_{\Delta 60}$ with 15.87 µg of longOVA peptide. This was calculated so that both groups were given the same mole of the epitope.*

3.3. Discussion

As pointed out in the "Aims of the Thesis", to present extracellular antigens on MHC I, DCs have to (1) be available at, or rapidly reach the site where antigens are present, (2) bind and internalise the antigens, (3) process the antigens in the proteasome and present antigen-derived peptides in the context of MHC molecules.

In Chapter 2, I presented data showing our efforts to optimise the binding and internalisation of OMVs, the antigen/adjuvant delivery system we use as a platform to develop vaccines against infectious diseases and cancer. I decorated the OMV surface with a DEC205-specific scFv with the idea of potentiating antigen up-take by DCs.

In this Chapter, I focused my attention on finding out the best strategy to optimise antigen presentation on MHC I. To address this issue, I used two epitopes broadly exploited to study $CD8^+$ T cell responses in C57BL6 mice: OVA and SV40. We first used synthetic peptides corresponding to the exact length of the epitopes (8 amino acids each), we mixed them ("adsorbed") with the OMVs and we established whether the peptide-OMV complexes could elicit epitope-specific T cells in C57BL6 mice. Our data show that, elevated frequencies of activated T cells were induced against both peptide epitopes, suggesting that, at least under the conditions used, OMVs represent an excellent adjuvant/delivery system for inducing cell-mediated immunity.

Now, with the configuration used, the OVA and SV40 peptides could potentially be presented on MHC I without needing to be internalised and processed: the peptides may in fact directly bind the surface-exposed MHC molecules. Therefore, we next asked the question whether similar epitope-specific T cell frequencies could be obtained if the epitopes were embedded within a longer amino acid sequence. In this configuration, the only way to induce epitope-specific T cells should be through peptide internalisation and processing by DCs. The data show that the two epitopes behave differently: while the "long SV40 peptide" continued to elicit very high T cell frequencies, the "long OVA peptide" did not. At present, we do not have an explanation for this difference, which could be attributed to differences in peptide internalisation, ubiquitination and/or processing by the immune-proteasome. However, it has to be pointed out that the SV40 long peptide consisted in two copies of the SV40 epitopes, flanking sequences and a linker (Table 4). On the other hand, "long OVA" contained only one copy of the epitope, flanked by a non-symmetric number of native amino acids present in the chicken

ovalbumin protein (Table 4). Such differences in configuration, mostly dictated by difficulties in synthesising a long OVA peptide carrying two copies of the epitope, could explain the T cell frequencies data. In this context, it is important to mention that Dekhtiarenko et al. showed that the C-terminal localisation of a T cell epitope radically improved immune protection by Cytomegalovirus-based vaccine vectors (Dekhtiarenko *et al.* 2016). Therefore, I hypothesise that placement of the SIINFEKL motif at the C-terminal end of the long peptide should improve the $CD8^+$ T cell response.

Such considerations are of particular importance to define the strategies to be used to combine T cell epitopes with OMVs. In the current study we have tested the T cell response elicited by synthetic peptides adsorbed to OMVs. An alternative strategy we have recently proposed (Grandi *et al.* 2017, 2018) is to engineer the OMV-producing strains in order to decorate OMVs with the epitopes fused to carrier proteins. Should this strategy be applied, the configuration used to create the fusion protein could strongly affect the frequency of epitope-specific T cells.

All this said, our data strongly suggest that to guarantee a consistent and optimal elicitation epitope-specific T cells with synthetic peptides adsorbed to OMVs, the use of peptides of the same length of the epitopes should be recommended.

The work described in this chapter delivers at least two additional messages. The first one is related to the dose of peptide to be used in combination with OMVs to elicit optimal T cell responses. Our data indicate that amounts of peptides as low as 0.5 µg are sufficient to induce excellent T cell frequencies. Moreover, increasing the doses too much (50 µg) tends to be detrimental to T cell response.

The second message concerns the OMVs used in this study. Such OMVs, named $OMV_{\Delta 60}$, derive from an *E. coli* derivative created in our laboratories by using Synthetic Biology. $OMV_{\Delta 60}$ features the absence of 60 endogenous proteins and the presence of a penta-acylated LPS. We showed that despite the fact that these vesicles have a reduced TLR4 agonistic activity, they maintain an excellent adjuvanticity. This property makes $OMV_{\Delta 60}$ an ideal adjuvant/delivery system for human use.

Chapter 4: *In situ* vaccination of tumours with OMVs

4.1. Introduction

As noted previously, DCs play a key role in determining the effectiveness of an anti-cancer immune response. To optimally induce anti-cancer $CD8^+$ T cell responses, DCs should (1) bind and internalise the antigen, (2) process the antigen and present cancer-specific epitopes in the context of MHC I molecules, and (3) be available at, or rapidly reach, the site where the cancer antigens are present or delivered by vaccination.

In the previous chapters I focused my attention on the first two steps of $CD8^+$ T cell induction. In this chapter, I was interested to see how the route of immunisation could influence the overall $CD8^+$ T cell response. Since it is known that DCs are present at the tumour microenvironment, we hypothesise that delivering the vaccine at the tumour site could be an efficient way not only to activate DCs with the vaccine adjuvant but also to provide the tumour resident DCs with the proper antigens. After antigen internalisation, such DCs should migrate to the draining lymph nodes and activate epitope-specific T cells, which would eventually move to the tumour site to exert their function.

As largely discussed in the Introduction, the concept of *in situ* vaccination is far from being new. In fact, it was first applied by Dr. Coley at the end of the nineteenth century with remarkable success (McCarthy 2006). In the last few years, thanks to the advances in our understanding of cancer immunology, *in situ* vaccination is attracting particular attention. In 2018, Sagiv-Barfi and colleagues showed that *in situ* vaccination of tumours can cause an abscopal effect (Sagiv-Barfi *et al.* 2018). Mice were implanted with syngeneic tumour cell lines at two distal sites and when one tumour was injected with unmethylated CpG and anti-OX40 antibody, they observed complete tumour regression of both injected and lateral tumours. Several *in situ* vaccination clinical trials using different adjuvants are being carried out with sometime spectacular results (Herr and Morales 2008; Hammerich *et al.* 2015, 2019; Frank *et al.* 2018; Aznar *et al.* 2019).

To the best of our knowledge, all *in situ* vaccination studies involve the use of adjuvants only, assuming that the cancer antigens are already available at the tumour

site. Our hypothesis is that the addition of the right, most immunogenic antigens to the adjuvants should further improve the effectiveness of *in situ* vaccination.

An additional motivation to use OMV-based vaccines for *in situ* vaccination, is that the mechanisms of action of OMVs should offer the possibility to combine more than one therapeutic regimen for cancer treatment.

Advances in cancer immunotherapy have shown that cancer patients benefit from combined treatment regimens (Kalbasi *et al.* 2013; Wolchok *et al.* 2017). Cancer vaccines are also showing the same trend. Cancer vaccines combined with anti-angiogenic therapies or immune checkpoint inhibitors have shown promising results (Lopes *et al.* 2018; Mougel *et al.* 2019). In addition, early-stage clinical trials revealed encouraging data for the combination of HPV cancer vaccines and immune checkpoint inhibitors (Shibata *et al.* 2019). It was also demonstrated that combination therapies passed toxicity and safety profiles and reduced drug resistance.

Considering the promising results of neoepitope-based cancer vaccines, *in situ* vaccination and oncolytic virotherapy (see Introduction), it would be interesting to understand whether these strategies combined can work synergistically. We consider our OMVs a suitable therapeutic modality to explore such combination for three reasons. Firstly, they are effective adjuvants and therefore they should be as good as other TLRs agonists in eliciting anti-cancer immune responses. Secondly, as I showed in Chapter 3, they can be decorated with cancer neoepitopes and elicit excellent epitope-specific T cells. Moreover, we have demonstrated that vaccination with the OVA peptide adsorbed to OMVs protect mice challenged with B16-OVA cell line from tumour growth (Figure 20) and we have shown that OMVs engineered with five CT26 neoepitopes (Kreiter *et al.* 2015) inhibited CT26 tumour growth in BALB/c mice (Figure 28). Thirdly, once internalised by neoplastic cells, OMVs have been shown to activate immunogenic cell death, mimicking oncolytic activity (Vanaja *et al.* 2016). OMVs are thought to trigger the cytosolic LPS signalling pathway, leading to NLRP3 activation, inflammasome assembly and pyroptosis. In contrast to apoptosis, cell death by pyroptosis results in cell lysis by plasma-membrane rupture and causes the release of damage-associated molecular pattern (DAMP) molecules (Baroja-Mazo *et al.* 2014; Inoue and Tani 2014; Xia *et al.* 2019). Therefore, they could allow us to join tumour antigen vaccines, adjuvanticity, immunogenicity and tumour cell cytotoxicity in one.

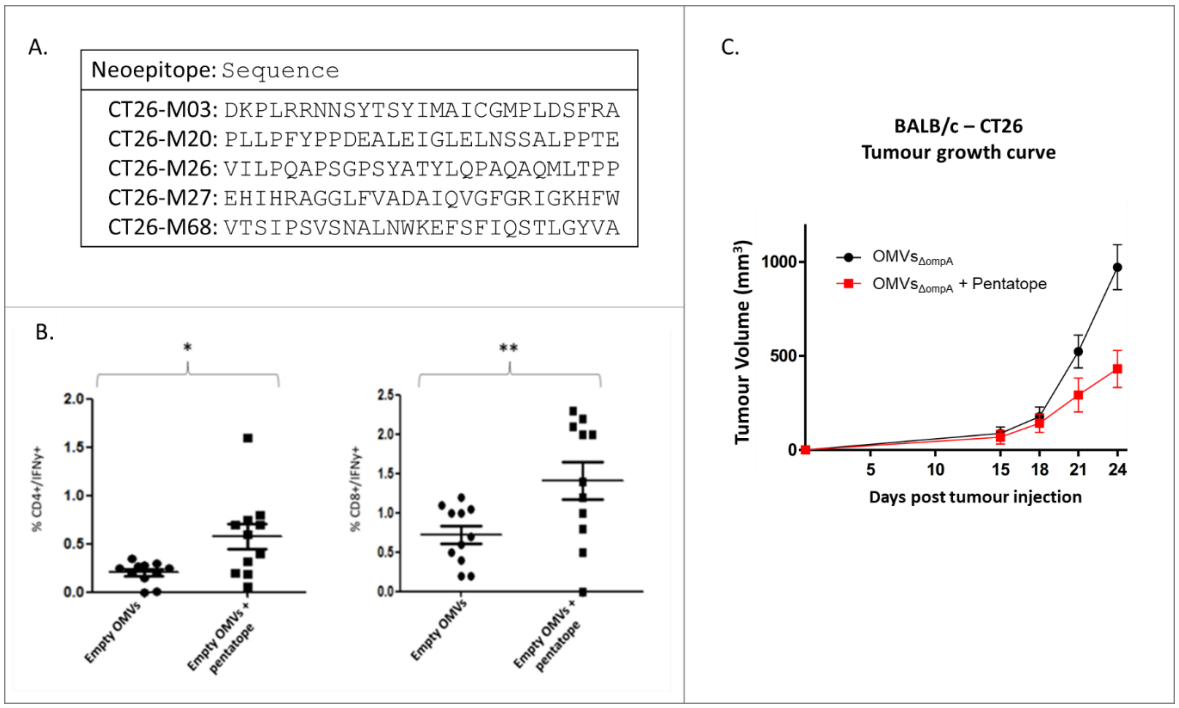

Figure 28: OMV vaccine with pentatope peptides adsorbd induces pentatope specific T cells and protects mice from CT26 tumours. *A, amino acid sequences of each of the pentatope peptides. B, BALB/c mice were vaccinated on day 0 and day 7 with either OMVs$_{\Delta ompA}$ or* OMVs$_{\Delta ompA}$ *adsobed with pentatope peptides. Spleens were collected on day 12. Splenocytes from each group stimulated in vitro with the five peptides of the pentatope or with a negative control peptide. CD4$^+$ and CD8$^+$ T cells expressing IFNγ were analysed by flow cytometry. C, BALB/c mice (n=14) were implanted with CT26 cells on day 0 and vaccinated on day 1, 4, 8, 11, 15, 18 and 21 with either OMVs$_{\Delta ompA}$ or* OMVs$_{\Delta ompA}$ *adsobed with pentatope peptides. Tumour growth was monitored from day 11, the mean (± s.e.m) tumour volume per group plotted. Data accumulated from two independent experiments of 6 mice/group and 8 mice/group, respectively.*

4.2. Results

4.2.1. $OMV_{\Delta 60}$ induced cancer cell lysis

Vanaja and colleagues showed that OMVs derived from *E. coli* BL21 are cytotoxic to the human cervical cancer cell line HeLa (Vanaja *et al.* 2016). Using the lactate dehydrogenase (LDH) assay they demonstrated 20% cell death of HeLa cells. To investigate the ability of our $OMV_{\Delta 60}$ to kill cancer cells in our mouse model, we incubated CT26 cells with increasing concentrations of OMVs for 24 hours and then measured LDH released into the supernatant. LDH is released into the cell culture supernatant during cytoplasmic membrane damage such as cell lysis. The presence of LDH is determined by its activity, which is measured following the two-step enzymatic reaction. LDH catalyses the conversion of lactate to pyruvate causing the reduction of NAD^+ to $NADH/H^+$. Then another catalyst, diaphorase, transfers the H/H^+ from $NADH/H^+$ to the yellow tetrazolium salt, which becomes reduced to form a red formazan product. The percentage of cytotoxicity was calculated so that the negative control was equal to 0% and the positive control equal to 100%. Both $OMVs_{\Delta 60}$ and $OMVs_{\Delta ompA}$ cause some cell killing. $OMVs_{\Delta ompA}$ caused a maximum of 10% cell death and $OMVs_{\Delta 60}$ approximately 7% cell death (Figure 29). In summary, our OMVs have some cytotoxic activity on CT26 cells following the trend observed by Vanaja et al.

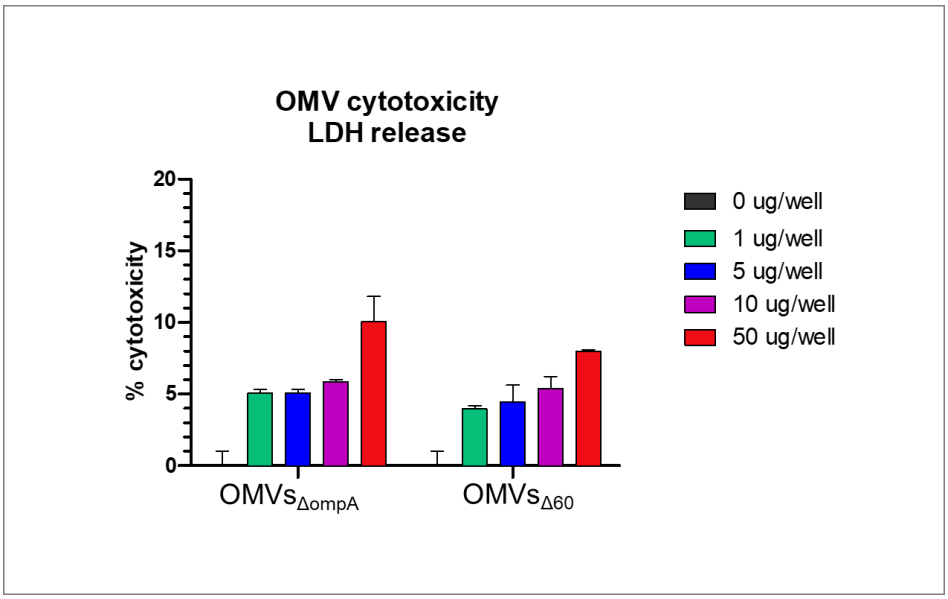

Figure 29: Analysis of OMV cytotoxicity to CT26 cells. *OMVs derived from strains BL21(DE3)ΔompA and BL21(DE3)Δ60 were incubated with 10,000 CT26 cells per well and at increasing concentrations. OMVs cytotoxicity was measured using the lactate dehydrogenase (LDH) release assay. The percentage cytotoxicity was calculated using the equation cytotoxicity % = (sample-negative)/(positive-negative)x100. The data are representative of four repeat experiments.*

4.2.2. *In situ* vaccination of OMVs inhibits growth of established tumours in the C57BL6-B16-OVA cancer model

The experimental design of our first *in situ* vaccination experiment involves the use of C57BL6 mice with syngeneic tumour cell line B16-OVA. B16-OVA contains a stably transfected plasmid encoding chicken ovalbumin, allowing its secretion into the B16F10 murine melanoma cells. It is a common tool for studying OVA as a model antigen in cancer immunology. We have already demonstrated in the previous chapter, that OMVs decorated with OVA peptide can stimulate an anti-OVA $CD8^+$ T cell response. We have also shown that mice bearing one tumour, have inhibited tumour growth when vaccinated with OMVs plus the OVA peptide. Here we designed a two-tumour experiment in order to assess the effect *in situ* vaccination of OMVs. We injected C57BL6 mice with B16-OVA cells at two sites, one on each flank. The tumour size was monitored every 2 days on both sides of the animal using a digital calliper and expressed as a volume (volume = $width^2$ x length x 0.5). When the tumour volume reached 50-100 mm^3 mice were vaccinated *in situ* directly into just one of the tumours. This was repeated every two days for three vaccinations in total (Figure 30A). Vaccination groups were as follows: PBS negative control, $OMVs_{\Delta 60}$ and $OMVs_{\Delta 60}$ with OVA 1X peptide adsorbed.

In the C57BL6-B16-OVA syngeneic model, the *in situ* vaccinated tumour, after vaccination with PBS control grew as expected (Figure 30C). However, the lateral tumour in the PBS control groups grew slower than that of the *in situ* tumour or did not grow. This may be an effect of the two-tumour model, as all mice had a dominant/primary (faster-growing) tumour which could induce an immune response acting at the distal tumour site. In all OMV treatment groups tumours vaccinated *in situ* regressed after vaccination. In particular, the $OMV_{\Delta 60}$ treatment caused complete regression of the *in situ* vaccinated tumours in 50% of the mice. The remaining 50% also experienced good tumour regression of the vaccinated tumour. Given the effective inhibition of $OMV_{\Delta 60}$ we could not observe any additional benefit of the combination of $OMVs_{\Delta 60}$ + OVA peptide. The tumour growth was similar for $OMVs_{\Delta 60}$ with or without the OVA peptide, conferring almost complete tumour inhibition (Figure 30). This inhibition was more effective than that previously observed with systemic vaccination (Figure 20B).

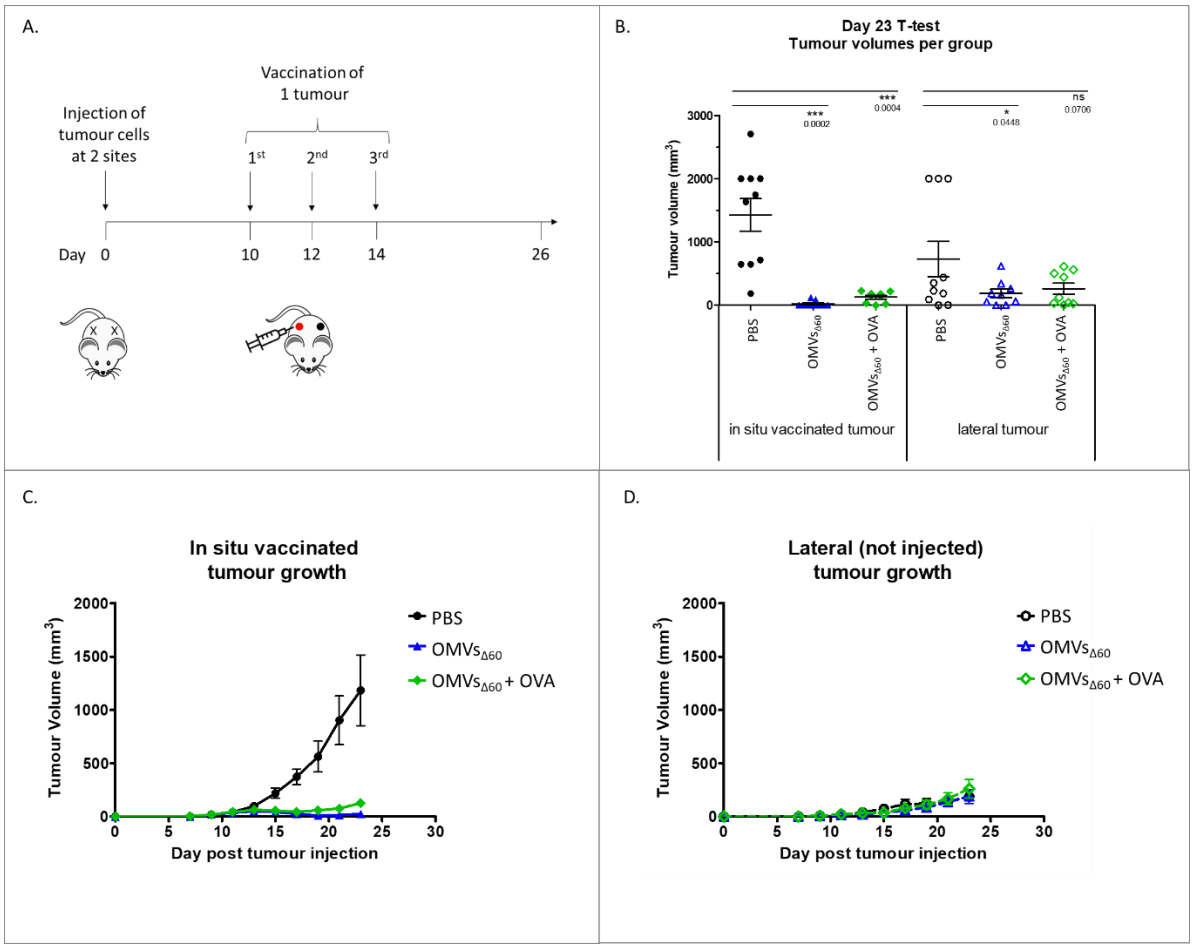

Figure 30: C57BL6 B16-OVA tumour growth with in situ vaccination tumour treatment. *Tumour cells were subcutaneously injected at two distal sites when tumour volume reached 50-100 mm^3, one tumour was vaccinated in situ. Then vaccinations were given every two days for three vaccinations with PBS, OMV$_{\Delta 60}$ or OMV$_{\Delta 60}$ adsorbed with 100 µg OVA. Tumour volumes of both the injected and later tumour were recorded every two days. A, Example vaccination schedule. B, Analysis of both situ injected tumour volumes and lateral tumour volumes in mice from each group at day 23. C, Tumour growth curves of tumours from each group that received in situ vaccination. D, Tumour growth curves of lateral tumours, not directly injected into. Humane endpoints were always respected therefore in the PBS group some of the mice were sacrificed earlier than day 26 and these mice were assigned single tumour volumes of 2000 mm^3. Statistical significance was calculated using an unpaired one-tailed T-test with Welch's correction. Not significant (ns)= P>0.1; *= P<0.1; **= P<0.01; ***= P<0.001.*

4.2.3. *In situ* vaccination of OMVs with neoepitopes inhibits tumour growth in both injected and lateral tumours

To confirm the effectiveness of *in situ* vaccination with OMV$_{\Delta 60}$, we used the BALB/c CT-26 mouse model. We had previously demonstrated that systemic immunisation of OMVs$_{\Delta ompA}$ engineered with five CT26 neoepitopes (pentatope) partially protects mice from tumour growth. For the two-tumour model, CT26 cells were injected subcutaneously at sites on both the right and left flank of the mice. As previously, tumour size was measured with a digital calliper and expressed as volume (volume = width^2 x length x 0.5). Bodyweight and mouse well-being were also closely

monitored. When tumour size reached 50-100 mm^3 mice were vaccinated *in situ* in just one of the tumours. Mice were given a total of 3 vaccinations every 2 days, into the same tumour. There were three treatment groups: PBS control, $OMV_{\Delta 60}$ and $OMV_{\Delta 60}$ + pentatope. Mice were sacrificed when the tumour volume of one tumour reached ≥ 2000 mm^3, or the sum of tumour volume reached 3000 mm^3.

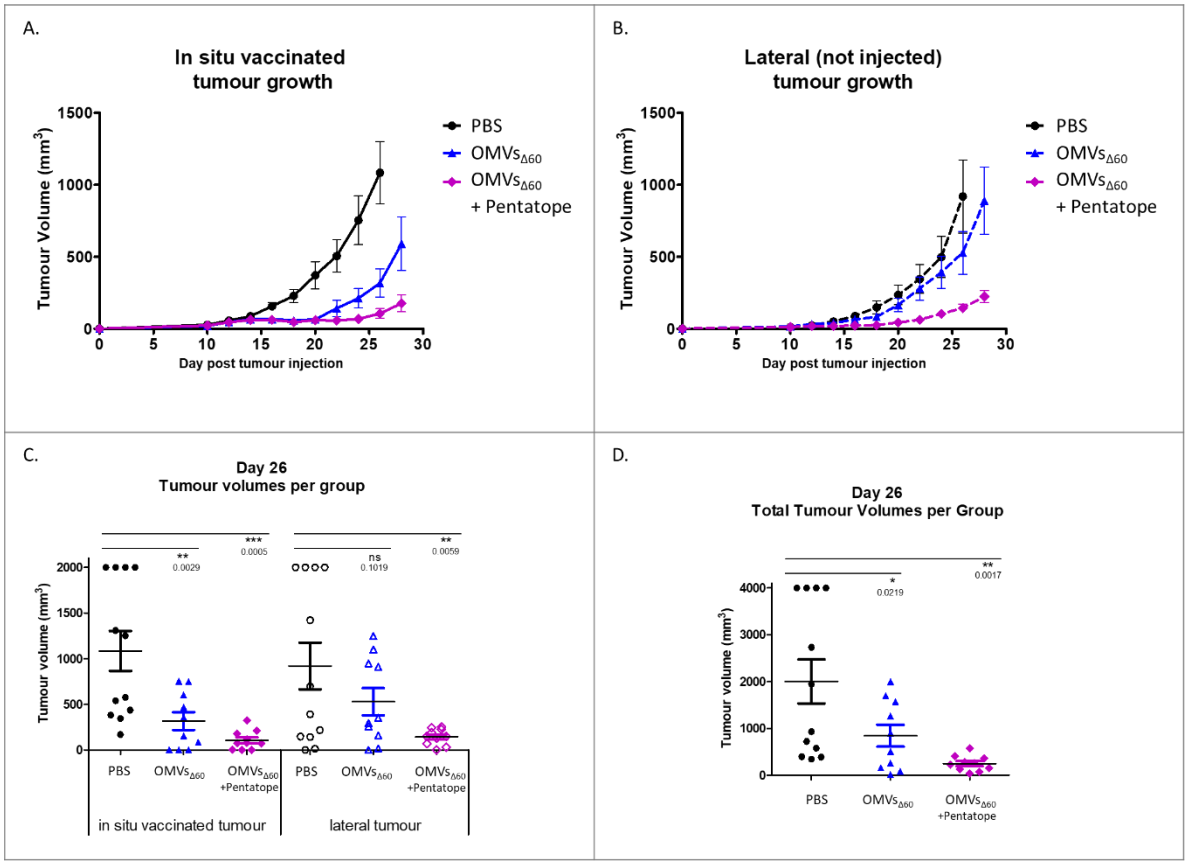

Figure 31: BALB/c CT26 tumour growth with in situ vaccination tumour treatment*. Tumour cells were subcutaneously injected at two distal sites when tumour volume reached 50-100 mm3, one tumour was vaccinated in situ. Then vaccinations were every two days for three vaccinations with PBS, $OMV_{\Delta 60}$ or $OMV_{\Delta 60}$ adsorbed with 100 µg pentatope. Tumour volumes of both the injected and later tumour were recorded every two days. A, Tumour growth curves of tumours from each group that received in situ vaccination. B, Tumour growth curves of lateral tumours, not directly injected into. C, Analysis of both situ injected tumour volumes and lateral tumour volumes in mice from each group at day 26. D, Analysis of the sum of tumour volumes per mouse in each group at day 26. Humane endpoints were always respected therefore in the PBS group some of the mice were sacrificed earlier than day 26 and these mice were assigned single tumour volumes of 2000 mm^3. Statistical significance was calculated using an unpaired one-tailed T-test with Welch's correction. Not significant (ns)= P>0.1; *= P<0.1; **= P<0.01; ***= P<0.001.*

In the PBS control group, after vaccination, both the *in situ* vaccinated tumour and the lateral tumour continued to grow as expected (Figure 31 A & B). In all OMV treatment groups, the *in situ* vaccinated tumour initially regressed after local vaccination and significantly inhibited tumour growth compared to PBS control (Figure 31 A). *In situ* vaccinated tumours in mice treated with $OMV_{\Delta 60}$ initially regressed, but

were generally re-growing 10 days after the first vaccination. This group also experienced a minimal effect on the lateral tumour, in which growth was slow during the vaccination period, but resumed as normal to match that of the PBS group (Figure 31B). Finally, $OMV_{\Delta 60}$ + pentatope *in situ* vaccination lead to tumour regression in 8 out of 10 of the vaccinated tumours and inhibition of the remaining two. Even with marginal re-growth at the end of the experiment, at day 26 the average size of tumours in the $OMV_{\Delta 60}$ + pentatope group was just 77.6 mm^3. The $OMV_{\Delta 60}$ + pentatope treatment was also effective at tumour inhibition of the lateral tumour as well as the locally vaccinated tumour (Figure 31C). This demonstrated an abscopal effect in this treatment group. It was also therefore the most effective as blocking total tumour growth in mice as demonstrated by analysis of the sum of the two tumours in the same mouse (Figure 31D).

4.3. Discussion

The aim of these experiments was to test whether OMVs are suitable *in situ* cancer vaccine agents and understand if the combination of OMV adjuvanticity, oncolytic activity and use as a peptide epitope vaccine vehicle, could effectively inhibit tumour growth when administered *in situ*. In addition, we wanted to understand whether this combination could lead to abscopal tumour immunity.

To be effective cancer vaccines must include adjuvants and protective antigens. As far as we know, data demonstrating *in situ* vaccination of tumours depends on the presence of tumour antigens within the injected tumour, and therefore relies on the simple administration of adjuvants only, or sometimes with immuno-potentiators. The rationale being that the presence of tumour antigens in the tumour is enough to promote anti-tumour immune responses and antigen spread. Data obtained both in preclinical and clinical experiments demonstrate that this is possible. Adjuvant only formulations are advantageous because they can be used against a wide variety of cancers in any patient. There is no need to know the cancer-specific or even patient-specific mutations. Meaning that this type of drug could be used on a large number of patients. Additionally, it would be more cost-effective to manufacture. These advantages are the reason that so far no attempts have been described investigating whether the addition of tumour-specific antigens to the adjuvant could potentiate the efficacy of classical *in situ* vaccination approaches.

With our experiments we have demonstrated that OMVs are excellent adjuvants for *in situ* vaccination. This is not surprising, considered the number of different MAMPs (LPS, lipoproteins, peptidoglycan, etc.) that decorate OMVs. Moreover, we believe that the effectiveness of OMVs in *in situ* vaccination is also mediated by their oncolytic activity. Such oncolytic activity, previously demonstrated by Vanaja et al., was confirmed to be also a property of our $OMV_{\Delta 60}$.

Probably the most important results from our work is that *in situ* vaccination could benefit from the addition of cancer neoepitopes. When we vaccinated BALB/c mice with PBS, $OMV_{\Delta 60}$ decorated with CT26-specific neoepitopes we inhibited the growth of both injected and lateral (not injected) tumours. In addition, this enhanced activity also led to the expansion of a sufficient number of T cells, which could enter the circulation and reach the distal tumour.

There are several limitations to the *in situ* experiments. One of which is the high concentration (100 µg) of peptide used in the OMV + peptide treatment groups for *in situ* vaccination compared to the 5 µg we used in the previous chapter for T cell response experiment. This is because the work was performed in parallel and we did not yet have the results of the OMVs with peptide titration experiments (Figure 25). Future studies will involve understanding the most efficient dose for the *in situ* vaccination modality. Another limitation is that we do not have data for tumour inhibition using *in situ* cancer vaccination in a tumour mouse model bearing just one tumour. This is because we first wanted to know if we could achieve an abscopal effect, in order to understand whether *in situ* cancer vaccination would be a good administration method for OMVs. We are now starting experiments with one tumour models as well as tumour infiltration lymphocytes studies.

Future experiments will also be addressed to better understand the mechanisms of action of OMV-based *in situ* vaccination. Due to their adjuvanticity, OMVs could stimulate the recruitment of DCs at the tumour site, thus facilitating the antigen uptake and processing. Also, OMVs could modify the cellular component, particularly the concentrations of macrophages, T_H1 cells and T_{REG}. Such experiments will be carried out by collecting the tumours, separating the different cellular populations and characterising them by flow cytometry.

Chapter 5: Final discussion

The unique adjuvanticity of OMVs means they are becoming more and more recognised as useful tools or vaccination. There are already examples in the clinic of OMVs as prophylactic vaccines against infectious diseases, such as Bexsero for meningitis B. However, there is far less work describing the use of OMVs for cancer vaccines or how OMVs can be used to elicit T cell responses to antigens. To further explore the OMV cancer vaccine platform we need to better understand (1) how OMVs can be used to elicit T cell responses against peptide antigens, (2) if OMV vaccines can enable cross-presentation of antigens, (3) the best method of administration of OMVs to achieve effective immunisation.

The goal of this thesis was to investigate antigen delivery and presentation of OMV-based cancer vaccines. I used a three-pronged approach. Firstly, I aimed to engineer OMVs with a construct for the expression of scFv on the surface, in order to target OMVs to the DEC205 receptor. Secondly, we studied the ability of OMVs induce $CD8^+$ T cell responses to peptide epitopes when they are adsorbed to OMVs and gain insight into the possible formulation of peptide antigens. Thirdly, we investigated the use of OMVs *in situ* cancer vaccination because we believed this mechanism may be the optimal method for OMV-based cancer vaccines.

We have achieved some important results with regard to the future design and administration of OMV based cancer vaccines.

Firstly, I demonstrated that OMVs can be engineered to express scFv on the surface. This was achieved by fusing lipidated FhuD2 to scFv. Though we had previously used FhuD2 as a carrier for a B cell specific polypeptide (Grandi *et al.* 2018), FhuD2 has not previously been described as a protein carrier able to chaperone large heterologous proteins, such as scFv into OMVs. In addition, I showed that the $OMVs_{\Delta 60}$, designed and engineered in our group over the last few years, are superior vehicles for the expression of the FhuD2-αmDEC205 fusion protein. Surface expression of FhuD2-αmDEC205 in $OMV_{\Delta 60}$ was greatly improved over that of expression in $OMV_{\Delta ompA}$. I was also able to engineer two other scFvs (HELD1.3 and mCD40), for which we demonstrated expression in OMVs and with a surface exposition. Then I showed increased internalisation of

FhuD2-αmDEC205 OMV over the control OMVs (FhuD2-αHELD1.3) after 30 minutes of incubation with JAWSII cells. Thus demonstrating that our FhuD2-αmDEC205 OMVs bind to mDEC205 and thus internalise more rapidly.

Secondly, we demonstrated that $OMVs_{\Delta 60}$ are an advantageous OMV cancer vaccine platform. We established that $OMVs_{\Delta 60}$ have better adjuvanticity versus reactogenicity profile than $OMVs_{\Delta ompA}$, in both mouse and human assays. When $OMVs_{\Delta 60}$ adsorbed with MHC I specific antigen peptides were used to vaccinate mice, a good $CD8^+$ T cell immune response was induced. As machine learning becomes an ever more important tool for drug discovery, there are now algorithms for predicting peptide processing for presentation on MHC molecules, such as those used in the immune epitope database (IEBD) analysis resource (Fleri *et al.* 2017). We believe that as this knowledge develops we will be able to design peptide and proteins with specific cleavage site that specifically direct processing toward MHC presentation. Studies into the design of synthetic long peptides will also contribute greatly to this cause by improving understand of requirements for flanking regions which convey efficient recessing for MHC presentation, such as work by Rabu et al (Rabu *et al.* 2019).

Thirdly, the incorporation of neoepitopes into *in situ* cancer vaccines can improve their therapeutic effect. The addition of the pentatope also caused inhibition of the second, lateral tumour, demonstrating an abscopal effect. This effect is incredibly important for cancer patients because it means that such a therapy could combat metastatic tumour growth. Or simply inhibit the growth of small secondary tumours which are not yet detectable and have yet to manifest clinically. It has been suggested that directly inducing antigen release is the critical step for initiating an abscopal immune response by *in situ* vaccination (Marabelle *et al.* 2017). If the presence of the right antigens is critical then it opens the door for the addition of tumour-specific antigens to *in situ* vaccine formulations. One of the advantages of classical *in situ* vaccination is that the identification of patient-specific epitopes is not required. However, here we showed for the first time that the efficacy of *in situ* vaccines can be improved by co-administration of cancer specific neoepitopes and adjuvants. The increased concentration of immunogenic and protective epitopes in the tumour microenvironment appears crucial for the efficacy of the *in situ* vaccine.

Chapter 6: Material and methods

6.1. Bacterial strains and culture conditions

OMVs were purified from *E. coli* BL21(DE3)Δ*ompA* (Fantappiè *et al.* 2014) strain or *E. coli* BL21(DE3)Δ*60* strain (Zanella *et al.* 2020). Whereas insertion of fusion proteins constructs into plasmids using the polymerase incomplete primer extension (PIPE) method (Klock and Lesley 2009) was carried out using the *E. coli* HK-100 strain.

OMV producing strains were routinely grown in Luria-Bertani (LB) broth (Miller) (Sigma L3522) at 30°C and/or 37°C and 200 rpm. When required, Ampicillin (Amp) was added to a final concentration of 100 µg/ml. Stock preparations of strains in LB and 20% glycerol were stored at -80°C. Each bacterial manipulation started from an over-night culture inoculated from a frozen stock or single colony on an LB agar plate.

6.1.1. Chemically competent cell preparation

All *E. coli* based strains were grown overnight in a volume of 5 mL of LB at 37°C and at 200 rpm. This was used to inoculate 100 mL of LB broth starting from OD_{600} = 0.1. The culture was incubated at 37°C, 200 rpm until an OD_{600} of 0.4-0.6 was reached. Bacterial suspension was centrifuged at 2500g for 20 min at 4°C. The bacterial pellet was resuspended in 40 ml of ice cold and $MgCl_2$ 100mM and left on ice for 30 minutes. The suspension was centrifuged at 2500g for 20 min at 4°C and resuspended in 4 ml of cold and sterile $CaCl_2$ 100 mM, glycerol 15% (v/v). Aliquots of 110 µl were stored at -80°C.

6.1.2. Chemically competent cell transformation

For transformation, 50 µl of chemically competent bacterial cells were thawed on ice and mixed with 100 ng of purified plasmid containing the gene of interest or a mix of amplified vector and insert with compatible overhangs (PIPE method). Tubes were incubated on ice for 30 minutes. Cell were heat-shocked at 42°C for 1 minute and immediately transferred on ice for 2 minutes. Recovery was performed at 37°C for 1 hour and shaking at 200 rpm in a final volume of 1 mL of LB and subsequently 500 ul were plated overnight on LB-Agar (Luria/Miller, Carl Roth, X969.2), containing Ampicillin at final concentration of 100 µg/mL.

6.2. Fusion protein construct generation

Plasmid insertions using the polymerase incomplete primer extension (PIPE) method. Full constructs containing the pet protein, lpp lipobox and leader sequence and FhuD2 were previously cloned in our laboratory in the pET21b+ plasmid. The synthetic gene encoding for the scFv of NLDC-145 (anti-mouse DEC205) was designed and purchased from GeneArt® Gene Synthesis (LifeTechnologies). The protein sequence was obtained from Demangel et al (Demangel *et al.* 2005) and codon optimised for expression in *E. coli*.

Anti-mouseDEC205 scFv codon optimised sequence:

```
GAA GTT AAA CTG CAG CAG AGC GGC ACC GAA GTT GTT AAA CCG GGT GCA AGC GTT AAA CTG  < 60
E   V   K   L   Q   Q   S   G   T   E   V   V   K   P   G   A   S   V   K   L

AGC TGT AAA GCA AGC GGT TAT ATC TTC ACC AGC TAT GAT ATT GAT TGG GTT CGT CAG ACA  < 120
S   C   K   A   S   G   Y   I   F   T   S   Y   D   I   D   W   V   R   Q   T

                  >VH domain
CCG GAA CAA GGT CTG GAA TGG ATT GGT TGG ATT TTT CCT GGT GAA GGT AGC ACC GAA TAT  < 180
P   E   Q   G   L   E   W   I   G   W   I   F   P   G   E   G   S   T   E   Y

AAC GAA AAA TTC AAA GGT CGT GCA ACC CTG AGC GTT GAT AAA AGC AGC AGC ACC GCA TAT  < 240
N   E   K   F   K   G   R   A   T   L   S   V   D   K   S   S   S   T   A   Y

ATG GAA CTG ACC CGT CTG ACC AGC GAA GAT AGC GCA GTT TAT TTC TGT GCA CGT GGT GAT  < 300
M   E   L   T   R   L   T   S   E   D   S   A   V   Y   F   C   A   R   G   D

TAT TAT CGT CGC TAT TTT GAT CTG TGG GGT CAG GGC ACC ACC GTT ACC GTT AGC AGC GGT  < 360
Y   Y   R   R   Y   F   D   L   W   G   Q   G   T   T   V   T   V   S   S   G

                  >Linker
GGT GGT GGT AGT GGT GGC GGT GGT TCA GGC GGT GGC GGT AGC GAT ATT CAG ATG ACC CAG  < 420
G   G   G   S   G   G   G   G   S   G   G   G   G   S   D   I   Q   M   T   Q

AGT CCG AGC TTT CTG AGC ACC AGC CTG GGT AAT AGC ATT ACC ATT ACC TGT CAT GCA AGC  < 480
S   P   S   F   L   S   T   S   L   G   N   S   I   T   I   T   C   H   A   S

CAG AAC ATT AAA GGT TGG CTG GCA TGG TAT CAG CAG AAA AGC GGT AAT GCA CCG CAG CTG  < 540
Q   N   I   K   G   W   L   A   W   Y   Q   Q   K   S   G   N   A   P   Q   L

                  >VL domain
CTG ATC TAT AAA GCC AGC AGC CTG CAG AGC GGT GTT CCG AGC CGT TTT AGC GGT AGC GGT  < 600
L   I   Y   K   A   S   S   L   Q   S   G   V   P   S   R   F   S   G   S   G

AGT GGC ACC GAT TAC ATT TTT ACC ATT AGC AAT CTG CAG CCG GAA GAT ATT GCA ACC TAT  < 660
S   G   T   D   Y   I   F   T   I   S   N   L   Q   P   E   D   I   A   T   Y

TAT TGT CAG CAC TAT CAG AGC TTT CCG TGG ACC TTT GGT GGT GGC ACC AAA CTG GAA ATT  < 720
Y   C   Q   H   Y   Q   S   F   P   W   T   F   G   G   G   T   K   L   E   I

AAA CGT GCA GCC  < 732
K   R   A   A
```

Sequences for the HELD1.3 Ab can be found at Uniprot P01820 for the VH region and P01635 for the VL region. Whereas the FGK45 sequence is deposited in NCBI under HQ662570.1 for the VH region and HQ662569.1 for the VL region (there are also respective protein IDs AEI27236.1 and AEI27235.1). All three scFv were cloned with the same $(G_4S)_3$ linker between the VH and VL region.

6.2.1. Cloning of fusion protein constructs

The polymerase incomplete primer extension (PIPE) method (Klock and Lesley 2009) was used for the cloning of the various constructs. To produce the final constructs the following plasmids were linearised: pET lpp, pET lpp-FhuD2 and pET pet, using forward and reverse primers for vector PCR (V-PIPE). The scFv was amplified using forward and reverse primers containing overhang regions to match the flanking insertion site of the respective plasmid (I-PIPE). The pET lpp1-9-ompA49-159-scFv (or pET lpp-TompA-scFv) required cloning of ompA49-159 out of the genome, and insertion of lpp aminoacids 2-9 by mutagenisis PIPE (M-PIPE). For PIPE method PCRs, Q5 high-fidelity DNA polymerase (NEB, M0491) used as according to manufacturer's instructions. A list of primer and plasmids used for cloning can be found in Table 5. The PCR products were digested with DpnI (NEB, R0176). Digested I-PIPE and V-PIPE products, combined (1:1 ratio, 2 µl final volume) and used to transform *E. coli* HK100 chemically competent cells. Positive clones identified by colony PCR as below. Construct sequences were confirmed by sequence analysis (Eurofins) before transformation into BL21(DE3)Δ*ompA* and BL21(DE3)Δ*60* strains.

Table 5: List of plasmids

Plasmid name	**Source**
pET21b+_lpp_FhuD2	In-house (Irene *et al.* 2019)
pET21b+_pet*	In-house - Constructed by colleagues in Siena
pET21b+_lpp_scFv mDEC205	Cloned
pET21b+_pet*_scFvmDEC205	Cloned
pET21b+_lpp1-9_TompA46-159_scFvmDEC205	Cloned
pET21b+_lpp_FhuD2_scFvmDEC205	Cloned
pET21b+_lpp_FhuD2_scFvHELD1.3	Cloned

pET21b+_lpp_FhuD2_scFvmCD40	Cloned

Table 6: List of primers used for cloning

Code #	Primer name	Sequence
Primers for vector PCR		
SI-03	vec_for_pET (no tail)	TAATGGCGAATGGGACGCGCCCTGTAG
SI-04	vec_rev_Lpp 1 (no tail)	GCAACCTGCCAGCAGAGTAGAACCCAG
SI-14	LF vec_petLS-for	TCTGCAGACAAAGACAACTCTGCG
SI-15	LF vec_omprev	GGCCTGCGCTACGGTAGCGAAA
SI-03	vec_for_pET (no tail)	TAATGGCGAATGGGACGCGCCCTGTAG
SI-11	vec_rev_OmpA159	GTTGTCCGGACGAGTGCCGATGGTG
SI-41	vec for FhuD2	GGGAACCAAGGTGAAAAAAATAACAAAGC
SI-42	vec rev lpp	CGTTGGACGGTCGTCTCATCTTGG
CI-1072	Nohis flag F	CATCACCATCACCATCACGATTACAAAGA
CI-1071	FhuD2-v-R	TTTTGCAGCTTTAATTAATTTTTC
Primers for I-PIPE		
SI-01	ins_for_Omp 46	CTGCTGGCAGGTTGCAACCCGTATGTTGGCTTTGAAATGGG
SI-02	ins_rev_Omp 159	tcccattcgccaTTAGTTGTCCGGACGAGTGCCGATG
SI-09	ins_for_scFv amDEC205 OmpA159	ACTCGTCCGGACAACGAAGTTAAACTGCAGCAGAGCGG
SI-10	ins_rev_scFv amDEC205 pET	tcccattcgccaTTAGGCTGCACGTTTAATTTCCAG
SI-12	ins_for_scFv amDEC205 LSOmpA	ACCGTAGCGCAGGCCGAAGTTAAACTGCAGCAGAGCGG
SI-13	ins_rev_scFv amDEC205 LSPet	GTCTTTGTCTGCAGAGGCTGCACGTTTAATTTCCAG
SI-16	ins_for_scFv amDEC205 Lpp1	CTGCTGGCAGGTTGCGAAGTTAAACTGCAGCAGAGCGG
SI-10	ins_rev_scFv amDEC205 pET	tcccattcgccaTTAGGCTGCACGTTTAATTTCCAG
SI-45	ins for scFvmDEC205 FhuD2tail	TAATTAAAGCTGCAAAAGAAGTTAAACTGCAGCAGAGCGG
SI-46	ins rev scFvmDEC205 pETtail	GATGGTGATGGTGATGTTAGGCTGCACGTTTAATTTCCAGTTTGG

SI-50	ins for scFv D1.3 FhuD2tail	TAATTAAAGCTGCAAAACAGGTGCAGCTGAAAGAAAGCGG
SI-51	ins rev scFv D1.3 pETtail	GATGGTGATGGTGATGTTAACGTTTAATTTCCAGTTTGGTGCCACC
SI-52	ins for scFv FGK45 FhuD2tail	TAATTAAAGCTGCAAAAGAAGTTCAGGTTGTTGAAAGTGATGG
SI-53	ins rev scFv FGK45 pETtail	GATGGTGATGGTGATGTTAACGTTTCAGTTCCAGTTTGGTGC
Primers for M-PIPE		
SI-17	ins_for_Lpp2-5	GCTCCAGCAACGCTAACCCGTATGTTGGCTTTGATG
SI-18	ins_rev_Lpp2-5	GTTAGCGTTGCTGGAGCAACCTGCCAGCAGAGTAG
SI-19	ins_for_Lpp6-9	CGCTAAAATCGATCAGAACCCGTATGTTGGCTTTGAAATGGG
SI-20	ins_rev_Lpp6-9	GTTCTGATCGATTTTAGCGTTGCTGGAGCAACCTGC
Primers for screening		
SI-58	for seq GGGGSG	GGTGGTGGTGGTAGTGGTGG
CI-1073	FhuD2 3'FOR	GTTGATGCTGGTACATACTGGTAC
CI-1004	T7 promoter	TAATACGACTCACTATAGGG
CI-1005	T7 term	GCTAGTTATTGCTCAGCGG

All primers with code number beginning SI were designed by myself and CI by Carmela Irene

6.2.1.1. Colony PCR and agarose gel electrophoresis

To check which colonies grown on the LB agar + Ampicillin plate contained the plasmid. The reaction mixture GoTaq® Green Master Mix 2X (Promega, M712B-C), forward and reverse primers 10 µM, bacterial cells picked from the plates and nuclease-free water to a final volume of 25 µl. PCR cycle programmed as according to GoTaq® instructions.

The PCR products were analysed by agarose gel electrophoresis (1% agarose gel) in tris-acetate-EDTA (TAE) buffer (Euroclone, EMR064001) at 100 V and the positive samples were cultured to extract the plasmid, subsequently sequenced. Forward and reverse primers used for each plasmid are in Table 6.

6.2.1.2. Plasmid purification

Overnight culture of single colonies were centrifuged at 4°C for 20 minutes at 2500g. Plasmid DNA was harvested from the pellet using the NucleoSpin Plasmid kit (Macherey-Nagel, 740588.250) following manufacturer protocol and the pDNA was eluted in 50 µl of sterile ultrapure H_2O.

6.3. OMV generation and purification

6.3.1. Small scale production for fusion protein expression

Recombinant clones were grown in 100 ml of LB broth and ampicillin (Carl Roth, K029.2) with a final concertation of 100 µg/mL, starting from an OD_{600} of 0.1, at 30°C. When a value of 0.4-0.6 of OD_{600} was reached, recombinant protein expression was induced by adding Isopropyl 6-D-1-thiogalactopyranoside (IPTG) (Carl Roth, CN08.3) to a final concentration of 0.1 mM. After 4 hours of incubation at 30°C and at 200 rpm, samples were centrifuged at 2500g for 20 min at 4°C. The supernatant, containing OMVs, was filtered using a 0.22 µm filter (Millipore, SLGP033RB).

OMVs were purified by centrifugation using the Optima X series ultracentrifuge (Beckman Coulter) with an SW-32-Ti swing rotor, at 32,000 rpm (~175,000g) for 2 hours at 4°C. OMVs contained in the pellet were resuspended in 100 µl of sterile PBS.

6.3.2. Medium scale fermentation for empty OMV production

E. coli BL21(DE3)Δ*ompA* or *E. coli* BL21(DE3)Δ*60* strains were cultured using the EZ control bioreactor (Applikon). Condition were set as follows: volume 2 l; temperature 30°C until OD_{600} = 0.5, then growth continued at 25°C; pH 6.8 (±0.2), dO_2 > 30%; rpm 280-500 rpm; at OD_{600} = 1.0 feed was performed by adding ampicillin (100 µg/ml), glycerol (15 g/l), $MgSO_4$ (0.25 g/l).

Culture supernatants were separated from living bacterial cells by a centrifugation step at 6,000g for 20 minutes followed by a filtration using a 0.22 µm filter (CytoOne® Bottle Top Filtration Unit, CC6032-9233). OMV were up concentrated and buffer exchanged into PBS using the tangential flow filtration system (ÄKTA flux) with a hollow fibre cartridge UFB-500-C-3MA (GE).

OMV concentrations were determined using the DC™ Protein Assay (Bio-Rad, 5000116).

6.4. SDS-PAGE and Western Blots

6.4.1. SDS-PAGE

OMVs were mixed with Laemmli loading buffer 2X (62.5 mM Tris-HCl, pH 6.8 buffer 25% glycerol 2% SDS 0.01% bromophenol blue, 2% dithiothreitol). Then denatured for 10 min at 95°C and loaded on an Any kD Criterion™ TGX™ precast polyacrylamide gel (Bio-Rad, 5678124) along with PM2610 protein marker (Smobio, PM2610) and run in Tris-glycine-SDS (TGS) (Biorad, 161-0772) running buffer at 180 volts for 50 minutes. The gel was stained with Problue Safe Stain (Giotto Biotech, G00PB001). Images of the gel were acquired using the Odyssey Infrared Imaging System (LI-COR Biosciences).

6.4.2. Western blot

OMV proteins separated by SDS-PAGE as above, (note gels were not stained). Proteins in the gels were transferred onto nitrocellulose membrane (iBlot™ Transfer Stack, nitrocellulose, Thermo Fisher Scientific) with iBlot® Dry Blotting System (Thermo Fisher Scientific). The membranes were blocked in blocking solution containing 10% skimmed milk and 0.05% Tween 20 dissolved in PBS (PBST) at room temperature (RT) for 30 minutes with agitation. Then stained with 0.5 µg/ml rabbit polyclonal α-FhuD2 antibodies (Genscript, epitope sequence: MDDGKTVDIPKDPK) in 3% skimmed milk in PBST, o/n at 4°C with agitation. After washing three times, for 5 minutes PBST, membranes were incubated with 1:2,000 dilution of peroxidase-conjugated anti-rabbit IgGs (Dako) for 1 hour in 3% skimmed milk in PBST. After three washing steps of 5 minutes in PBST and one wash of 5 minutes in PBS, proteins were detected using the ECL Star Enhanced Chemiluminescent Substrate (EuroClone, EMP001005) and imaged using the ChemiDOC (BioRAD) instrument.

6.5. Phase partitioning with Triton X-114

Protein phase partitioning with Triton X-114 (Sigma, 93422) was performed as follows. 50 µg of OMVs were diluted in 450 µl of PBS, then ice cold TritonX-114 (10%) was added to a final concentration of 1% and the OMV-containing solution was incubated at 4 °C for 1 hour shaking. The solution was then heated at 37 °C for 10 minutes and the aqueous phase was separated from the detergent by centrifugation at

13,000g for 10 minutes. Proteins in both phases were then precipitated by standard chloroform/methanol procedure, separated by SDS-PAGE electrophoresis and the protein of interest visualised by Western blot.

6.6. Flow cytometry of Bacteria

Bacterial strains were grown at 37°C and 200 rpm in LB medium (starting OD_{600} = 0.1) and, when the cultures reached an OD_{600} of 0.5, protein expression was induced by addition of 0.1 mM IPTG for 2 hours. After induction, a volume corresponding to OD_{600} =1 was collected from each culture and centrifuged at 14,000 rpm for 10 minutes. Using 1 ml of the buffer PBS with Bovine serum albumin (Fischer, 11413164) at 1% (PBS/BSA 1%) to resuspend pelleted bacteria. It was further diluted 1:50 in PBS/BSA 1%. Bacteria were seeded for staining at 50 µl/well in a 96-well plate. 50 µl of 2x solution of rabbit α-FhuD2 antibodies (final concentration 8 µg/ml) in PBS/BSA 1% was added in selected wells and cell incubated for 1 hour at 4°C. Cells were then washed 3 times with 200 µl/well of PBS/BSA 1% and centrifuged centrifuge for 10 minutes at 3,500 rpm at 4°C. Buffer was removed from the pellets and 100 µl/well of Alexa Fluor®488 α-rabbit IgG (Thermo Fisher Scientific) diluted 1:200 (final concentration 10 µg/ml) in PBS/BSA 1% were added in selected wells and incubated for 1 hour at 4°C in the dark. Cells were then washed twice with 200 µl/well of PBS/BSA 1% and centrifuged centrifuge for 10 minutes at 3,500 rpm and 4°C. Cells were fixed with 100 µl PBS/Formaldehyde 2% for 15 minutes at room temperature. Cells were then washed twice with 200 µl/well of PBS. Finally, cells were resuspended in 200 µl of PBS for analysis by flow cytometry using the FACS Canto (Becton Dickinson). Data were analysed using FlowJo v10.1.

6.7. Mammalian cell lines and culture

6.7.1. Cell lines and complete culture media

The human THP-1 monocytes (ATCC® TIB-202™) were a kind gift from the Department of Biomedical and Clinic Sciences at the University of Florence. THP-1 cells were cultured in Roswell Park Memorial Institute (RPMI1640) medium (Corning 15-040-CVR), with 10% heat inactivated foetal bovine serum (FBS) (Thermo Fisher Scientific,

10270-106), 2mM L-glutamine (Fisher scientific, 25030081), 1X Penicillin/Streptomycin (EuroClone, ECB3001D) and 0.05 mM 2-mercaptoethanol.

HEK-Blue™ mTLR4 cell line (Invivogen, hkb-mtlr4) is a reporter gene cell line, developed by co-transfection of the mTLR4 gene, the MD-2/CD14 co-receptor genes and a secreted embryonic alkaline phosphatase (SEAP) reporter gene into HEK293 cells. HEK-Blue™ mTLR4 cell were cultures as per manufacturer's instructions. Briefly, endotoxin free Dulbecco's modified Eagle's medium (DMEM) (Corning, 15-017-CVR), containing 10% heat inactivated fetal bovine serum (FBS) endotoxin free (Thermo Fisher Scientific, 10270-106), 2nM L-glutamine (Fisher scientific, 25030081) and 1X Penicillin/Streptomycin (EuroClone, ECB3001D) 1X. With HEK-Blue selection reagents (250X) to maintain expression of mTLR4 and co-receptors.

HEK-Blue™ hTLR4 cell line (Invivogen, hkb-hTLR2) is a reporter gene cell line, developed by co-transfection of the hTLR2mTLR4 gene, the CD14 co-receptor genes and a secreted embryonic alkaline phosphatase (SEAP) reporter gene into HEK293 cells. HEK-Blue™ hTLR2 cell were cultures as per manufacturer's instructions. Briefly, Dulbecco's modified Eagle's medium (DMEM) (Corning, 15-017-CVR), containing 10% heat inactivated fetal bovine serum (FBS), 2nM L-glutamine (Fisher scientific, 25030081) and 1X Penicillin/Streptomycin (EuroClone, ECB3001D) 1X. With HEK-Blue selection reagents (250X) to maintain expression of hTLR2 and co-receptor and reporter gene.

Mouse CT26 colon carcinoma cell line (ATCC® CRL-2638) were a kind gift from the Department of Biomedical and Clinic Sciences at the University of Florence. CT26 cells were cultured in RPMI1640 medium, with 10% heat inactivated FBS, 2mM L-glutamine and 1X Penicillin/Streptomycin.

Mouse melanoma B16-OVA cell line, is the B16F10 cell line transfected with a plasmid carrying a complete copy of chicken ovalbumin (OVA) and the Geneticin (G418) resistance gene, and was kindly provided by Cristian Capasso and prof. Vincenzo Cerullo from the Laboratory of Immunovirotherapy, Drug Research Program, Faculty of Pharmacy, University of Helsinki. B16-OVA cells were cultured in RPMI1640 medium, with 10% heat inactivated FBS, 2mM L-glutamine, 1X Penicillin/Streptomycin and Geneticin (G418) (Euroclone, 11413164) at 500 μg/ml.

Mouse immature dendritic cells JAWSII (ATCC® CRL-11904™) is an immortalised cell line derived from the bone marrow of C57BL6 mice. They were cultured in complete culture medium containing Alpha minimum essential medium with ribonucleosides, deoxyribonucleosides (Sigma, M6199), 4 mM L-glutamine, 1 mM sodium pyruvate, 20 % FBS and 5 ng/ml murine GM-CSF (PeproTech, 315-03).

6.7.2. Cell thawing, passage and cryopreservation

Cryopreserved cell were thawed in a water bath at 37°C until approximately 90% thawed. The 1 ml aliquot of cells was then added to 9 ml of prewarmed complete culture medium, spun at 300g for 4 min and media discarded. Cells were resuspended in 10 ml of prewarmed complete culture medium and added to a tissue culture flask for incubated at 37°C with 5% CO_2.

All cell lines were cultured at 37°C with 5% CO_2. When cells reached between 70-90% confluence, culture medium was removed by aspiration and discarded. Cells were then rinsed with Dulbecco's phosphate buffered saline (DPBS) containing no $CaCl_2$ and no $MgCl_2$ to remove the culture media. Typically, 3 ml of 1X Trypsin ethylenediaminetetraacetic acid (EDTA) (Life Technologies) was added per T75 tissue culture flask (Corning) and cell/Trypsin mixture was incubated at 37°C with 5% CO2 for a maximum of 5 min. Cells were periodically observed by microscope until cells detached from the flask surface. Remaining attached cells were detached by gentle tapping. Complete growth medium (as detailed above) was then added and cells were removed, spun at 300g for 4 minutes and resuspended in complete growth medium.

Cells were cryopreserved at a density of 2-5 x 10^6 cells/ml in 1 ml aliquots in freezing medium (FBS containing 10% dimethyl sulfoxide (DMSO) (Sigma, D2650)). The cells were aliquoted in cryovials (Corning) and frozen at -80°C at 1°C per minute using a 'Mr Frosty' freezing container (Nalgene), then transferred for storage in liquid nitrogen (LN_2).

6.8. *In vitro* cell assays

6.8.1. Internalisation of OMVs

Mouse dendritic cell line JAWSII cells were seeded at 3 x 10^4 cells in 100 µl of complete culture medium, in a 96-well optical plate for microscopy. The next day I incubated 10 µg/ml of OMVs from BL21(DE3)Δ*60-FhuD2-amDEC205* and BL21(DE3)Δ*60-FhuD2-aHELD1.3* with these cells for 2, 30, 90 and 180 minutes. At the end of the incubation period, the media (with OMVs) were removed and cells fixed and permeabilised using Cytofix/Cytoperm (Beckton Dickenson). Cells were subsequently blocked with mouse Fc Block (BD Pharmingen, 553142) for 15 minutes before staining with the anti-LPS antibody (Hycult Biotech, HM6011-1A) at a final concentration of 1.7 µg/ml for 1 hour. After washing three time with PBS the secondary antibody, anti-mouse AlexaFlour 488 (Thermo, A11001) was incubated with the cell at 2 µg/ml for 45 minutes. Then was twice with PBS and store overnight at 4°C. The next day cells were stained with CellMask™ Deep Red Plasma membrane Stain (Thermo, C10046) at final concentration 2.5 µg/ml and Hoechst 33342 (Thermo, H3570) at 1 µg/ml for 40 min. Cell washed with PBS and stored in PBS for imaging. Images were collected at 100 X using the Nikon Eclipse TI2 spinning disk confocal microscope, with the help of staff in the Advanced Imaging Core facility (CIBIO).

6.8.2. Internalisation analysis

Image analysis was performed using ImageJ and a semi-automated macro to count cells and OMVs per cell in each image. The original macro was written by Michela Roccuzzo at Advanced Imaging Core facility (AICF) of CIBIO, we then edited it together to best fit and analyse the data correctly. Using the macro we obtained the number of OMVs per cell. The data column statistics were analysed and showed a non-Gaussian distribution. Therefore, I used the Kruskal–Wallis test (also known as one-way ANOVA on ranks) to compare groups, then subsequently used the Dunn's multiple comparisons test to compare the difference in the sum of ranks between two groups. The scatter plot as statistical analysis were performed using GraphPad Prism 5.

6.8.3. DC biomarker analysis

The JAWSII cells counted and resuspended at 2.5 x 10^5 cells/ml in complete media. In a 12-well culture plate, 1.5 ml per well was seeded. OMVs derived from

BL21(DE3)Δ*60-FhuD2-αmDEC205* or BL21(DE3)Δ*60* were added to give a final concentration of 25 µg/ml. An equivalent volume of PBS added to control wells. Each treatment was given in a total of 4 wells. The cells and OMVs were incubated for 72 hours at 37°C with 5% CO_2. Then to one well of each OVA peptide (SIINFEKL) was added at a final concentration of 96.3 ng/ml (or 100nM) for 2 hours. Subsequently cells were harvested from the wells using a 1 ml syringe plunger. Cell centrifuged at 300g for 5 min at 4°C and resuspended in PBS/FBS 5% and pre-incubated with Fc Block for 15 minutes. Then seeded into a 96-well round bottom plate to allow for single staining. Specific antibodies and their final experimental concentrations are given in Table 7 below:

Table 7: Antibodies for the detection of DC biomarkers

Antibody target	Fluorophore	Provider	Catalogue #	Final concentration
Fc block (α-CD16/CD32)		BD Pharmingen	553142	10 µg/ml
CD80 (hamster IgG2)	PE	BD Pharmingen	553769	2 µg/ml
hamster IgG2	PE isotype control	BD Pharmingen	550085	2 µg/ml
CD86 (rat IgG2a k)	PE	BD Pharmingen	553692	2 µg/ml
rat IgG2a k	PE isotype control	BD Pharmingen	553930	2 µg/ml
MHCII (rat IgG2a k)	APC	Miltenyi Biotech	130-102-139	3 µg/ml
rat IgG2a k	APC isotype control	Miltenyi Biotech	130-103-085	3 µg/ml
H-2kb/SIINFEKL (m IgG1)	PE	Miltenyi Biotech	130-102-180	3 µg/ml
Mouse IgG1	PE isotype control	Miltenyi Biotech	130-098-845	3 µg/ml

After staining for 1 hour, cells were washed and resuspended with PBS for flow cytometry analysis using the BD FACS Canto. Data analysis was performed using FlowJo v.10. Bar charts were made using GraphPad Prism 5.

6.8.4. THP-1 cell hIL-6 release assay for adjuvanticity and reactogenicity

THP-1 cells were thawed, cultures maintained at a concentration of 2-4 x 10^5 viable cells/ml. Passage performed when cell concentration reached 8x10^5 cells/ml. Monocytes were differentiated into macrophages by adding 100 ng/ml of phorbol 12-myristate 13-acetate (PMA) to the culture for 48 hours. Then, 24 hours before the assay the media was refreshed. Cell were removed from the flask by trypsinisation. Cell resuspended in complete medium at 2 x 10^6 cell/ml and 50 µl per well seeded in a 96-well flat bottom plate. Six 10-fold serial dilutions of $OMV_{\Delta ompA}$ and $OMV_{\Delta 60}$ were made from a concentration of 2000 ng/mL to 0.02 ng/mL in RPMI complete medium. Then 50 µl of the dilutions were added to the cells and incubated for 24 hours at 37°C, 5% CO_2.

Supernatant was collected and hIL-6 release measured using the human IL-6 ELISA Assay (Invitrogen 88-7066) according to the manufacturers' protocol.

6.8.5. HEK Blue™ TLR activation assays

6.8.5.1. Mouse TLR4 activation assay

HEK-Blue™ mTLR4 cells were seeded and treated as per the manufacturers' protocol. OMVs derived from BL21(DE3)Δ*ompA* and BL21(DE3)Δ*60* were tested for mTLR4 activation. LPS (200 ng/mL) was used as positive control and endotoxin free water as a negative control. OMVs were initially diluted at 100 ng/ml ($OMVs_{\Delta ompA}$) or at 10 ng/mL ($OMVs_{\Delta 60}$) and then eight 10-fold serial dilutions prepared. 20 µl of each dilution were put in a 96-well flat bottom plate and then 180 µl per well of HEK-Blue™ mTLR4 cells (140,000 cells/ml) added. After 17 hours of incubation, 20 µl of supernatant was transferred in a new 96-well flat bottom plate, 180 µl of Quanti-Blue™ added and incubated for 30 minutes at 37°C. The absorbance of colorimetric reaction was measured at an absorbance of 655 nm using the Infinite M200PRO Plate reader (TECAN).

6.8.5.2. Human TLR2 activation assay

HEK-Blue™ hTLR2 cells were seeded and treated as per the manufacturers' protocol. OMVs derived from BL21(DE3)Δ*ompA* and BL21(DE3)Δ*60* were tested for hTLR2 activation. Pam3CSK4 (Pam3CysSerLys4) (Invivogen, tlrl-pms), a synthetic triacylated lipopeptide, was used as positive control and water as a negative control. OMVs were initially diluted at 100 ng/ml and then eight 10-fold serial dilutions prepared. 20 µl of each dilution were put in a 96-well flat bottom plate and then 180 µl per well of HEK-Blue™ hTLR2 cells (140,000 cells/ml) added. After 17 hours of incubation, 20 µl of supernatant was transferred in a new 96-well flat bottom plate, 180 µl of Quanti-Blue™ added and incubated for 30 minutes at 37°C. The absorbance of colorimetric reaction was measured at an absorbance of 655 nm using the Infinite M200PRO Plate reader (TECAN).

6.8.6. Lactate dehydrogenase (LDH) release cytotoxicity assay

CT26 cells were seeded at 10,000 cells per well in 100µl of RPMI1640 without phenol red (Corning, 17-105-CVR), with 10% FBs (heat inactivated), 2mM L-glutamine and 1X penicillin/streptomycin, in a 96-well flat bottom, tissue culture treated plate.

Then incubated overnight at 37°C, 5% CO_2. The next day, the culture medium was carefully removed so as not to disturb the cells. Treatments and controls were added in a final volume of 200 µl of treatment media (RPMI1640 without phenol red, 2mM L-glutamine and 1X Penicillin/Streptomycin and 1.25% FBS). Negative control was treatment media only, positive control was Triton X-100 (Merck, T8787) at 0.1%. OMVs, derived from BL21(DE3)Δ*ompA* and BL21(DE3)Δ*60*, added in the following concentrations: 1 µg/well; 5 µg/well; 10 µg/well; 50 µg/well. Treated cells were incubated for 24 hours at 37°C 5% CO_2. The plate was centrifuged for 10 min at 250g and 100 µl of cell-free supernatant was transferred to a clear flat bottom 96-well plate. Subsequently, 100 µl of freshly prepared reaction mixture (catalyst and INT dye solution) was added and incubated for 30 minutes at room temperature in the dark. Then the reaction was stopped with 1M HCl. The absorbance of colorimetric reaction was measured at 492 nm (reference wavelength: 620 nm) using an Infinite M200PRO Plate reader (TECAN). The percentage cytotoxicity was calculated as follows:

$$cytotoxicity\ \% = \frac{sample\ value - negative\ value}{positive\ value - negative\ value} \times 100$$

6.9. *In vivo* experiments

6.9.1. Animal studies

BALB/c and C57BL/6N (referred to as C57BL6) mouse strains were obtained from Charles River Laboratories (Italy). All mice were monitored twice a day to evaluate any early signs of pain and distress, such as respiration rate, posture, and weight loss according to humane endpoints. Animals showing such conditions were anaesthetised and subsequently euthanised in accordance with experimental protocols, which were reviewed and approved by the Animal Ethical Committee of the University of Trento and the Italian Ministry of Health.

6.9.2. Vaccination for T cell response analysis

To analyse T cell response, mice were subcutaneously injected with 10 µg of OMVs with various amount of epitope peptide (as specified for each experiment). Vaccinations were performed on day 0 and on day 7. On day 12, spleens were collected and processed for the splenocyte re-stimulation assay and subsequent T cell analysis.

6.9.3. Splenocyte re-stimulation assay

Spleens were collected from each mouse in 3 ml of RPMI + 10% FBS + penicillin/streptomycin (complete culture media). They were subsequently homogenised and filtered through a 70 µm cell strainer. Splenocytes were suspended in complete culture media, counted and seeded in a round bottom 96-well plate at a concentration of 30×10^6 cells/ml. peptides used for negative control and re-stimulation depended upon which epitope was being analysed in which mouse model. Cells were stimulated with a final concentration of 5 µg/ml of negative control peptide (B16-M30 for BALB/c and AH1 for C57BL6), or 5 µg/ml of OVA (SIINFEKL), 5 µg/ml of SV40 (VVYDFLKL) or 5 µg/ml each of a mix of the pentatope peptides (M03, M20, M26, M27, and M68 peptides). As positive control, cells were stimulated with phorbol 12-myristate 13-acetate (PMA, 20 ng/ml) and Ionomycin (2 uM). After 2 h of stimulation at 37°C with 5% CO_2, BD GolgiStop (Beckton Dickenson) was added to each well and cells incubated for 4 h at 37°C with 5% CO_2 as per manufacturer's instructions. Splenocytes were then washed with PBS twice, stained with NearIR Live/Dead cell stain (Thermo Fisher) and incubated for 20 min at room temperature in the dark. After three washes with PBS, splenocytes were permeabilised and fixed using BD Cytofix/Cytoperm (Beckton Dickenson) according to the manufacturer's protocol. Splenocytes were stored at 4°C in PBS/BSA. Staining continued with a mix of the following fluorescent-labelled antibodies: Anti CD3-APC (BioLegend), Anti-CD4-BV510 (BioLegend), anti-CD8-PECF594 (BD) and IFN–γ-BV785 (BioLegend). Samples were analysed on a BD LSRII FACS and data analysed using FlowJo V.10 software. Graphs were plotted using Prism 5.0 software (GraphPad).

6.9.4. *In situ* vaccination of mice bearing two tumours

We used two syngeneic mouse models, Balb/C with CT-26 colon carcinoma cells and C57BL6 with B16-OVA melanoma cell line expressing chicken ovalbumin. Female mice (Balb/C and C57BL6) were 7 weeks old when the experiments began. CT26 and B16-OVA tumour cells (1.5×10^5 and 2.8×10^5, respectively) were injected subcutaneously at sites on both the right and left flank of the respective mouse strain. Tumour size was monitored every 2 days on both sides of the animals with a digital calliper and expressed as volume (volume = (width^2 x length)/2). Body weight and mouse well-being were also closely monitored. When tumour size reached at ≥50-100 mm^3 mice were vaccinated *in situ* in one of the tumours. PBS, OMVs (10 µg /injection) or

OMVs + 1X peptides (10ug + 100ug /injection) were injected in a volume of 50 µl. For pentatope peptides 20µg of each peptide was used. Mice were given a total of three vaccinations every two days. They were sacrificed when the sum of the tumour volume per mouse reached ≥ 2000 mm^3 or when splenocytes needed to be analysed. The investigator was not blinded to the group allocation during the experiment and/or when assessing the outcome.

Bibliography

Alaniz R. C., B. L. Deatherage, J. C. Lara, and B. T. Cookson, 2007 Membrane Vesicles Are Immunogenic Facsimiles of Salmonella typhimurium That Potently Activate Dendritic Cells, Prime B and T Cell Responses, and Stimulate Protective Immunity In Vivo . J. Immunol. 179: 7692–7701. https://doi.org/10.4049/jimmunol.179.11.7692

Ammi R., J. De Waele, Y. Willemen, I. Van Brussel, D. M. Schrijvers, *et al.*, 2015 Poly(I:C) as cancer vaccine adjuvant: Knocking on the door of medical breakthroughs. Pharmacol. Ther. 146: 120–131.

Apostolopoulos V., T. Thalhammer, A. G. Tzakos, L. Stojanovska, V. Apostolopoulos, *et al.*, 2013 Targeting antigens to dendritic cell receptors for vaccine development. J. Drug Deliv. 2013: 869718. https://doi.org/10.1155/2013/869718

Arnold R., Y. Galloway, A. McNicholas, J. O'Hallahan, and J. O'Hallahan, 2011 Effectiveness of a vaccination programme for an epidemic of meningococcal B in New Zealand. Vaccine 29: 7100–7106. https://doi.org/S0264-410X(11)01118-2 [pii]10.1016/j.vaccine.2011.06.120

Atkins M. B., M. T. Lotze, J. P. Dutcher, R. I. Fisher, G. Weiss, *et al.*, 1999 High-dose recombinant interleukin 2 therapy for patients with metastatic melanoma: Analysis of 270 patients treated between 1985 and 1993. J. Clin. Oncol. 17: 2105–2116. https://doi.org/10.1200/jco.1999.17.7.2105

Aznar M. A., N. Tinari, A. J. Rullán, A. R. Sánchez-Paulete, M. E. Rodriguez-Ruiz, *et al.*, 2017 Intratumoral Delivery of Immunotherapy—Act Locally, Think Globally. J. Immunol. 198: 31–39. https://doi.org/10.4049/jimmunol.1601145

Aznar M. A., L. Planelles, M. Perez-Olivares, C. Molina, S. Garasa, *et al.*, 2019 Immunotherapeutic effects of intratumoral nanoplexed poly I:C. J. Immunother. Cancer 7: 116. https://doi.org/10.1186/s40425-019-0568-2

Baroja-Mazo A., F. Martín-Sánchez, A. I. Gomez, C. M. Martínez, J. Amores-Iniesta, *et al.*, 2014 The NLRP3 inflammasome is released as a particulate danger signal that amplifies the inflammatory response. Nat. Immunol. 15: 738–748. https://doi.org/10.1038/ni.2919

Bartlett D. L., Z. Liu, M. Sathaiah, R. Ravindranathan, Z. Guo, *et al.*, 2013 Oncolytic viruses as therapeutic cancer vaccines. Mol. Cancer 12.

Bast R. C., B. Zbar, T. Borsos, and H. J. Rapp, 1974 BCG and Cancer. N. Engl. J. Med. 290: 1458–1469.

Baumeister S. H., G. J. Freeman, G. Dranoff, and A. H. Sharpe, 2016 Coinhibitory Pathways in Immunotherapy for Cancer. Annu. Rev. Immunol. 34: 539–573. https://doi.org/10.1146/annurev-immunol-032414-112049

Berlanda Scorza F., A. M. Colucci, L. Maggiore, S. Sanzone, O. Rossi, *et al.*, 2012 High Yield Production Process for Shigella Outer Membrane Particles, (S. Bereswill, Ed.). PLoS One 7: e35616. https://doi.org/10.1371/journal.pone.0035616

Bernadac A., M. Gavioli, J. C. Lazzaroni, S. Raina, R. Lloubes, *et al.*, 1998 Escherichia coli tol-pal mutants form outer membrane vesicles. J Bacteriol 180: 4872–4878.

Bird R. E., K. D. Hardman, J. W. Jacobson, S. Johnson, B. M. Kaufman, *et al.*, 1988 Single-chain antigen-binding proteins. Science (80-.). 242: 423–426. https://doi.org/10.1126/science.3140379

Birkholz K., M. Schwenkert, C. Kellner, S. Gross, G. Fey, *et al.*, 2010 Targeting of DEC-205 on human dendritic cells results in efficient MHC class II-restricted antigen presentation. Blood 116: 2277–2285. https://doi.org/10.1182/blood-2010-02-268425

Bishop R. E., H. S. Gibbons, T. Guina, M. S. Trent, S. I. Miller, *et al.*, 2000 Transfer of palmitate from phospholipids to lipid A in outer membranes of Gram-negative bacteria. EMBO J. 19: 5071–5080. https://doi.org/10.1093/emboj/19.19.5071

Bonifaz L., D. Bonnyay, K. Mahnke, M. Rivera, M. C. Nussenzweig, *et al.*, 2002 Efficient targeting of protein antigen to the dendritic cell receptor DEC-205 in the steady state leads to antigen presentation on major histocompatibility complex class I products and peripheral CD8+ T cell tolerance. J. Exp. Med. 196: 1627–1638. https://doi.org/10.1084/jem.20021598

Bonifaz L. C., D. P. Bonnyay, A. Charalambous, D. I. Darguste, S.-I. Fujii, *et al.*, 2004 In vivo targeting of antigens to maturing dendritic cells via the DEC-205 receptor improves T cell vaccination. J. Exp. Med. 199: 815–24. https://doi.org/10.1084/jem.20032220

Boulot G., J. L. Eiselé, G. A. Bentley, T. N. Bhat, E. S. Ward, *et al.*, 1990 Crystallization and preliminary X-ray diffraction study of the bacterially expressed Fv from the monoclonal anti-lysozyme antibody D1.3 and of its complex with the antigen, lysozyme. J. Mol. Biol. 213: 617–619. https://doi.org/10.1016/S0022-2836(05)80248-7

Bozzacco L., C. Trumpfheller, F. P. Siegal, S. Mehandru, M. Markowitz, *et al.*, 2007 DEC-205 receptor on dendritic cells mediates presentation of HIV gag protein to CD8+ T cells in a spectrum of human MHC I haplotypes. Proc. Natl. Acad. Sci. U. S. A. 104: 1289–

1294. https://doi.org/10.1073/pnas.0610383104

Bray F., J. Ferlay, I. Soerjomataram, R. L. Siegel, L. A. Torre, *et al.*, 2018 Global cancer statistics 2018: GLOBOCAN estimates of incidence and mortality worldwide for 36 cancers in 185 countries. CA. Cancer J. Clin. 68: 394–424. https://doi.org/10.3322/caac.21492

Burnet M., 1957 Cancer-A Biological Approach* Iii. Viruses Associated With Neoplastic Conditions. Br. Med. J. 1: 841. https://doi.org/10.1136/bmj.1.5023.841

Chabner B. A., and T. G. Roberts, 2005 Chemotherapy and the war on cancer. Nat. Rev. Cancer 5: 65–72.

Chang M. H., 2009 Cancer prevention by vaccination against hepatitis B. Recent results cancer Res. Cancer Prev. II 181: 85–94.

Chen D. J., N. Osterrieder, S. M. Metzger, E. Buckles, A. M. Doody, *et al.*, 2010 Delivery of foreign antigens by engineered outer membrane vesicle vaccines. Proc Natl Acad Sci U S A 107: 3099–3104. https://doi.org/0805532107 [pii]10.1073/pnas.0805532107

Chen D. S., and I. Mellman, 2013 Oncology Meets Immunology: The Cancer-Immunity Cycle. Immunity 39: 1–10. https://doi.org/10.1016/j.immuni.2013.07.012

Chen P., X. Liu, Y. Sun, P. Zhou, Y. Wang, *et al.*, 2016 Dendritic cell targeted vaccines: Recent progresses and challenges. Hum. Vaccin. Immunother. 12: 612–622. https://doi.org/10.1080/21645515.2015.1105415

Chen Q., S. Rozovsky, and W. Chen, 2017a Engineering multi-functional bacterial outer membrane vesicles as modular nanodevices for biosensing and bioimaging. Chem. Commun. 53: 7569–7572. https://doi.org/10.1039/C7CC04246A

Chen B. Y., G. Zhou, Q. L. Li, J. S. Lu, D. Y. Shi, *et al.*, 2017b Enhanced effects of DNA vaccine against botulinum neurotoxin serotype A by targeting antigen to dendritic cells. Immunol. Lett. 190: 118–124. https://doi.org/10.1016/j.imlet.2017.08.004

Ciabattini A., A. M. Cuppone, R. Pulimeno, F. Iannelli, G. Pozzi, *et al.*, 2006 Stimulation of human monocytes with the gram-positive vaccine vector Streptococcus gordonii. Clin. Vaccine Immunol. 13: 1037–1043. https://doi.org/10.1128/CVI.00110-06

Collin M., and V. Bigley, 2018 Human dendritic cell subsets: an update. Immunology 154: 3–20.

Cowles C. E., Y. Li, M. F. Semmelhack, I. M. Cristea, and T. J. Silhavy, 2011 The free and bound forms of Lpp occupy distinct subcellular locations in Escherichia coli. Mol. Microbiol. 79: 1168–1181. https://doi.org/10.1111/j.1365-2958.2011.07539.x

Daugherty P. S., M. J. Olsen, B. L. Iverson, and G. Georgiou, 1999 Development of an optimized expression system for the screening of antibody libraries displayed on the Escherichia coli surface. Protein Eng. 12: 613–21. https://doi.org/10.1093/PROTEIN/12.7.613

Deatherage B. L., J. C. Lara, T. Bergsbaken, S. L. R. Barrett, S. Lara, *et al.*, 2009 Biogenesis of bacterial membrane vesicles. Mol. Microbiol. 72: 1395–1407. https://doi.org/10.1111/j.1365-2958.2009.06731.x

Dekhtiarenko I., R. B. Ratts, R. Blatnik, L. N. Lee, S. Fischer, *et al.*, 2016 Peptide Processing Is Critical for T-Cell Memory Inflation and May Be Optimized to Improve Immune Protection by CMV-Based Vaccine Vectors, (L. J. Sigal, Ed.). PLOS Pathog. 12: e1006072. https://doi.org/10.1371/journal.ppat.1006072

Demangel C., J. Zhou, A. B. H. Choo, G. Shoebridge, G. M. Halliday, *et al.*, 2005 Single chain antibody fragments for the selective targeting of antigens to dendritic cells. Mol. Immunol. 42: 979–985. https://doi.org/10.1016/j.molimm.2004.09.034

Dhodapkar M. V., M. Sznol, B. Zhao, D. Wang, R. D. Carvajal, *et al.*, 2014 Induction of Antigen-Specific Immunity with a Vaccine Targeting NY-ESO-1 to the Dendritic Cell Receptor DEC-205. Sci. Transl. Med. 6.

Dighe A. S., E. Richards, L. J. Old, and R. D. Schreiber, 1994 Enhanced in vivo growth and resistance to rejection of tumor cells expressing dominant negative IFNγ receptors. Immunity 1: 447–456. https://doi.org/10.1016/1074-7613(94)90087-6

Dillekås H., M. S. Rogers, and O. Straume, 2019 Are 90% of deaths from cancer caused by metastases? Cancer Med. 8: 5574–5576. https://doi.org/10.1002/cam4.2474

Dougan M., and G. Dranoff, 2009 Immune Therapy for Cancer. Annu. Rev. Immunol. 27: 83–117. https://doi.org/10.1146/annurev.immunol.021908.132544

Dougan M., G. Dranoff, and S. K. Dougan, 2019 Cancer Immunotherapy: Beyond Checkpoint Blockade. Annu. Rev. Cancer Biol. 3: 55–75. https://doi.org/10.1146/annurev-cancerbio-030518-055552

Dudley M. E., and D. C. Roopenian, 1996 Loss of a unique tumor antigen by cytotoxic T lymphocyte immunoselection from a 3-methylcholanthrene-induced mouse sarcoma reveals secondary unique and shared antigens. J. Exp. Med. 184: 441–447. https://doi.org/10.1084/jem.184.2.441

Dunn G. P., A. T. Bruce, H. Ikeda, L. J. Old, and R. D. Schreiber, 2002 Cancer immunoediting: From immunosurveillance to tumor escape. Nat. Immunol. 3: 991–998.

Dunn G. P., L. J. Old, and R. D. Schreiber, 2004 The Three Es of Cancer Immunoediting. Annu. Rev. Immunol. 22: 329–360. https://doi.org/10.1146/annurev.immunol.22.012703.104803

Ehrlich P., 1909 Ueber den jetzigen stand der karzinomforschung. Ned. Tiijdschrift voor Geneeskd. 5: 273–290.

Ellis T. N., and M. J. Kuehn, 2010 Virulence and Immunomodulatory Roles of Bacterial Outer Membrane Vesicles. Microbiol. Mol. Biol. Rev. 74: 81–94. https://doi.org/10.1128/mmbr.00031-09

Ellis T. N., S. A. Leiman, and M. J. Kuehn, 2010 Naturally produced outer membrane vesicles from Pseudomonas aeruginosa elicit a potent innate immune response via combined sensing of both lipopolysaccharide and protein components. Infect. Immun. 78: 3822–3831. https://doi.org/10.1128/IAI.00433-10

Emens L. A., P. A. Ascierto, P. K. Darcy, S. Demaria, A. M. M. Eggermont, *et al.*, 2017 Cancer immunotherapy: Opportunities and challenges in the rapidly evolving clinical landscape. Eur. J. Cancer 81: 116–129.

Fantappiè L., M. de Santis, E. Chiarot, F. Carboni, G. Bensi, *et al.*, 2014 Antibody-mediated immunity induced by engineered Escherichia coli OMVs carrying heterologous antigens in their lumen. J Extracell Vesicles 3: 1–14. https://doi.org/10.3402/jev.v3.2401524015 [pii]

Fantappiè L., C. Irene, M. De Santis, A. Armini, A. Gagliardi, *et al.*, 2017 Some Gram-negative Lipoproteins Keep Their Surface Topology When Transplanted from One Species to Another and Deliver Foreign Polypeptides to the Bacterial Surface. Mol. Cell. Proteomics 16: 1348–1364. https://doi.org/10.1074/mcp.M116.065094

Fleri W., S. Paul, S. K. Dhanda, S. Mahajan, X. Xu, *et al.*, 2017 The immune epitope database and analysis resource in epitope discovery and synthetic vaccine design. Front. Immunol. 8: 278.

Francisco J. A., R. Campbell, B. L. Iverson, and G. Georgiou, 1993 Production and fluorescence-activated cell sorting of Escherichia coli expressing a functional antibody fragment on the external surface. Proc. Natl. Acad. Sci. 90: 10444–10448. https://doi.org/10.1073/pnas.90.22.10444

Frank M. J., P. M. Reagan, N. L. Bartlett, L. I. Gordon, J. W. Friedberg, *et al.*, 2018 In situ vaccination with a tlr9 agonist and local low-dose radiation induces systemic responses in untreated indolent lymphoma. Cancer Discov. 8.

https://doi.org/10.1158/2159-8290.CD-18-0743

Fyfe G., R. I. Fisher, S. A. Rosenberg, M. Sznol, D. R. Parkinson, *et al.*, 1995 Results of treatment of 255 patients with metastatic renal cell carcinoma who received high-dose recombinant interleukin-2 therapy. J. Clin. Oncol. 13: 688–696. https://doi.org/10.1200/JCO.1995.13.3.688

Gaciarz A., J. Veijola, Y. Uchida, M. J. Saaranen, C. Wang, *et al.*, 2016 Systematic screening of soluble expression of antibody fragments in the cytoplasm of E. coli. Microb. Cell Fact. 15.

Gardner T., B. Elzey, and N. M. Hahn, 2012 Sipuleucel-T (Provenge) autologous vaccine approved for treatment of men with asymptomatic or minimally symptomatic castrate-resistant metastatic prostate cancer. Hum. Vaccin. Immunother. 8: 534–539. https://doi.org/10.4161/hv.19795

Gerke C., A. M. Colucci, C. Giannelli, S. Sanzone, C. G. Vitali, *et al.*, 2015 Production of a Shigella sonnei vaccine based on generalized modules for membrane antigens (GMMA), 1790GAHB. PLoS One 10. https://doi.org/10.1371/journal.pone.0134478

Gerritzen M. J. H., D. E. Martens, R. H. Wijffels, L. van der Pol, and M. Stork, 2017 Bioengineering bacterial outer membrane vesicles as vaccine platform. Biotechnol. Adv. 35: 565–574. https://doi.org/10.1016/j.biotechadv.2017.05.003

Giuliani M. M., J. Adu-Bobie, M. Comanducci, B. Aricò, S. Savino, *et al.*, 2006 A universal vaccine for serogroup B meningococcus. Proc. Natl. Acad. Sci. U. S. A. 103: 10834–10839. https://doi.org/10.1073/pnas.0603940103

Grandi A., M. Tomasi, and G. Grandi, 2016 Vaccinology: The art of putting together the right ingredients. Hum. Vaccines Immunother. 12: 1311–1317. https://doi.org/10.1080/21645515.2015.1123829

Grandi A., M. Tomasi, I. Zanella, L. Ganfini, E. Caproni, *et al.*, 2017 Synergistic Protective Activity of Tumor-Specific Epitopes Engineered in Bacterial Outer Membrane Vesicles. Front. Oncol. 7: 253. https://doi.org/10.3389/fonc.2017.00253

Grandi A., L. Fantappiè, C. Irene, S. Valensin, M. Tomasi, *et al.*, 2018 Vaccination With a FAT1-Derived B Cell Epitope Combined With Tumor-Specific B and T Cell Epitopes Elicits Additive Protection in Cancer Mouse Models. Front. Oncol. 8: 481. https://doi.org/10.3389/fonc.2018.00481

Green D. S., M. D. Bodman-Smith, A. G. Dalgleish, and M. D. Fischer, 2007 Phase I/II study of topical imiquimod and intralesional interleukin-2 in the treatment of accessible

metastases in malignant melanoma. Br. J. Dermatol. 156: 337–345. https://doi.org/10.1111/j.1365-2133.2006.07664.x

Guerra N., Y. X. Tan, N. T. Joncker, A. Choy, F. Gallardo, *et al.*, 2008 NKG2D-Deficient Mice Are Defective in Tumor Surveillance in Models of Spontaneous Malignancy. Immunity 28: 571–580. https://doi.org/10.1016/j.immuni.2008.02.016

Haan J. M. M. Den, S. M. Lehar, and M. J. Bevan, 2000 CD8+ but not CD8- dendritic cells cross-prime cytotoxic T cells in vivo. J. Exp. Med. 192: 1685–1695. https://doi.org/10.1084/jem.192.12.1685

Hammerich L., A. Binder, and J. D. Brody, 2015 In situ vaccination: Cancer immunotherapy both personalized and off-the-shelf. Mol. Oncol. 9: 1966–1981.

Hammerich L., N. Bhardwaj, H. E. Kohrt, and J. D. Brody, 2016 *In situ* vaccination for the treatment of cancer. Immunotherapy 8: 315–330. https://doi.org/10.2217/imt.15.120

Hammerich L., T. U. Marron, R. Upadhyay, J. Svensson-Arvelund, M. Dhainaut, *et al.*, 2019 Systemic clinical tumor regressions and potentiation of PD1 blockade with in situ vaccination. Nat. Med. 25: 814–824. https://doi.org/10.1038/s41591-019-0410-x

Hanahan D., and R. A. Weinberg, 2000 The hallmarks of cancer. Cell 100: 57–70.

Hanahan D., and R. A. Weinberg, 2011 Hallmarks of cancer: The next generation. Cell 144: 646–674.

Harrington K., D. J. Freeman, B. Kelly, J. Harper, and J. C. Soria, 2019 Optimizing oncolytic virotherapy in cancer treatment. Nat. Rev. Drug Discov.

He X., S. I. Abrams, and J. F. Lovell, 2018 Peptide Delivery Systems for Cancer Vaccines. Adv. Ther. 1: 1800060. https://doi.org/10.1002/adtp.201800060

Herr H. W., and A. Morales, 2008 History of Bacillus Calmette-Guerin and Bladder Cancer: An Immunotherapy Success Story. J. Urol. 179: 53–56. https://doi.org/10.1016/j.juro.2007.08.122

Holliger P., and P. J. Hudson, 2005 Engineered antibody fragments and the rise of single domains. Nat. Biotechnol. 23: 1126–1136. https://doi.org/10.1038/nbt1142

Hollingsworth R. E., and K. Jansen, 2019 Turning the corner on therapeutic cancer vaccines. npj Vaccines 4: 7. https://doi.org/10.1038/s41541-019-0103-y

Hopfinger G., U. Jäger, and N. Worel, 2019 CAR-T Cell Therapy in Diffuse Large B Cell Lymphoma: Hype and Hope. HemaSphere 3: e185. https://doi.org/10.1097/hs9.0000000000000185

Huston J. S., D. Levinson, M. Mudgett-Hunter, M. S. Tai, J. Novotny, *et al.*, 1988 Protein engineering of antibody binding sites: Recovery of specific activity in an anti-digoxin single-chain Fv analogue produced in Escherichia coli. Proc. Natl. Acad. Sci. U. S. A. 85: 5879–5883. https://doi.org/10.1073/pnas.85.16.5879

Inaba K., W. J. Swiggard, M. Inaba, J. Meltzer, A. Miryza, *et al.*, 1995 Tissue Distribution of the DEC-205 Protein That Is Detected by the Monoclonal Antibody NLDC-145: I. Expression on Dendritic Cells and Other Subsets of Mouse Leukocytes. Cell. Immunol. 163: 148–156. https://doi.org/10.1006/cimm.1995.1109

Inoue H., and K. Tani, 2014 Multimodal immunogenic cancer cell death as a consequence of anticancer cytotoxic treatments. Cell Death Differ. 21: 39–49.

Irene C., L. Fantappiè, E. Caproni, F. Zerbini, A. Anesi, *et al.*, 2019 Bacterial outer membrane vesicles engineered with lipidated antigens as a platform for Staphylococcus aureus vaccine. Proc. Natl. Acad. Sci. 116: 1–9. https://doi.org/10.1073/pnas.1905112116

Jiang W., W. J. Swiggard, C. Heufler, M. Peng, A. Mirza, *et al.*, 1995 The receptor DEC-205 expressed by dendritic cells and thymic epithelial cells is involved in antigen processing. Nature 375: 151–155.

Jiang X., C. Shen, J. Rey-Ladino, H. Yu, and R. C. Brunham, 2008 Characterization of murine dendritic cell line JAWS II and primary bone marrow-derived dendritic cells in Chlamydia muridarum antigen presentation and induction of protective immunity. Infect. Immun. 76: 2392–401. https://doi.org/10.1128/IAI.01584-07

Joffre O. P., E. Segura, A. Savina, and S. Amigorena, 2012 Cross-presentation by dendritic cells. Nat. Rev. Immunol. 12: 557–569. https://doi.org/10.1038/nri3254

Jorgensen T. N., C. Haase, and B. K. Michelsen, 2002 Treatment of an Immortalized APC Cell Line with Both Cytokines and LPS Ensures Effective T-Cell Activation In Vitro. Scand. J. Immunol. 56: 492–503. https://doi.org/10.1046/j.1365-3083.2002.01166.x

Kalbasi A., C. H. June, N. Haas, and N. Vapiwala, 2013 Radiation and immunotherapy: A synergistic combination. J. Clin. Invest. 123: 2756–2763.

Kaparakis-Liaskos M., and R. L. Ferrero, 2015 Immune modulation by bacterial outer membrane vesicles. Nat. Rev. Immunol. 15: 375–387. https://doi.org/10.1038/nri3837

Kaplan D. H., V. Shankaran, A. S. Dighe, E. Stockert, M. Aguet, *et al.*, 1998 Demonstration of an interferon γ-dependent tumor surveillance system in immunocompetent mice.

Proc. Natl. Acad. Sci. U. S. A. 95: 7556–7561. https://doi.org/10.1073/pnas.95.13.7556

Kaplon H., M. Muralidharan, Z. Schneider, and J. M. Reichert, 2020 Antibodies to watch in 2020. MAbs 12. https://doi.org/10.1080/19420862.2019.1703531

Karaki S., H. Pere, C. Badoual, and E. Tartour, 2016 Hope in the Long Road Toward the Development of a Therapeutic Human Papillomavirus Vaccine. Clin. Cancer Res. 22: 2317–2319. https://doi.org/10.1158/1078-0432.CCR-16-0216

Kaufman H. L., F. J. Kohlhapp, and A. Zloza, 2015 Oncolytic viruses: A new class of immunotherapy drugs. Nat. Rev. Drug Discov. 14: 642–662.

Kenter G. G., M. J. P. Welters, A. R. P. M. Valentijn, M. J. G. Lowik, D. M. A. Berends-van der Meer, *et al.*, 2009 Vaccination against HPV-16 Oncoproteins for Vulvar Intraepithelial Neoplasia. N. Engl. J. Med. 361: 1838–1847. https://doi.org/10.1056/NEJMoa0810097

Kesty N. C., and M. J. Kuehn, 2004 Incorporation of heterologous outer membrane and periplasmic proteins into Escherichia coli outer membrane vesicles. J Biol Chem 279: 2069–2076. https://doi.org/10.1074/jbc.M307628200M307628200 [pii]

Khalil D. N., N. Suek, L. F. Campesato, S. Budhu, D. Redmond, *et al.*, 2019 In situ vaccination with defined factors overcomes T cell exhaustion in distant tumors. J. Clin. Invest. 129: 3435–3447. https://doi.org/10.1172/jci128562

Khan S., M. S. Bijker, J. J. Weterings, H. J. Tanke, G. J. Adema, *et al.*, 2007 Distinct uptake mechanisms but similar intracellular processing of two different toll-like receptor ligand-peptide conjugates in dendritic cells. J. Biol. Chem. 282: 21145–21159. https://doi.org/10.1074/jbc.M701705200

Khong H. T., and N. P. Restifo, 2002 Natural selection of tumor variants in the generation of “tumor escape” phenotypes. Nat. Immunol. 3: 999–1005. https://doi.org/10.1038/ni1102-999

Kidner T. B., D. L. Morton, D. J. Lee, M. Hoban, L. J. Foshag, *et al.*, 2012 Combined intralesional bacille calmette-guérin (BCG) and topical imiquimod for in-transit melanoma. J. Immunother. 35: 716–720. https://doi.org/10.1097/CJI.0b013e31827457bd

Kim Y. J., R. Neelamegam, M. A. Heo, S. Edwardraja, H. J. Paik, *et al.*, 2008a Improving the productivity of single-chain Fv antibody against c-Met by rearranging the order of its variable domains. J. Microbiol. Biotechnol. 18: 1186–1190. https://doi.org/7448 [pii]

Kim J.-Y., A. M. Doody, D. J. Chen, G. H. Cremona, M. L. Shuler, *et al.*, 2008b Engineered bacterial outer membrane vesicles with enhanced functionality. J. Mol. Biol. 380: 51–66. https://doi.org/10.1016/j.jmb.2008.03.076

Kim O. Y., B. S. Hong, K.-S. Park, Y. J. Yoon, S. J. Choi, *et al.*, 2013 Immunization with Escherichia coli outer membrane vesicles protects bacteria-induced lethality via Th1 and Th17 cell responses. J. Immunol. 190: 4092–4102. https://doi.org/jimmunol.1200742 [pii] 10.4049/jimmunol.1200742

Klebanoff C. A., N. Acquavella, Z. Yu, and N. P. Restifo, 2011 Therapeutic cancer vaccines: Are we there yet? Immunol. Rev. 239: 27–44. https://doi.org/10.1111/j.1600-065X.2010.00979.x

Klock H. E., and S. A. Lesley, 2009 The Polymerase Incomplete Primer Extension (PIPE) Method Applied to High-Throughput Cloning and Site-Directed Mutagenesis, pp. 91–103 in *Methods in molecular biology (Clifton, N.J.)*,.

Koebel C. M., W. Vermi, J. B. Swann, N. Zerafa, S. J. Rodig, *et al.*, 2007 Adaptive immunity maintains occult cancer in an equilibrium state. Nature 450: 903–907. https://doi.org/10.1038/nature06309

Kohlhapp F. J., and H. L. Kaufman, 2016 Molecular pathways: Mechanism of action for talimogene laherparepvec, a new oncolytic virus immunotherapy. Clin. Cancer Res. 22: 1048–1054. https://doi.org/10.1158/1078-0432.CCR-15-2667

Kreiter S., M. Vormehr, N. van de Roemer, M. Diken, M. Löwer, *et al.*, 2015 Mutant MHC class II epitopes drive therapeutic immune responses to cancer. Nature 520: 692–696. https://doi.org/10.1038/nature14426

Kulp A., and M. J. Kuehn, 2010 Biological Functions and Biogenesis of Secreted Bacterial Outer Membrane Vesicles. Annu Rev Microbiol 64: 163–184. https://doi.org/10.1146/annurev.micro.091208.073413

Kyi C., R. L. Sabado, Y. M. Saenger, M. R. Posner, M. Donovan, *et al.*, 2016 In situ, therapeutic vaccination against refractory solid cancers with intratumoral Poly-ICLC: A phase I study. J. Clin. Oncol. 34: 3086–3086. https://doi.org/10.1200/jco.2016.34.15_suppl.3086

Labrijn A. F., M. L. Janmaat, J. M. Reichert, and P. W. H. I. Parren, 2019 Bispecific antibodies: a mechanistic review of the pipeline. Nat. Rev. Drug Discov.

Lahoud M. H., F. Ahmet, J. G. Zhang, S. Meuter, A. N. Policheni, *et al.*, 2012 DEC-205 is a cell surface receptor for CpG oligonucleotides. Proc. Natl. Acad. Sci. U. S. A. 109:

16270–16275. https://doi.org/10.1073/pnas.1208796109

Lakhrif Z., A. Moreau, B. Hérault, A. Di-Tommaso, M. Juste, *et al.*, 2018 Targeted Delivery of Toxoplasma gondii Antigens to Dendritic Cells Promote Immunogenicity and Protective Efficiency against Toxoplasmosis. Front. Immunol. 9. https://doi.org/10.3389/fimmu.2018.00317

Lamm D. L., 1992 Long-term results of intravesical therapy for superficial bladder cancer. Urol. Clin. North Am. 19: 573–80.

Laughlin R. C., M. Mickum, K. Rowin, L. G. Adams, and R. C. Alaniz, 2015 Altered host immune responses to membrane vesicles from Salmonella and Gram-negative pathogens. Vaccine 33: 5012–5019. https://doi.org/10.1016/j.vaccine.2015.05.014

Launay O., A. G. W. Ndiaye, V. Conti, P. Loulergue, A. S. Sciré, *et al.*, 2019 Booster Vaccination With GVGH Shigella sonnei 1790GAHB GMMA Vaccine Compared to Single Vaccination in Unvaccinated Healthy European Adults: Results From a Phase 1 Clinical Trial. Front. Immunol. 10: 335. https://doi.org/10.3389/fimmu.2019.00335

Lee M. S., D. H. Kim, H. Kim, H. S. Lee, C. Y. Kim, *et al.*, 1998 Hepatitis B vaccination and reduced risk of primary liver cancer among male adults: A cohort study in Korea. Int. J. Epidemiol. 27: 316–319. https://doi.org/10.1093/ije/27.2.316

Lennerz V., M. Fatho, C. Gentilini, R. A. Frye, A. Lifke, *et al.*, 2005 The response of autologous T cells to a human melanoma is dominated by mutated neoantigens. Proc. Natl. Acad. Sci. U. S. A. 102: 16013–16018. https://doi.org/10.1073/pnas.0500090102

Lin L., L. Yan, Y. Liu, F. Yuan, H. Li, *et al.*, 2019 Incidence and death in 29 cancer groups in 2017 and trend analysis from 1990 to 2017 from the Global Burden of Disease Study. J. Hematol. Oncol. 12: 96. https://doi.org/10.1186/s13045-019-0783-9

Lipford G. B., M. Hoffman, H. Wagner, and K. Heeg, 1993 Primary in vivo responses to ovalbumin. Probing the predictive value of the Kb binding motif. J. Immunol. 150: 1212–22.

Lopes A., K. Vanvarenberg, Š. Kos, S. Lucas, D. Colau, *et al.*, 2018 Combination of immune checkpoint blockade with DNA cancer vaccine induces potent antitumor immunity against P815 mastocytoma. Sci. Rep. 8. https://doi.org/10.1038/s41598-018-33933-7

Lum B. L., and F. M. Torti, 1991 Adjuvant Intravesicular Pharmacotherapy for Superficial Bladder Cancer. JNCI J. Natl. Cancer Inst. 83: 682–694. https://doi.org/10.1093/jnci/83.10.682

Macri C., C. Dumont, A. P. Johnston, and J. D. Mintern, 2016 Targeting dendritic cells: a promising strategy to improve vaccine effectiveness. Clin. Transl. Immunol. 5: e66. https://doi.org/10.1038/cti.2016.6

Maito F. L. D. M., A. P. D. de Souza, L. Pereira, M. Smithey, D. Hinrichs, *et al.*, 2012 Intratumoral TLR-4 Agonist Injection Is Critical for Modulation of Tumor Microenvironment and Tumor Rejection. ISRN Immunol. 2012: 1–11. https://doi.org/10.5402/2012/926817

Makita S., K. Yoshimura, and K. Tobinai, 2017 Clinical development of anti-CD19 chimeric antigen receptor T-cell therapy for B-cell non-Hodgkin lymphoma. Cancer Sci. 108: 1109–1118.

Marabelle A., L. Tselikas, T. de Baere, and R. Houot, 2017 Intratumoral immunotherapy: using the tumor as the remedy. Ann. Oncol. 28: xii33–xii43. https://doi.org/10.1093/annonc/mdx683

McCarthy E. F., 2006 The toxins of William B. Coley and the treatment of bone and soft-tissue sarcomas. Iowa Orthop. J. 26: 154–158.

Miller K. D., J. Weaver-Feldhaus, S. A. Gray, R. W. Siegel, and M. J. Feldhaus, 2005 Production, purification, and characterization of human scFv antibodies expressed in Saccharomyces cerevisiae, Pichia pastoris, and Escherichia coli. Protein Expr. Purif. 42: 255–267. https://doi.org/10.1016/j.pep.2005.04.015

Mishra R. P. N., P. Mariotti, L. Fiaschi, S. Nosari, S. Maccari, *et al.*, 2012 Staphylococcus aureus FhuD2 Is Involved in the Early Phase of Staphylococcal Dissemination and Generates Protective Immunity in Mice. J. Infect. Dis. 206: 1041–1049. https://doi.org/10.1093/infdis/jis463

Miyaji E. N., E. Carvalho, M. L. S. Oliveira, I. Raw, and P. L. Ho, 2011 Trends in adjuvant development for vaccines: DAMPs and PAMPs as potential new adjuvants. Brazilian J. Med. Biol. Res. = Rev. Bras. Pesqui. medicas e Biol. 44: 500–13. https://doi.org/10.1590/s0100-879x2011007500064

Moore M. W., F. R. Carbone, and M. J. Bevan, 1988 Introduction of soluble protein into the class I pathway of antigen processing and presentation. Cell 54: 777–785. https://doi.org/10.1016/S0092-8674(88)91043-4

Moshiri A., A. Dashtbani-Roozbehani, S. N. Peerayeh, and S. D. Siadat, 2012 Outer membrane vesicle: A macromolecule with multifunctional activity. Hum. Vaccines Immunother. 8: 953–955.

Mougel A., M. Terme, and C. Tanchot, 2019 Therapeutic cancer vaccine and combinations with antiangiogenic therapies and immune checkpoint blockade. Front. Immunol. 10.

Mumberg D., M. Wick, and H. Schreiber, 1996 Unique tumor antigens redefined as mutant tumor-specific antigens. Semin. Immunol. 8: 289–293.

Murphy K., and C. Weaver, 2016 *Janeway's Immunobiology*. Garland Science, New York.

Mylin L. M., A. M. Deckhut, R. H. Bonneau, T. D. Kierstead, M. J. Tevethia, *et al.*, 1995 Cytotoxic T lymphocyte escape variants, induced mutations, and synthetic peptides define a dominant H-2Kb-restricted determinant in simian virus 40 tumor antigen. Virology 208: 159–172. https://doi.org/10.1006/viro.1995.1139

Mylin L. M., T. D. Schell, D. Roberts, M. Epler, A. Boesteanu, *et al.*, 2000 Quantitation of CD8+ T-Lymphocyte Responses to Multiple Epitopes from Simian Virus 40 (SV40) Large T Antigen in C57BL/6 Mice Immunized with SV40, SV40 T-Antigen-Transformed Cells, or Vaccinia Virus Recombinants Expressing Full-Length T Antigen or Epitope Minigenes. J. Virol. 74: 6922–6934. https://doi.org/10.1128/jvi.74.15.6922-6934.2000

Narita S. ichiro, and H. Tokuda, 2017 Bacterial lipoproteins; biogenesis, sorting and quality control. Biochim. Biophys. Acta - Mol. Cell Biol. Lipids 1862: 1414–1423.

Ngu L. N., N. N. Nji, G. E. Ambada, B. Sagnia, C. N. Sake, *et al.*, 2019 In vivo targeting of protein antigens to dendritic cells using anti-DEC-205 single chain antibody improves HIV Gag specific CD4 $^{+}$ T cell responses protecting from airway challenge with recombinant vaccinia-gag virus. Immunity, Inflamm. Dis. 7: 55–67. https://doi.org/10.1002/iid3.151

O'Donoghue E. J., and A. M. Krachler, 2016 Mechanisms of outer membrane vesicle entry into host cells. Cell. Microbiol. 18: 1508–1517. https://doi.org/10.1111/cmi.12655

Obiero C. W., A. G. W. Ndiaye, A. S. Sciré, B. M. Kaunyangi, E. Marchetti, *et al.*, 2017 A Phase 2a Randomized Study to Evaluate the Safety and Immunogenicity of the 1790GAHB Generalized Modules for Membrane Antigen Vaccine against Shigella sonnei Administered Intramuscularly to Adults from a Shigellosis-Endemic Country. Front. Immunol. 8: 1884. https://doi.org/10.3389/fimmu.2017.01884

Ott P. A., Z. Hu, D. B. Keskin, S. A. Shukla, J. Sun, *et al.*, 2017 An immunogenic personal neoantigen vaccine for patients with melanoma. Nature 547: 217–221. https://doi.org/10.1038/nature22991

Park K.-S., K.-H. Choi, Y.-S. Kim, B. S. Hong, O. Y. Kim, *et al.*, 2010 Outer Membrane Vesicles Derived from Escherichia coli Induce Systemic Inflammatory Response Syndrome, (O.

Neyrolles, Ed.). PLoS One 5: e11334. https://doi.org/10.1371/journal.pone.0011334

Park J. S., W. C. Lee, K. J. Yeo, K. S. Ryu, M. Kumarasiri, *et al.*, 2012 Mechanism of anchoring of OmpA protein to the cell wall peptidoglycan of the gram-negative bacterial outer membrane. FASEB J. 26: 219–228. https://doi.org/10.1096/fj.11-188425

Peters C., and S. Brown, 2015 Antibody-drug conjugates as novel anti-cancer chemotherapeutics. Biosci. Rep. 35: 225.

Petzold C., S. Schallenberg, J. N. H. Stern, and K. Kretschmer, 2012 Targeted antigen delivery to DEC-205+ dendritic cells for tolerogenic vaccination. Rev. Diabet. Stud. 9: 305–318. https://doi.org/10.1900/RDS.2012.9.305

Pierce R. H., J. S. Campbell, S. I. Pai, J. D. Brody, and H. E. K. Kohrt, 2015 In-situ tumor vaccination: Bringing the fight to the tumor. Hum. Vaccines Immunother. 11: 1901–1909. https://doi.org/10.1080/21645515.2015.1049779

Pol S., 2015 Hepatitis: HBV vaccine - The first vaccine to prevent cancer. Nat. Rev. Gastroenterol. Hepatol. 12: 190–191.

Pol L. van der, M. Stork, and P. van der Ley, 2015 Outer membrane vesicles as platform vaccine technology. Biotechnol. J. 10: 1689–1706. https://doi.org/10.1002/biot.201400395

Postow M. A., J. Chesney, A. C. Pavlick, C. Robert, K. Grossmann, *et al.*, 2015 Nivolumab and ipilimumab versus ipilimumab in untreated melanoma. N. Engl. J. Med. 372: 2006–2017. https://doi.org/10.1056/NEJMoa1414428

Prasad V., 2018 Tisagenlecleucel - The first approved CAR-T-cell therapy: Implications for payers and policy makers. Nat. Rev. Clin. Oncol. 15: 11–12.

Qu C., T. Chen, C. Fan, Q. Zhan, Y. Wang, *et al.*, 2014 Efficacy of Neonatal HBV Vaccination on Liver Cancer and Other Liver Diseases over 30-Year Follow-up of the Qidong Hepatitis B Intervention Study: A Cluster Randomized Controlled Trial, (A. Singal, Ed.). PLoS Med. 11: e1001774. https://doi.org/10.1371/journal.pmed.1001774

Rabu C., L. Rangan, L. Florenceau, A. Fortun, M. Charpentier, *et al.*, 2019 Cancer vaccines: designing artificial synthetic long peptides to improve presentation of class I and class II T cell epitopes by dendritic cells. Oncoimmunology 8. https://doi.org/10.1080/2162402X.2018.1560919

Radoja S., T. D. Rao, D. Hillman, and A. B. Frey, 2000 Mice Bearing Late-Stage Tumors Have Normal Functional Systemic T Cell Responses In Vitro and In Vivo. J. Immunol. 164:

2619–2628. https://doi.org/10.4049/jimmunol.164.5.2619

Raja J., J. M. Ludwig, S. N. Gettinger, K. A. Schalper, and H. S. Kim, 2018 Oncolytic virus immunotherapy: future prospects for oncology. J. Immunother. Cancer 6: 140. https://doi.org/10.1186/s40425-018-0458-z

Rehman H., A. W. Silk, M. P. Kane, and H. L. Kaufman, 2016 Into the clinic: Talimogene laherparepvec (T-VEC), a first-in-class intratumoral oncolytic viral therapy. J. Immunother. Cancer 4. https://doi.org/10.1186/s40425-016-0158-5

Rodrigo G., M. Gruvegård, and J. Van Alstine, 2015 Antibody Fragments and Their Purification by Protein L Affinity Chromatography. Antibodies 4: 259–277. https://doi.org/10.3390/antib4030259

Rolink A., F. Melchers, J. Andersson, V. Steward, F. . Alt, *et al.*, 1996 The SCID but Not the RAG-2 Gene Product Is Required for Sμ–Sε Heavy Chain Class Switching. Immunity 5: 319–30. https://doi.org/10.1016/S1074-7613(00)80258-7

Rosalia R. A., E. D. Quakkelaar, A. Redeker, S. Khan, M. Camps, *et al.*, 2013 Dendritic cells process synthetic long peptides better than whole protein, improving antigen presentation and T-cell activation. Eur. J. Immunol. 43: 2554–2565. https://doi.org/10.1002/eji.201343324

Rosenberg S. A., and M. T. Lotze, 1986 Cancer Immunotherapy Using Interleukin-2 and Interleukin-2-Activated Lymphocytes. Annu. Rev. Immunol. 4: 681–709. https://doi.org/10.1146/annurev.iy.04.040186.003341

Rosenqvist E., E. A. Hoiby, E. Wedege, K. Bryn, J. Kolberg, *et al.*, 1995 Human antibody responses to meningococcal outer membrane antigens after three doses of the Norwegian group B meningococcal vaccine. Infect Immun 63: 4642–4652.

Rosenthal K. S., and D. H. Zimmerman, 2006 Vaccines: All things considered. Clin. Vaccine Immunol. 13: 821–829.

Rosenthal J. A., C.-J. Huang, A. M. A. Doody, T. Leung, K. Mineta, *et al.*, 2014 Mechanistic insight into the TH1-biased immune response to recombinant subunit vaccines delivered by probiotic bacteria-derived outer membrane vesicles, (Y. Chung, Ed.). PLoS One 9: e112802. https://doi.org/10.1371/journal.pone.0112802 PONE-D-14-26349 [pii]

Rötzschke O., K. Falk, S. Stevanovic, G. Jung, P. Walden, *et al.*, 1991 Exact prediction of a natural T cell epitope. Eur. J. Immunol. 21: 2891–2894. https://doi.org/10.1002/eji.1830211136

Rueda P., G. Morón, J. Sarraseca, C. Leclerc, and J. I. Casal, 2004 Influence of flanking sequences on presentation efficiency of a CD8+ cytotoxic T-cell epitope delivered by parvovirus-like particles. J. Gen. Virol. 85: 563–572. https://doi.org/10.1099/vir.0.19525-0

Sagiv-Barfi I., D. K. Czerwinski, S. Levy, I. S. Alam, A. T. Mayer, *et al.*, 2018 Eradication of spontaneous malignancy by local immunotherapy. Sci. Transl. Med. 10: eaan4488. https://doi.org/10.1126/scitranslmed.aan4488

Sahin U., E. Derhovanessian, M. Miller, B. P. Kloke, P. Simon, *et al.*, 2017 Personalized RNA mutanome vaccines mobilize poly-specific therapeutic immunity against cancer. Nature 547: 222–226. https://doi.org/10.1038/nature23003

Sallets A., S. Robinson, A. Kardosh, and R. Levy, 2018 Enhancing immunotherapy of STING agonist for lymphoma in preclinical models. Blood Adv. 2: 2230–2241. https://doi.org/10.1182/bloodadvances.2018020040

Sato-Kaneko F., S. Yao, A. Ahmadi, S. S. Zhang, T. Hosoya, *et al.*, 2017 Combination immunotherapy with TLR agonists and checkpoint inhibitors suppresses head and neck cancer. JCI insight 2. https://doi.org/10.1172/jci.insight.93397

Schreiber R. D., L. J. Old, and M. J. Smyth, 2011 Cancer immunoediting: Integrating immunity's roles in cancer suppression and promotion. Science (80-.). 331: 1565–1570.

Schumacher T. N., and R. D. Schreiber, 2015 Neoantigens in cancer immunotherapy. Science (80-.). 348: 69–74.

Schwechheimer C., and M. J. Kuehn, 2015 Outer-membrane vesicles from Gram-negative bacteria: biogenesis and functions. Nat Rev Microbiol 13: 605–619. https://doi.org/nrmicro3525 [pii]10.1038/nrmicro3525

Sell S., 2017 Cancer immunotherapy: Breakthrough or "deja vu, all over again"? Tumor Biol. 39: 1–14. https://doi.org/10.1177/1010428317707764

Serruto D., M. J. Bottomley, S. Ram, M. M. Giuliani, and R. Rappuoli, 2012 The new multicomponent vaccine against meningococcal serogroup B, 4CMenB: immunological, functional and structural charaterization of the antigens. Vaccine 30: B87–B97. https://doi.org/10.1016/j.vaccine.2012.01.033

Sevastsyanovich Y. R., D. L. Leyton, T. J. Wells, C. a Wardius, K. Tveen-Jensen, *et al.*, 2012 A generalised module for the selective extracellular accumulation of recombinant proteins. Microb. Cell Fact. 11: 69. https://doi.org/10.1186/1475-2859-11-69

Shibata T., B. J. Lieblong, T. Sasagawa, and M. Nakagawa, 2019 The promise of combining cancer vaccine and checkpoint blockade for treating HPV-related cancer. Cancer Treat. Rev. 78: 8–16.

Shrimpton R. E., M. Butler, A. S. Morel, E. Eren, S. S. Hue, *et al.*, 2009 CD205 (DEC-205): A recognition receptor for apoptotic and necrotic self. Mol. Immunol. 46: 1229–1239. https://doi.org/10.1016/j.molimm.2008.11.016

Sierra G. V, H. C. Campa, N. M. Varcacel, I. L. Garcia, P. L. Izquierdo, *et al.*, 1991 Vaccine against group B Neisseria meningitidis: protection trial and mass vaccination results in Cuba. NIPH Ann. 14: 110–195.

Somerville J. E., L. Cassiano, B. Bainbridge, M. D. Cunningham, and R. P. Darveau, 1996 A novel Escherichia coli lipid A mutant that produces an antiinflammatory lipopolysaccharide. J. Clin. Invest. 97: 359–365. https://doi.org/10.1172/JCI118423

Souchon H., N. Doyen, M. M. Riottot, F. Rougeon, and R. J. Poljak, 1990 Nucleotide sequence of the VH,VL regions of an anti-idiotopic antibody reacting with a private idiotope of the anti-lysozyme D1.3 antibody. Mol. Immunol. 27: 429–433. https://doi.org/10.1016/0161-5890(90)90167-X

Stathopoulos C., G. Georgiou, and C. F. Earhart, 1996 Characterization of Escherichia coli expressing an Lpp'OmpA(46-159)-PhoA fusion protein localized in the outer membrane. Appl Microbiol Biotechnol 45: 112–119.

Steeghs L., A. M. Keestra, A. van Mourik, H. Uronen-Hansson, P. van der Ley, *et al.*, 2008 Differential activation of human and mouse Toll-like receptor 4 by the adjuvant candidate LpxL1 of Neisseria meningitidis. Infect. Immun. 76: 3801–7. https://doi.org/10.1128/IAI.00005-08

Steinman R. M., and Z. A. Cohn, 1973 Identification of a novel cell type in peripheral lymphoid organs of mice: I. Morphology, quantitation, tissue distribution. J. Exp. Med. 137: 1142–1162. https://doi.org/10.1084/jem.137.5.1142

Steinman R. M., and M. D. Witmer, 1978 Lymphoid dendritic cells are potent stimulators of the primary mixed leukocyte reaction in mice. Proc. Natl. Acad. Sci. U. S. A. 75: 5132–5136. https://doi.org/10.1073/pnas.75.10.5132

Szekeres Z., M. Herbáth, Z. Szittner, K. Papp, A. Erdei, *et al.*, 2011 Modulation of the humoral immune response by targeting CD40 and FcyRII/III; delivery of soluble but not particulate antigen to CD40 enhances antibody response with a Th1 bias. Mol. Immunol. 49: 155–162. https://doi.org/10.1016/j.molimm.2011.08.008

Tanaka Y., and S. S. Tevethia, 1988 In vitro selection of SV40 T antigen epitope loss variants by site-specific cytotoxic T lymphocyte clones. J. Immunol. 140: 4348–54.

Tomasi M., 2018 Bacterial outer membrane vesicles (OMVs) as a platform for personalized cancer vaccines (Doctoral thesis)

Topalian S. L., C. G. Drake, and D. M. Pardoll, 2015 Immune checkpoint blockade: A common denominator approach to cancer therapy. Cancer Cell 27: 450–461.

Tran E., P. F. Robbins, and S. A. Rosenberg, 2017 "Final common pathway" of human cancer immunotherapy: targeting random somatic mutations. Nat. Immunol. 18: 255–262. https://doi.org/10.1038/ni.3682

Tsao M. S., K. M. Kerr, S. Dacic, Y. Yatabe, and F. R. Hirsch, 2017 *IASLC ATLAS OF PD-L1 IMMUNOHISTOCHEMISTRY TESTING IN LUNG CANCER Conquering Thoracic Cancers Worldwide*. Aurora, Colorado.

Tsuji T., J. Matsuzaki, M. P. Kelly, V. Ramakrishna, L. Vitale, *et al.*, 2011 Antibody-Targeted NY-ESO-1 to Mannose Receptor or DEC-205 In Vitro Elicits Dual Human CD8 + and CD4 + T Cell Responses with Broad Antigen Specificity . J. Immunol. 186: 1218–1227. https://doi.org/10.4049/jimmunol.1000808

Uto T., T. Fukaya, H. Takagi, K. Arimura, T. Nakamura, *et al.*, 2016 Clec4A4 is a regulatory receptor for dendritic cells that impairs inflammation and T-cell immunity. Nat. Commun. 7. https://doi.org/10.1038/ncomms11273

Vaks L., and I. Benhar, 2014 Production of stabilized scFv antibody fragments in the E. coli bacterial cytoplasm. Methods Mol. Biol. 1060: 171–184. https://doi.org/10.1007/978-1-62703-586-6_10

Vanaja S. K., A. J. Russo, B. Behl, I. Banerjee, M. Yankova, *et al.*, 2016 Bacterial Outer Membrane Vesicles Mediate Cytosolic Localization of LPS and Caspase-11 Activation. Cell 165: 1106–1119. https://doi.org/10.1016/j.cell.2016.04.015

Velga E., V. De Lorenzo, L. A. Fernández, E. Veiga, V. De Lorenzo, *et al.*, 1999 Probing secretion and translocation of a β-autotransporter using a reporter single-chain Fv as a cognate passenger domain. Mol. Microbiol. 33: 1232–1243. https://doi.org/10.1046/j.1365-2958.1999.01571.x

Villadangos J. A., and P. Schnorrer, 2007 Intrinsic and cooperative antigen-presenting functions of dendritic-cell subsets in vivo. Nat. Rev. Immunol. 7: 543–555.

Wang R., S. Xiang, Y. Feng, S. Srinivas, Y. Zhang, *et al.*, 2013 Engineering production of functional scFv antibody in E. coli by co-expressing the molecule chaperone Skp.

Front. Cell. Infect. Microbiol. 3. https://doi.org/10.3389/fcimb.2013.00072

Wang C., J. Dickie, R. V. Sutavani, C. Pointer, G. J. Thomas, *et al.*, 2018 Targeting head and neck cancer by vaccination. Front. Immunol. 9.

Ward E. S., D. Güssow, A. D. Griffiths, P. T. Jones, and G. Winter, 1989 Binding activities of a repertoire of single immunoglobulin variable domains secreted from Escherichia coli. Nature 341: 544–546. https://doi.org/10.1038/341544a0

Wculek S. K., F. J. Cueto, A. M. Mujal, I. Melero, M. F. Krummel, *et al.*, 2019 Dendritic cells in cancer immunology and immunotherapy. Nat. Rev. Immunol. 1–18. https://doi.org/10.1038/s41577-019-0210-z

Wolchok J. D., V. Chiarion-Sileni, R. Gonzalez, P. Rutkowski, J. J. Grob, *et al.*, 2017 Overall Survival with Combined Nivolumab and Ipilimumab in Advanced Melanoma. N. Engl. J. Med. 377: 1345–1356. https://doi.org/10.1056/NEJMoa1709684

Wong K. K., W. W. A. Li, D. J. Mooney, and G. Dranoff, 2016 Advances in Therapeutic Cancer Vaccines, pp. 191–249 in *Advances in Immunology*, Academic Press Inc.

Xia X., X. Wang, Z. Cheng, W. Qin, L. Lei, *et al.*, 2019 The role of pyroptosis in cancer: pro-cancer or pro-“host”? Cell Death Dis. 10.

Yang A., E. Farmer, T. C. Wu, and C. F. Hung, 2016 Perspectives for therapeutic HPV vaccine development. J. Biomed. Sci. 23: 1–19. https://doi.org/10.1186/s12929-016-0293-9

Yarchoan M., A. Hopkins, and E. M. Jaffee, 2017 Tumor mutational burden and response rate to PD-1 inhibition. N. Engl. J. Med. 377: 2500–2501.

Zanella I., 2019 Construction and characterization of proteome-minimized OMVs from E. coli and their exploitation in infectious disease and cancer vaccines (Doctoral thesis)

Zanella I., E. König, M. Tomasi, A. Gagliardi, S. J. Isaac, *et al.*, 2020 Proteome-minimized Outer Membrane Vesicles from Escherichia coli as a vaccine platform for infectious diseases and cancer. Submitted.

Zapala L., N. Drela, J. Bil, D. Nowis, G. W. Basak, *et al.*, 2011 Optimization of activation requirements of immature mouse dendritic JAWSII cells for in vivo application. Oncol. Rep. 25: 831–840. https://doi.org/10.3892/or.2010.1128

Zariri A., J. Beskers, B. van de Waterbeemd, H. J. Hamstra, T. H. E. Bindels, *et al.*, 2016 Meningococcal outer membrane vesicle composition-dependent activation of the innate immune response. Infect. Immun. 84: 3024–3033. https://doi.org/10.1128/IAI.00635-16

Zerbini F., I. Zanella, D. Fraccascia, E. König, C. Irene, *et al.*, 2017 Large scale validation of

an efficient CRISPR/Cas-based multi gene editing protocol in Escherichia coli. Microb. Cell Fact. 16: 68. https://doi.org/10.1186/s12934-017-0681-1

Zhang Y., Z. Fang, R. Li, X. Huang, and Q. Liu, 2019 Design of Outer Membrane Vesicles as Cancer Vaccines: A New Toolkit for Cancer Therapy. Cancers (Basel). 11: 1314. https://doi.org/10.3390/cancers11091314

Publications

Proteome-minimized Outer Membrane Vesicles from *Escherichia coli* as a vaccine platform for infectious diseases and cancer

*Zanella I, König E, Tomasi M, Gagliardi A, **Isaac SJ**, Grigolato M, Frattini L, Zerbini F, Fantappiè L, Irene C, Caproni E, Corbellari R, Valensin S, Bini L, Ashhab Y, Grandi A and Grandi G*

Manuscript submitted

I performed and analysed in situ vaccination experiments. I contributed to OMV production and purification, as well as manuscript editing.

Bacterial outer membrane vesicles engineered with lipidated antigens as a platform for *Staphylococcus aureus* vaccine

*Irene C, Fantappiè L, Caproni E, Zerbini F, Anesi A, Tomasi M, Zanella I, Stupia S, Prete S, Valensin S, König E, Frattini L, Gagliardi A, **Isaac SJ**, Grandi A, Guella G, and Grandi G*

PNAS 2019 October 22, 116 (43) 21780-21788

I contributed to OMV engineering and manuscript editing.

Vaccination with a FAT1-Derived B Cell Epitope Combined with Tumor-Specific B and T Cell Epitopes Elicits Additive Protection in Cancer Mouse Models

*Grandi A, Fantappiè L, Irene C, Valensin S, Tomasi M, Stupia S, Corbellari R, Caproni E, Zanella I, **Isaac SJ**, Ganfini L, Frattini L, König E, Gagliardi A, Tavarini S, Sammicheli C, Parri M, Grandi G*

Front Oncol. 2018 Oct 26;8:481.

I contributed to protein analysis including Western blots and ELISA, as well as editing of the manuscript.

Synergistic Protective Activity of Tumor-Specific Epitopes Engineered in Bacterial Outer Membrane Vesicles

*Grandi A, Tomasi M, Zanella I, Ganfini L, Caproni E, Fantappiè L, Irene C, Frattini L, **Isaac SJ**, König E, Zerbini F, Tavarini S, Sammicheli C, Giusti F, Ferlenghi I, Parri M, Grandi G*.

Front Oncol. 2017 Nov 7;7:253.

I contributed to strain engineering, OMV preparation and characterisation.

Acknowledgements

Firstly, I would like to thank my PhD advisor, Prof. Guido Grandi for giving me the opportunity to do my PhD in his laboratory. I have learned so much throughout this experience and as a consequence have grown as a scientist and a person.

Thank you to all the past and present members of the Laboratory of Synthetic and Structural Vaccinology. Particularly, Mirel who took me under his wing from the start, helping me to get to grips with how things work, not just in the lab but at CIBIO and in Trento. Francesca for your positive energy and guidance. Carmela, for having an infectious drive to get things done as well as being a great teacher. Ilaria, for your calm perspective and great chats. Luca for getting me skiing. Enrico, for being the other foreigner! And providing a non-stop flow of Dad jokes. Alvise, for your energy and enthusiasm. Also to all our colleagues based in Siena, doing their best not to let distance separate us. Thanks Laura, Assunta, Elena, Simone and of course Alberto for your positivity and consistent willingness to help.

I'd like to also thank all the students, Masters and Bachelors, that passed through our lab on their own journeys. You brought liveliness and more curiosity to the lab. Thanks Stefania for your cheer and compassion. Thank you Martina! You were a pleasure to supervise and you can't image just how you also helped me grow.

I need to also give my appreciation to the Advanced Imaging facility, thanks Michela and Giorgina. Also thanks to everyone working in MOF, with a special thanks to Marta for your unlimited patience while training me. Additionally, never would have made it without the help and support of Isabella R.

Everyone in the 32nd cycle, just knowing we were all in the same boat was enough. A special thanks to Mariachiara for being such a supportive friend, Veronica for our chats in Red 5, Caterina and Nausicaa for good gabble and spritz (but maybe not enough). Ade, for all our chats (in the muva tongue n all) and being a supportive friend.

All my friends near and far, so many of you have made my day so many times with words of encouragement and affection. Especially you Daniela, Olivia, Saiqa, Simone and Tara, thanks for not letting me forget myself.

My Family, you make me strong, thanks for making sure I always believed in myself. A special thank you to you Mum and Dad.

Cristiano, could not have done it without you!...and your unwavering love and support.